NASA Technical Paper 1742

A Simulator Study for the Development and Evaluation of Operating Procedures on a Supersonic Cruise Research Transport To Minimize Airport-Community Noise

William D. Grantham, Paul M. Smith,
and Perry L. Deal

NOVEMBER 1980

NASA

NASA Technical Paper 1742

A Simulator Study for the Development and Evaluation of Operating Procedures on a Supersonic Cruise Research Transport To Minimize Airport-Community Noise

William D. Grantham
Langley Research Center
Hampton, Virginia

Paul M. Smith
Kentron International, Inc.
Hampton, Virginia

Perry L. Deal
Langley Research Center
Hampton, Virginia

NASA
National Aeronautics
and Space Administration

Scientific and Technical
Information Branch

1980

SUMMARY

Piloted-simulator studies have been conducted to determine takeoff and landing operating procedures for a supersonic cruise research transport concept that result in predicted noise levels which meet current Federal Aviation Administration (FAA) noise-certification standards. The results of these studies indicate that with the use of standard FAA noise-certification test procedures, the simulated aircraft did not meet the FAA traded-noise-level standards during takeoff and landing. With the use of advanced test procedures, however, this simulated aircraft did meet the traded-noise-level standards for average flight crew skills. The advanced takeoff procedures developed involve violating three of the current Federal Aviation Regulations (FAR) noise-test conditions. These violations are thrust cutback at altitudes below 214 m (700 ft), thrust cutback level below that presently allowed, and configuration change (other than raising the landing gear). Of these rule violations, thrust cutback at altitudes below 214 m (700 ft) is of primary importance. That is, only minor noise-reduction benefits were realized by violating the other rules listed. It was not necessary to violate any FAR noise-test conditions during landing approach. However, it was determined that a decelerating approach produced lower noise levels at the FAR measuring station and reduced the effective perceived noise level contour areas by as much as 74 percent. The advanced takeoff and landing-approach procedures developed and evaluated during this study did not compromise flight safety.

Automation of some of the aircraft functions reduced pilot workload when performing the advanced procedure takeoffs and landings. The development of a simple head-up display to assist in the takeoff flight mode proved to be adequate for performing the task.

INTRODUCTION

The continued increase in size and power of commercial transport aircraft has caused considerable concern about the noise environment in the vicinity of major airports. This concern has manifested itself in the form of government noise regulations for all civilian subsonic transports as well as local opposition to airport expansion and restricted hours of operation.

Figure 1 indicates the noise limits as a function of aircraft weight allowed by the current Federal Aviation Regulations (FAR, ref. 1). It also presents the "noisiness" of some present-day jet transports (ref. 2) relative to this noise standard as well as to each other. Note that the majority of the "narrow-body" subsonic aircraft do not meet these noise standards for takeoff or approach and that neither the Concorde nor the TU-144 supersonic transports meet these standards for takeoff, sideline, or approach. In general the "wide-body" subsonic aircraft, powered by high-bypass-ratio engines, do meet the noise standards in reference 1.

The U.S. Department of Transportation and the National Aeronautics and Space Administration (NASA) have supported work on the development of two methods to reduce the noise from the narrow-body subsonic aircraft: (1) Nacelle redesign with extensive use of sound-absorption material, and (2) equip aircraft with large-diameter, single-stage fan engines with nacelle redesign including use of sound-absorption material. Other than conventional aircraft-operation procedures could also be used to reduce airport-community noise. Considerable literature is available showing the noise-reduction benefits during landing approaches for present-day subsonic jet transports by using steeper than normal approaches, two-segment approaches, and decelerating approaches. (See refs. 3 to 6.)

Since 1972, the NASA Langley Research Center (LaRC) has been working in advanced supersonic technology for potential application to future U.S. transport aircraft. Among the significant advances which have been made during this period is the development of a new engine concept that is a duct-burning turbofan variable-stream-control engine (VSCE), which has the potential to operate with less jet noise during takeoffs and landings than conventional turbojets. The improvement is attributed to coannular-nozzle-jet noise relief. Therefore, the present simulation study was conducted in an attempt to develop operational procedures for a typical supersonic cruise research (SCR) transport concept that would reduce the airport-community noise during both takeoffs and landings. (See refs. 7 and 8.)

The noise-certification standards in reference 1 for subsonic transport aircraft specify takeoff and landing "piloting" procedures that require constant flight speed and no configuration changes (except the landing gear may be retracted after lift-off). It should be considered, however, that a supersonic transport with VSCE's will have airframe-engine characteristics that are different from present-day subsonic jet transports, and if these characteristics are utilized properly, they could significantly reduce community noise during takeoff and landing. For example, the variable engine inlet and exhaust nozzles allow for tailoring of engine performance while minimizing engine noise; the relatively high thrust-to-weight ratio allows rapid acceleration to optimum climb speeds; and the relatively simple high-lift flap system makes the SCR transport concept amenable to automated operation.

The subject-piloted simulator study was conducted using the AST-105-1 SCR transport concept to determine: (1) Advanced takeoff and landing procedures for which the FAR noise-level requirements could be met; (2) if a pilot with average skills could perform the task of flying the suggested profiles without compromising flight safety; (3) the degree of automation required; and (4) the pilot information displays required.

Noise predictions were made with the aircraft noise prediction program (ANOPP, ref. 9). This program uses time-dependent trajectory and engine data to predict the time-dependent one-third octave band spectra at a set of observer positions. These spectra are then integrated to obtain perceived noise and effective perceived noise. The ANOPP includes noise-source prediction modules for jet mixing noise, jet shock-cell noise, compressor noise, combustion

noise, turbine noise, and airframe noise. In the present study, only the jet-mixing-noise module was used. The ANOPP was also used to determine noise contours for the simulated takeoffs and landings.

Use of trade names or names of manufacturers in this report does not constitute an official endorsement of such products or manufacturers, either expressed or implied, by the National Aeronautics and Space Administration.

SYMBOLS AND DEFINITIONS

Values are given in both the International Systems of Units (SI) and U.S. Customary Units. The measurements and calculations were made in U.S. Customary Units. Dots over symbols denote differentiation with respect to time.

AK_V	gain on airspeed error
GK_I	integrator gain
G	acceleration and deceleration engine inverse time constants, sec^{-1}
h	altitude, m (ft)
K	gain
$K_{s,\theta}$	switching gain
M	Mach number
s	Laplace operator
T	thrust, N (lbf)
T_g	gross thrust
t	time, sec
t_1	deceleration time, sec
V	airspeed, knots
V_c	climb speed, knots
V_R	rotation speed, knots
$V_{R,I}$	desired airspeed upon completion of deceleration, knots
$\dot{V}_{SMOOTH}$	velocity rate limit, knots/sec
V_1	decision speed (engine failure speed + ΔV for a 2-sec reaction time), knots

V_2	airspeed of aircraft at obstacle, knots
V^*	reference airspeed, knots
W	airplane weight, N (lbf)
X	distance from brake release, m (ft)
α	angle of attack, deg
γ	flight-path angle, deg
δ_f	trailing-edge flap deflection, deg
δ_{SB}	speed-brake deflection, deg
ε	error
θ	pitch attitude, deg
τ	time constant, sec
τ_B	pitch-attitude-bias time constant, sec
ϕ	angle of roll, deg
ψ	heading angle, deg

Subscripts:

B	bias
C	commanded
FI	flight idle
IAS	indicated airspeed
IC	initial condition
LG	landing gear
LO	lift-off
MAX	maximum
MIN	minimum
N	net

PFD	pitch-command sensitivity to flight director
PIL	pilot
SB	speed brake
trim	trim condition
V	velocity
VFD	velocity flight director
θ	pitch

Abbreviations:

ADI	attitude-director indicator
Adv	advanced
ANOPP	aircraft noise prediction program
eng	engine
EPNL	effective perceived noise level, dB
FAA	Federal Aviation Administration
FAR	Federal Aviation Regulations
IAS	indicated airspeed
Mod	modified
PLA	power lever angle
PNLT	tone-corrected perceived noise level
proc	procedure
SCR	supersonic cruise research
Std	standard
TH	track/hold
VMS	Langley Visual/Motion Simulator
VSCE	variable-stream-control engine

DESCRIPTION OF SIMULATED AIRPLANE*

The SCR transport concept simulated in this study was a resized version of the configuration in reference 10 and is described in detail in reference 11. Reference 11 also contains the mass and dimensional characteristics, control-surface deflections and deflection-rate limits, and most of the aerodynamic data used in this study. A three-view sketch of the simulated airplane is presented in figure 2.

The static aerodynamic data were estimated based on the low-speed wind-tunnel test results of references 12 and 13 and corrected for configuration differences. The control surfaces used for low-speed lateral control consisted of outboard ailerons, outboard flaperons, and inboard flaperons. The lateral-control system was designed in such a manner that all lateral-control surfaces were driven by the commanded aileron deflection, and each surface was deflected so that all reached their limit simultaneously. The rigid lateral-control data were taken from reference 12 and modified to account for the size and location of the control surfaces on the subject airplane. An all-movable vertical tail was used for low-speed directional control and its effectiveness was estimated by using the data from reference 12. The reduction of lateral-control effectiveness due to wing flexibility was taken from reference 14, and the reduction of directional-control effectiveness due to fuselage transverse bending was based on unpublished results. To facilitate steep decelerating approaches, a speed brake was designed which incorporated bifurcated "rudders" on the two wing fins. To minimize ground roll following touchdown, the speed brakes and wing spoilers were used.

The aerodynamic effects of ground proximity were obtained from the test data of reference 15. The dynamic aerodynamic derivatives were estimated by using a combination of the forced-oscillation test data of reference 16 and the estimation techniques of reference 17.

The variable-stream-control engine concept, designated VSCE-516, was selected for this study. The engine was scaled to meet the takeoff design thrust-to-weight ratio of 0.254 for the simulated SCR transport. The engine-performance data generated by the manufacturer was provided in the form of an unpublished-data package which included the performance for a standard day plus 10°C. The engine performance for a standard day plus 10°C was used for the takeoff and landing analyses as well as the subsequent noise analyses made during this study. Since the response characteristics of the VSCE-516 engine were not known, the response times were varied from fast to very slow. Unless specifically noted the fast engine-response characteristics were used for the results discussed. (The impact of the engine-response times on flight safety was evaluated and will be discussed.)

---

*The work-up and analyses of the aerodynamic and geometric data packages utilized for this SCR simulation program were performed under contract number NAS1-16000 by Paul M. Smith of Kentron International Inc.

DESCRIPTION OF SIMULATION EQUIPMENT

Studies of advanced takeoff and landing procedures for a typical SCR transport concept were made with the general-purpose cockpit of the Langley Visual/Motion Simulator (VMS). This is a ground-based motion simulator with six degrees of freedom. For this study it had a transport-type cockpit which was equipped with conventional flight and engine-thrust controls and with a flight-instrument display representative of those found in current transport airplanes. (See fig. 3.) Instruments that indicated angle of attack, angle of sideslip, pitch rate, and flap angle were also provided. A conventional cross-pointer-type flight-director instrument was used, and the command bars (cross pointers) were driven by the main computer program. The horizontal bar of the ADI was used for flight-path-control command during landing approaches and as a simplified airspeed-control command during takeoffs. This "takeoff" director was programmed with two options: (1) The option of commanding the pilot to climb at an airspeed of $V_2 + \Delta V$, or (2) the option of commanding the pilot to climb at an IAS of 250 knots. (See fig. 4 for block diagram of the takeoff director.)

The control forces on the wheel, column, and rudder pedals were provided by a hydraulic system coupled with an analog computer. The system allows for the usual variable-feel characteristics of stiffness, damping, coulomb friction, breakout forces, detents, and inertia.

The airport-scene display used an "out-the-window" virtual image system of the beam-splitter, reflective-mirror type. (See fig. 5.) In addition to the airport scene presented on the out-the-window virtual image system, a "head-up" display was superimposed on the same system. (See fig. 6.) The head-up portion of the display consisted of angle-of-attack, pitch-rate, and climb-gradient presentations that were used only for the takeoff and climb maneuvers. The head-up display was not used for landing approaches.

The motion-performance characteristics of the VMS system possess time lags of less than 50 msec. The washout system used to present the motion-cue commands to the motion base was nonstandard. (See ref. 18.)

A runway "model" was programmed that was considered to have certain roughness characteristics and a slope from the center to the edge representing a runway crown. Only a dry runway was considered in this study.

The only aural cues provided were engine noises and landing-gear extension and retraction noises.

TESTS AND PROCEDURES

The tests consisted of simulated takeoffs and landings using "standard" as well as "advanced" procedures. The term "standard procedures," as used in this report, refers to those procedures that adhere to all present Federal Aviation Regulations, whereas the "advanced procedures" used do not adhere to all of the FAR, particularly those regulations that pertain to aircraft noise-certification procedures.

A NASA test pilot participated in the simulation program, and his comments dictated the type of pilot-information displays and the degree of automation that was developed for performing the task of "flying" the various takeoff and landing procedures used in this study. In addition to the normal-type displays used in current subsonic jet transports, the pilot-information displays consisted of a takeoff director and a head-up display, both previously described in this paper and used only during takeoff and climb. The automated features consisted of an autothrottle for controlling airspeed and an autodeceleration control. The autodeceleration control was programmed as a part of the autothrottle and was used only when the deceleration switch was activated by the pilot. The autothrottle portion of the system was sometimes used for both takeoffs and landings, whereas the autodeceleration mode was only used during landing approaches. (See fig. 7 for block diagram of autothrottle.)

By operating the VSCE's used in this study at maximum allowable turbine-inlet temperature, the maximum thrust is increased approximately 16 percent. The higher values of thrust allow the achievement of higher speeds, increased lift-drag ratio, better climb performance, and permitted larger power cutbacks, resulting in lower community noise. Therefore, the initial thrust used for takeoffs in this study was 116.4 percent of normal rated takeoff thrust unless otherwise noted. Since the thrust-response characteristics were not known for this engine, various response times were simulated and evaluated as to the effects they have on the advanced operating procedures developed for community noise reduction as well as the effects on flight safety.

All computations were made for a standard day plus 10°C. Also, constant weights were used for takeoff (W = 3051 kN (686 000 lbf)) and approach and landing (W = 1745 kN (392 250 lbf)). No weight changes due to fuel consumption were considered. Current Federal Aviation Regulations were adhered to at all times throughout this simulation study, with the exception of some of those presented in reference 1. Some of the aircraft noise-certification procedures presented in reference 1 were not followed at all times in order to determine the benefits (i.e., noise reductions) that may be realized should these "rules" be changed. Specifically, the rules listed in reference 1 that were not always followed during the present study are:

(1) A constant takeoff configuration must be maintained throughout the takeoff-noise test, except the landing gear may be retracted.

(2) Takeoff power or thrust must be used from the start of takeoff roll to an altitude above the runway of at least 214 m (700 ft).

(3) Upon reaching an altitude of 214 m (700 ft) or greater, the takeoff power or thrust may not be reduced below that needed to maintain level flight with one engine inoperative or to maintain a 4-percent climb gradient, whichever power or thrust is greater.

(4) A steady approach speed must be established and maintained over the approach-measuring point.

(5) The approaches must be conducted with a steady glide angle of $3^{\circ} \pm 0.5^{\circ}$.

Noise characteristics of the simulated SCR concept at the three measuring stations prescribed in reference 1 and indicated in figure 8 were calculated for both takeoffs and landing approaches with the NASA aircraft noise prediction program (ANOPP) described in reference 9. Noise contours were also developed with the data output from this noise-prediction program.

Takeoffs were performed with rotation speeds from 172 to 200 knots of IAS, and the climb speeds varied from 211 to 250 knots of IAS. During these takeoffs, thrust reductions (cutbacks) were made as a function of distance from brake release and/or altitude. These thrust reductions were made manually as well as automatically. It should be mentioned that after the "final" thrust reduction was made (always prior to reaching the flyover noise-measuring point), the climb gradient was reduced to 0.04 ($\gamma \approx 2.3^{\circ}$).

Landing approaches were made at: (1) Constant speed for various constant glide angles, (2) constant speed for various segmented glide angles, and (3) decelerating speed for various constant glide angles. The glide angles varied from 3° to 6°, and the approach speeds varied from 250 to 158 knots of IAS.

The results of this study, derived with the aforementioned evaluation procedures, are primarily presented in the form of effective perceived noise level (EPNL) reductions as a function of piloting techniques used to perform takeoffs and landings with the simulated SCR transport concept. The significant results are reviewed in the following sections.

RESULTS AND DISCUSSION

The results of this study are discussed in terms of the previously stated objectives and are primarily presented in the form of effective perceived noise level (EPNL), as the piloting technique (operational procedure) varied during takeoffs and landings on the simulated SCR transport concept. The noise levels discussed pertain to jet noise only.

For clarity and completeness, some of the data presented in reference 7 are resubmitted in this paper.

Takeoffs

Takeoffs were performed with rotation speeds V_R from 172 to 200 knots of IAS, an angular-rotation rate $\dot{\theta}$ of 3°/sec, and "initial" rotation angles of attack α_{INT} from 4° to 8° (depending on the desired climb speed V_C). The α_{INT} as used here is the angle of attack to which the pilot rotates and maintains until V_2 is achieved.

<u>Determination of rotation speed</u>.- The procedures used to determine the minimum and maximum rotation speeds to be used in this simulation study are those given in reference 19. In general, the range of V_R used was selected from the V_1 information determined on the simulator and presented in figure 9. The V_1

concept was developed for civil air transport certification, and its intent is to provide the pilot sufficient information to decide whether to refuse or to continue the takeoff. If the pilot elects to refuse the takeoff, the total distance required for the maneuver (from brake release to V_1 to full stop) is called the accelerate-stop distance. If the pilot elects to continue the takeoff, the total distance required from brake release to V_1 to an altitude of 10.7 m (35.0 ft) is called the takeoff distance. (As can be seen from fig. 9, the intersection of the two curves (balanced field length) occurs at approximately 172 knots of IAS.) In addition, reference 19 states that the critical engine-inoperative takeoff distance for a rotation speed of 5 knots less than V_R must not exceed the corresponding critical engine-inoperative takeoff distance for the established V_R. Therefore, it can be seen from the takeoff-distance curve of figure 9 that the minimum "established" V_R should be no less than approximately 185 knots of IAS. However, for the present simulation program, a minimum $V_R = V_1 = 172$ knots of IAS (three-engine balanced field length) was chosen in order to get the maximum possible variable range for V_R and the corresponding V_c. From the accelerate-stop-distance curve in combination with the takeoff-distance curve of figure 9, the maximum V_R chosen to be used in this simulation study was 200 knots of IAS, because of tire speed limitations. Thus, the range of rotation speeds used in this study was from 172 to 200 knots of IAS, resulting in lift-off speeds from 193 to 215 knots of IAS.

Angular-rotation rate.- An angular-rotation rate $\dot{\theta}$ of approximately 3°/sec was used for all takeoffs. This value was selected by considering aft-fuselage scrape as well as pilot-passenger comfort. It was also noted that the nominal angular-rotation rate used by the pilots when flying the Concorde simulation (ref. 20) was approximately 2.8°/sec.

Initial rotation angle of attack.- The initial α selected for each takeoff varied depending upon the selected rotation speed and climb speed. For example, for a selected V_R of 172 knots of IAS and a climb speed of $V_2 + 10$ knots of IAS, the initial α used for the best climb performance was determined to be approximately 8°, whereas for a selected V_R of 200 knots of IAS and a V_c of 250 knots of IAS, the initial α used for the best performance was determined to be approximately 4°.

Minimum flyover noise during takeoff.- For simulated takeoff procedures with no power cutbacks, the flyover EPNL at the reference 1 measuring point was calculated to be approximately 118.0 dB, regardless of the selected rotation speed or the selected climb speed, and the sideline EPNL was calculated to be greater than 116.0 dB for all takeoffs.

The scheme used to determine a piloting technique that would result in acceptable noise levels for both flyover and sideline was to first define the minimum-flyover-noise procedure with no consideration for the sideline noise generated. Reference 1 states, in part, that: (1) Takeoff power or thrust must be used from the start of takeoff roll to an altitude of at least 214 m (700 ft) for airplanes with more than three engines; (2) upon reaching an altitude of 214 m, the power or thrust may not be reduced below that needed to maintain level flight with one engine inoperative or to maintain a 4-percent climb gradient, whichever power or thrust is greater; and (3) a speed of at least $V_2 + 10$ knots must be maintained throughout the takeoff-noise test. Therefore,

the first task was to determine the amount of allowable thrust cutback, and this is indicated in figure 10. For indicated airspeeds greater than approximately 240 knots, the four-engine, 4-percent climb-gradient criterion should be used, whereas the three-engine, zero climb-gradient criterion should be used for indicated airspeeds below 240 knots. For the present study, the four-engine, 4-percent climb-gradient criterion was used for all climb speeds considered since it was more beneficial at the lower climb speeds (V_C < 240 knots of IAS) and was almost as beneficial at the higher climb speeds (V_C > 240 knots of IAS). Therefore, the net thrust was reduced to 71 percent at the cutback point when the slowest climb speed was flown ($V_R = 172$ and $V_C = V_2 + 10 = 211$ knots of IAS), and was reduced to 58 percent at the cutback point when a climb speed of 250 knots of IAS was flown. (It should be noted that the maximum airspeed allowed below an altitude of 3048 m (10 000 ft) is 250 knots of IAS because of air traffic control considerations.)

The "ideal" cutback altitudes were then determined from the lowest V_R and V_C investigated (172 and 211 knots of IAS, respectively) as well as the highest V_R and V_C investigated (200 and 250 knots of IAS, respectively), and the results are presented in figure 11. Indications are that for $V_R = 172$ and $V_C = 211$ knots of IAS, the ideal cutback altitude, from the standpoint of EPNL, was approximately 400 m (1312 ft); for $V_R = 200$ and $V_C = 250$ knots of IAS, the ideal cutback altitude was approximately 290 m (951 ft). Figure 11 also indicates that the faster climb speed, which allowed more thrust cutback, was approximately 2.0-dB less noisy than the slower climb speed (EPNL of 107.7 dB compared with 109.6 dB), even though the cutback altitude was approximately 110 m (361 ft) lower. It should also be noted that the minimum flyover EPNL for the technique with $V_R = 200$ knots of IAS and $V_C = 250$ knots of IAS was slightly lower than the maximum level allowed (EPNL of 108.0 dB, ref. 1).

These two takeoff profiles are presented in figure 12. The piloting procedures used were: (1) Accelerate from brake release to $V_R = 172$ and 200 knots of IAS); (2) at V_R, rotate the airplane at an angular-rotation rate of 3°/sec to an angle of attack of 8° and 4° and maintain α until V_2 is achieved; (3) after attaining V_2, the pilot merely "flew" the takeoff-director commands, which in these cases commanded climb speeds of $V_2 + 10 = 211$ and 250 knots of IAS; and (4) upon attaining the designated "ideal" cutback altitudes (400 m (1312 ft) and 290 m (951 ft)), the copilot reduced the net thrust to 71 percent and 58 percent and the pilot simultaneously reduced the climb gradient to 0.04 in each instance. The results indicate that the airplane was at an altitude of 492 m (1614 ft) when it flew over the noise-measuring station (a distance of 6500 m (21 325 ft) from brake release) for the slower V_R and V_C compared with an altitude of 420 m (1378 ft) for the faster V_R and V_C. The calculated flyover perceived noise levels (PNL's) and effective perceived noise levels (EPNL's) are also presented in figure 12, and indicate that the maximum calculated PNL's for the slower and faster takeoffs were 110.8 dB and 109.6 dB, resulting in EPNL's of 109.6 dB and 107.7 dB. Therefore, it was concluded that the faster rotation and climb speeds were more beneficial from a noise standpoint, and thus the majority of the takeoffs made and discussed throughout the remainder of this paper pertain to rotation speeds of 200 knots of IAS and climb speeds of 250 knots of IAS.

Figure 13 indicates that for climb speeds greater than approximately 233 knots of IAS on a 4-percent climb gradient, less thrust is required to trim for $\delta_f = 10^{\circ}$ than for $\delta_f = 20^{\circ}$. For example, at $V_c = 250$ knots of IAS, 2-percent less thrust is required to trim for the $\delta_f = 10^{\circ}$ configuration than for the $\delta_f = 20^{\circ}$ configuration ($T_N = 56$ percent compared with $T_N = 58$ percent). Figure 14 presents the flyover EPNL differences due to raising the flaps to 10° (for $V_c > 233$ knots of IAS) and indicates that since the incremental EPNL was less than 1.0 dB for any cutback altitude, the configuration change would probably not be justified. (It should be noted that ref. 1 requires a constant configuration throughout the takeoff-noise test, with the exception of landing-gear retraction.)

During the generation of the flight profiles necessary to calculate the corresponding EPNL's shown in figures 11 and 14, it was found that the rate of thrust cutback and the rate of climb-gradient change were very important as to whether the desired climb speed was maintained. Therefore, instead of manually reducing the thrust to the specified level (depending upon the V_c and δ_f), the autothrottle was activated at various altitudes and, again, the climb gradient was reduced to 0.04. These results are presented in figure 15 and compared with the results for manual-throttle cutbacks. The results indicate that the use of the autothrottle reduces the EPNL approximately 1.0 dB for the "ideal" cutback altitude (290 m (951 ft)). The resulting flight profiles are presented in figure 16. Note that although the same approximate altitude (417 m (1368 ft)) was achieved at the flyover-noise-measuring station (6500 m (21 325 ft) from brake release), the calculated values for PNL and EPNL are somewhat different, even though both takeoffs were for the same configuration and the same takeoff procedures were used - with the exception of the method used to reduce the thrust at the designated altitude. The differences in the EPNL's were attributed to the differences in the thrust management. Note from the net-thrust trace that for the manual-cutback procedure, the copilot gradually reduced the thrust from T_{MAX} to 58 percent with no overshoot. However, when the thrust was reduced with the autothrottle, an overshoot in thrust resulted (T_N became as low as approximately 44 percent at one instance), and therefore the EPNL was lower at the measuring station due to the lower values of net thrust. Also note that the climb speed was maintained relatively constant at approximately 250 knots of IAS during both flights.

Obviously it will be necessary to use the minimum amount of thrust during takeoff in order to keep the sideline noise at a minimum. However, sufficient thrust must be used to keep the takeoff flyover EPNL at 110.0 dB or less in order to even consider using the present FAR trade-off capabilities. Therefore, takeoffs were performed for which only 100 percent of the thrust was used. Figure 17 presents the calculated flyover EPNL's against various cutback altitudes for initial values of thrust of 100 percent and 116.4 percent. The minimum flyover EPNL that was calculated was greater than 111.0 dB when 100 percent thrust was used for takeoff, regardless of the cutback altitude, compared with a minimum EPNL of less than 108.0 dB when maximum available thrust (116.4 percent) was used for takeoff. It was therefore concluded that an initial value of thrust greater than 100 percent must be used in order to achieve a flyover EPNL equal to or less than 110.0 dB. Furthermore, these results indicated that at some point during the early stages of the takeoff the thrust must be reduced below 100 percent in order to reduce the sideline EPNL being generated. Side-

line EPNL was greater than 110.0 dB even when only 100 percent thrust was used for takeoff. (As mentioned previously, the sideline EPNL was greater than 116.0 dB for the maximum-thrust takeoff.)

Summary of results pertaining to minimum flyover noise during takeoff.- With no consideration given to the sideline noise being generated, various takeoff procedures were used in an attempt to define the "best" piloting procedure that could be used in order to create the minimum effective perceived noise level at the flyover noise-measuring station of reference 1 (6500 m (21 235 ft) from brake release). The more significant results are as follows:

1. With no power cutbacks the flyover EPNL was approximately 118 dB, regardless of the rotation speed or climb speed.

2. For the noise-abatement takeoff procedures presently allowed by the Federal Aviation Regulations (ref. 1), the maximum allowed rotation speed and climb speed (V_R = 200 and V_c = 250 knots of IAS) were the most beneficial for creating the minimum noise at the designated flyover-noise-measuring station. This takeoff procedure with thrust reduction above an altitude of 214 m (700 ft) resulted in a flyover EPNL of 107.7 dB, which met the 108.0-dB requirement of reference 1.

3. Minor additional noise benefits could be realized by reducing the flap deflections from 20° to 10° for indicated airspeeds greater than approximately 233 knots.

4. Additional noise benefits were gained by activating the autothrottle rather than manual-throttle manipulations at the "ideal" cutback altitude.

The best advanced piloting procedure used during this study for minimum flyover noise, disregarding the sideline noise being generated, was as follows:

(1) With maximum available thrust (116.4 percent), accelerate the airplane from brake release to 200 knots of IAS.

(2) At V = 200 knots of IAS, rotate the airplane at an angular-rotation rate of 3°/sec to an angle of attack of 4°. Retract the landing gear after lift-off.

(3) Maintain $\alpha \approx 4^{\circ}$ until V_2 is achieved; V_2 is defined as the aircraft velocity at a hypothetical obstacle (h_{LG} = 10.7 m (35.0 ft)).

(4) Accelerate the airplane from V_2 to a climb speed of 250 knots of IAS. (V_c = 250 knots of IAS is the maximum speed allowed below an altitude of 3048 m (10 000 ft)).

(5) Prior to achieving V_c = 250 knots, reduce the flap deflections from 20° to 10°.

(6) At an altitude of 290 m (951 ft), activate the autothrottle and reduce the climb gradient to 0.04.

This takeoff procedure resulted in a flyover EPNL of 106.7 dB, which is 1.3 dB less than the maximum allowed EPNL of 108.0 dB (ref. 1).

<u>Sideline-noise considerations during takeoffs</u>.- In an attempt to determine a takeoff procedure that would allow the use of the aforementioned noise trade-offs between the flyover, sideline, and approach EPNL's and thus meet the 108.0-dB requirements of reference 1, various piloting procedures were used during simulated takeoffs. Because it was determined earlier that the most advantageous procedure for flyover noise was to rotate as late as possible and climb as fast as possible, the majority of the "sideline-noise" takeoffs were made for which V_R was 200 knots and V_C was 250 knots of IAS.

Figure 18 indicates the sideline EPNL's calculated for a standard procedure takeoff (i.e., no FAR rules broken). Note that the sideline EPNL approaches 108.0 dB approximately 1800 m (5906 ft) after brake release and has exceeded 110.0 dB prior to lift-off (X = 2496 m (8189 ft)). The maximum sideline EPNL is 114.8 dB. Therefore some degree of power cutback is required prior to lift-off in order to keep the sideline EPNL equal to or less than 110.0 dB, the maximum level that would allow the use of the aforementioned noise-trade-off criteria.

Various piloting techniques were used in an attempt to determine the "optimum" takeoff procedure insofar as the minimum sideline and flyover jet noise were concerned. Power cutbacks were made at various distances from brake release as well as at various altitudes in an attempt to keep the sideline noise to a minimum. Then a "final" power cutback was made (sometimes autothrottle was used) and the climb gradient was reduced to 0.04 prior to reaching the flyover-noise measuring station in order to keep the flyover EPNL to a minimum. The objective was to keep the sideline EPNL equal to or less than 110.0 dB and at the same time keep the flyover EPNL equal to or less than 109.0 dB.

The profile for a typical takeoff with "advanced" procedures is presented in figure 19. The piloting procedures used were as follows:

(1) With the flaps set at 20° and with maximum available thrust, accelerate the airplane from brake release to $V = 200$ knots of IAS.

(2) At $V = 200$ knots of IAS, rotate at $\dot{\theta} \approx 3°/\text{sec}$ to an angle of attack of approximately 4°. At $X \approx 2225$ m (7300 ft) and $V \approx 208$ knots of IAS, reduce the net thrust to 110 percent.

(3) After lift-off ($X \approx 2500$ m (8202 ft) and $V \approx 217$ knots of IAS), raise the landing gear and accelerate to V_2 while maintaining $\alpha \approx 4°$.

(4) At V_2 (approximately 235 knots of IAS), reduce the net thrust to 90 percent, and by following the commands of the takeoff director, accelerate to 250 knots of IAS. Prior to $V_C = 250$ knots, raise the flaps from 20° to 10°.

(5) Continue the climbout at $V_C = 250$ knots of IAS. At an altitude of approximately 185 m (607 ft), activate the autothrottle and reduce the climb gradient to 0.04.

With data obtained from this simulation study, an optimization technique described in reference 21 has been shown to identify a takeoff strategy comparable to advanced procedure I presented in figure 19 of this report.

Figure 20 indicates that the sideline EPNL exceeds 108.0 dB at $X \approx 2700$ m (8858 ft) and that the maximum sideline EPNL is 109.8 dB at $X \approx 3350$ m (10 991 ft). Note that the maximum sideline EPNL for this advanced-procedure takeoff is approximately 5.0 dB lower than that calculated for the standard-procedure takeoff. The flight profile of this advanced-procedure takeoff (fig. 19) shows that an altitude of 254 m (833 ft) was attained at the flyover-noise measuring station and that the calculated flyover EPNL was 108.1 dB. It should also be mentioned that the autothrottle caused the net thrust to overshoot the allowed level of 56 percent. (T_N actually became as low as 38 percent at one point and was less than 56 percent for approximately 5 sec, which corresponded to the time just prior to and immediately after flying over the flyover-noise-measuring station.) It is believed that although this large, temporary thrust reduction exceeded the allowed limit (fig. 13), flight safety would not be jeopardized in that, for example, should an engine fail during the time the autothrottle had driven the thrust to this "unacceptably" low level, the autothrottle would very quickly command sufficient thrust on the remaining three engines to maintain an indicated airspeed of 250 knots. It is therefore believed that this piloting procedure is a realistic and safe takeoff procedure if autothrottle is used, and that by utilizing the aforementioned trade-off criteria, the traded EPNL can be kept below 108.0 dB at the designated measuring stations, assuming the approach EPNL is no more than 105.0 dB.

Effects of modifying the VSCE engine for maximum coannular-nozzle acoustic benefit.- It was determined during the simulation program that very large cutbacks in thrust were possible in order to reduce the flyover noise during takeoff. It was realized at that time that the design of the simulated VSCE was such that the coannular-nozzle acoustic reduction was lost for thrust settings below approximately 60 percent. Therefore, in general, the flyover jet-noise levels discussed previously would be somewhat lower if the coannular-nozzle noise-alleviation effects could be maintained for thrust settings lower than 60 percent. Reference 22 presents the method used in the ANOPP (ref. 9) for predicting coannular-jet noise based on a test-data correlation formulated in reference 23.

The engine designers were asked to investigate the impact of retaining the coannular-nozzle acoustic benefit at cutback thrust settings approaching 40 percent. These data were supplied for use in the simulation study with the warning that design changes to the "current" VSCE might be required, with potential impact on weight and performance. Nevertheless, these "modified" engine data were used to repeat some of the advanced-procedure takeoffs, and the results indicated that although the engine modification did not improve the maximum sideline EPNL, the flyover EPNL was reduced approximately 2.0 dB. For example, repeating the takeoff procedure indicated in figure 19 but with the modified VSCE reduced the flyover jet noise from 108.1 dB to 106.0 dB. (The maximum sideline EPNL remained at 109.8 dB.)

A new takeoff procedure was developed for use with the modified engine in an attempt to further reduce the sideline-noise level (allowing the flyover EPNL

to increase above 106.0 dB) and thus reduce the traded-noise level. (The noise trade-offs allowed by ref. 1 will be discussed later in this paper.) The takeoff profile for the piloting procedure developed is presented in figure 21. The procedure was as follows:

(1) With the flaps set at 20° and with maximum available thrust, accelerate the airplane from brake release to $V = 200$ knots of IAS.

(2) At $V = 200$ knots of IAS, rotate at $\dot{\theta} \approx 3°/\text{sec}$ to an initial angle of attack of approximately 4°.

(3) After lift-off ($X \approx 2496$ m (8188 ft) and $V \approx 218$ knots of IAS), raise the landing gear and accelerate to V_2 while maintaining $\alpha \approx 4°$.

(4) At V_2 (approximately 235 knots of IAS), reduce the net thrust to 75 percent and, by following the commands of the takeoff director, accelerate to 250 knots of IAS. Prior to attaining $V_c = 250$ knots of IAS, raise the flaps from 20° to 10°.

(5) Continue the climbout at $V_c = 250$ knots. At an altitude of approximately 152 m (500 ft), activate the autothrottle and reduce the climb gradient to 0.04.

Figure 21 indicates that the flyover EPNL was 106.8 dB; the maximum sideline EPNL was 108.2 dB at $X \approx 2743$ m (9000 ft). Thus the traded EPNL could be as low as 106.2 dB. An interesting point to be noted here is that the maximum sideline noise occurred prior to reaching the end of the runway.

Keeping the sideline noise on the airport property.- As stated previously in this paper, some of the aircraft noise-certification procedures given in reference 1 were not followed at all times during the present study in order to determine the benefits (noise reductions) that may be realized should these "rules" be changed. The rules that were not always followed are presented in the "Tests and Procedures" section in detail but, briefly, the rules that were not adhered to during the advanced-procedure takeoff designated advanced procedure II are: (1) Thrust cutbacks were made prior to achieving an altitude of 214 m (700 ft); (2) the airplane configuration was changed during the noise test in that the flap deflections did not remain constant; and (3) at the "final" cutback station the autothrottle commanded values of thrust which, for a brief period of time, were less than those presently allowed.

Figure 22 shows the effect of various takeoff procedures on the effective perceived noise calculated at the reference 1 sideline-noise-measuring station. Note that for either of the advanced procedures presented the sideline EPNL's were below the allowable level of 108.0 dB at distances from brake release that might be considered to be "off the airport property." (The sideline EPNL calculated for the advanced procedure II takeoff did not exceed 108.0 dB past the end of the 3505-m (11 500-ft) runway.) It was therefore hypothesized that if the present noise-certification rules were changed so that the sideline EPNL was not restricted to a maximum of 108.0 dB on airport properties, advanced procedures could be developed that would further reduce the flyover noise as well as the overall traded noise. (Note that the present sideline-noise limit of 108.0 dB

does not apply prior to airplane lift-off.) Such a relaxation of the sideline noise "restriction area" would also allow the development of takeoff procedures that would not require violating all of the three aforementioned takeoff-noise-certification rules. For example, with the piloting procedure designated advanced procedure II (fig. 21) but without any configuration change (the flaps remain at 20°) and without allowing the autothrottle to drive the net thrust below the allowable limit of 58 percent, the maximum sideline EPNL was again calculated to be 108.2 dB at $X \approx 2743$ m (9000 ft) and the flyover EPNL was 109.5 dB. (Note that the flyover EPNL increased from 106.8 dB to 109.5 dB.) However, if no restriction on sideline noise was considered prior to reaching a distance from brake release of 4420 m (14 500 ft) (914 m (3000 ft) beyond the end of the runway), the flyover EPNL could be reduced from 109.5 dB to 107.2 dB, although the sideline EPNL would be well above 108.0 dB prior to this point. (See fig. 23.) This could be accomplished by breaking only one of the aforementioned rules of reference 1; that is, the only rule that was not followed was that thrust cutback was made prior to achieving an altitude of 214 m (700 ft). The only difference in the piloting procedures used for these two takeoffs was the altitude at which the first thrust cutback was made. (The final cutback was made at the same distance from brake release during both takeoffs.) A maximum sideline EPNL of 108.2 dB was calculated when the first thrust cutback was made at V_2 (h_{LG} = 10.7 m (35.0 ft)), whereas a maximum sideline EPNL of 112.8 dB was calculated when the first thrust cutback was made at $h \approx 61$ m (200 ft).

It was concluded then that the simulated SCR transport concept with the modified variable-stream-control engines can meet the 108.0-dB takeoff EPNL standards of reference 1 through the use of advanced operating procedures. The advanced operating procedures involve violating three of the noise-certification rules: (1) Thrust cutbacks are made prior to achieving an altitude of 214 m (700 ft); (2) a constant configuration is not maintained in that the flaps are raised from 20° to 10° during the early stages of the takeoff; and (3) for a brief period of time following the "final" thrust cutback, thrust levels will be below those presently allowed. It was also concluded, however, that only the rule violation listed as (1) would be necessary to meet the takeoff noise standards if the sideline-noise restriction area did not include the distance from brake release to 4420 m (14 500 ft), which might be considered to be "airport property" on many of the international airports of today.

Landing Approaches

Reference 1 states that a constant airspeed and configuration must be maintained on a constant glide angle of $3^\circ \pm 0.5^\circ$ throughout the landing-approach noise test. However, all of these "rules" were varied in an attempt to determine the noise benefits that could be realized should they be changed. During this simulation study, landing approaches were made at: (1) Constant speed at various constant glide angles; (2) constant speed at various segmented glide angles; and (3) decelerating speed at various constant glide angles. (Decelerating speed for various segmented glide angles was not studied.) The glide angles varied from 3° to 6° and the approach speeds varied from 250 to 158 knots of IAS.

Reference 1 landing-approach test procedure.- The landing-approach EPNL calculated for a constant indicated airspeed of 158 knots, a constant configuration, and a constant glide angle of 3° was 101.5 dB at the reference 1 measuring station (2000 m (6562 ft) from the threshold, on the extended centerline of the runway; see fig. 8). This was sufficiently low to allow the use of the aforementioned noise-trade-off rules of reference 1.

Constant speed for various constant glide angles.- Landing approaches were made with a constant configuration and a constant indicated airspeed of 158 knots for various constant glide angles. In addition to the "standard" 3° glide angle, glide angles of 4°, 5°, and 6° were used and the resulting EPNL's calculated for the reference 1 measuring station were 96.8, 92.3, and 86.9 dB. Figure 24 presents the calculated EPNL's at various distances from the runway threshold for the various simulated glide angles. Although the calculated EPNL for the 6° glide-angle approach was 14.6 dB less than the EPNL calculated for the 3° glide angle (at the ref. 1 measuring station), the rate of sink for the 6° approach was considered by the pilot to be too high at the lower altitudes. For the 6° approach and an indicated airspeed of 158 knots, the rate of sink was approximately 525 m/min (1723 ft/min). A pilot prefers to have a rate of sink no greater than approximately 305 m/min (1000 ft/min) at altitudes below 152 m (500 ft). The rate of sink for a glide angle of only 4° also would be greater than 305 m/min. It may therefore be hypothesized that a two-segment approach would alleviate the unacceptably high rate of sink at altitudes below 152 m and at the same time reduce the approach noise.

Constant speed at various segmented glide angles.- Landing approaches were made with a constant configuration and a constant indicated airspeed of 158 knots for various segmented glide angles. Two-segment approaches were made for which the first segment was 6°, 5°, or 4° and the second segment was 3° in each instance. Various altitudes were also used for the "transition" maneuver. It was determined that although the two-segment approach may be beneficial for reducing the noise-contour area, the noise calculated for the reference 1 measuring station would not be reduced since the transition altitude would have to be too high in order not to exceed the maximum desired rate of sink below 152 m (500 ft). Figure 25 shows a comparison of the calculated landing-approach EPNL's at various distances from the runway threshold for a two-segment ($6^{\circ}/3^{\circ}$) and a single-segment (3°) approach. Note that the two-segment-approach EPNL at the reference 1 measuring station is higher than that for the 3° approach. This higher noise level at the measuring station is due to the increase in thrust required to transition from the 6° glide angle to the 3° glide angle and maintain indicated airspeed at 158 knots. (See fig. 26.) As might be expected, however, figure 25 shows that the two-segment approach is much less noisy at distances from the runway threshold greater than the glide-angle transition point.

The effects of various procedures for takeoffs and landings on the calculated noise contours will be discussed later in this paper.

Decelerating speeds for various constant glide angles.- The decelerating approaches simulated during the present study had initial indicated airspeeds of 200 and 250 knots, with the final airspeed being 158 knots in each instance. The decelerations were initiated at the outer marker (approximately 8149 m

(26 735 ft) from the runway threshold) and were completed at the reference 1 measuring station. It should be noted that speed brakes were sometimes used during the decelerating approaches.

The calculated EPNL's at the measuring station for the decelerating approaches were somewhat lower than EPNL's for constant-speed approaches regardless of the initial airspeed. Figure 27 presents a comparison of the calculated EPNL's for a constant-speed approach and two decelerating approaches for a constant glide angle of 3°. When the airplane was decelerated from 200 to 158 knots of IAS the calculated EPNL at the reference 1 measuring station was approximately 1.0 dB less than when the airplane was flown at a constant speed of 158 knots; the decelerating approach which initiated at 250 knots of IAS was approximately 3.0 dB less noisy than the constant 158-knot approach. It may also be noted in figure 27 that the approach EPNL calculated for the two decelerating-speed approaches at distances from the runway threshold greater than the reference 1 measuring station were similar and that both were as much as 12.0 dB less than that for the constant-speed approach at some points. This indicates that the areas of the landing-approach noise contours would be appreciably reduced by flying a decelerating approach. In addition, a comparison of figures 24 and 27 indicates that the calculated EPNL's at distances from the runway threshold greater than the reference 1 measuring station are similar for a constant-speed, 5° glide-angle approach (fig. 24) and a decelerating-speed, 3° glide-angle approach (fig. 27).

Summary of results pertaining to landing-approach noise tests.- It was determined that the calculated landing-approach EPNL for the simulated SCR transport concept with the present-day test procedures from reference 1 is 101.5 dB, which is well below the maximum allowed level of 108.0 dB. It was also found that substantial noise-reduction benefits could be gained by increasing the glide angle and flying a constant airspeed, although glide angles greater than approximately 3° resulted in unacceptably high rates of sink below an altitude of 152 m (500 ft). Minor noise-reduction benefits at the reference 1 measuring station were realized by flying decelerating approaches. It must be noted, however, that although the decelerating approaches produced only minor benefits at the reference 1 measuring station (2000 m (6562 ft) short of the runway threshold), decelerating approaches should be very beneficial for reducing the area of the approach-noise contours. The area of the approach-noise contours could also be reduced by flying two-segment approaches, although the two-segment approaches flown did not reduce the effective perceived noise levels at the reference 1 measuring station.

It is also concluded from these results that these calculated noise levels underscore the need for examining noise sources other than jet-exhaust noise such as engine-fan, compressor, turbine, combustor, and airframe noise. For example, during the landing approach the engine-fan noise of a variable-stream-control engine may be greater than the engine jet noise associated with the relatively low jet velocities. (Thrust settings near flight idle were used on the landing approaches during the present SCR simulation study.) To reduce the fan-inlet and fan-exhaust noise levels, the inlet and exhaust ducts could be acoustically treated to absorb the peak-tone noise levels. However, the inlet duct for supersonic aircraft configurations is generally of a complex nature and not readily adaptable for installation of acoustic liners.

Another means of reducing the inlet peak-tone noise, however, is to choke the inlet throat during the landing approach. The static data from reference 24 show that as the inlet-throat Mach number was increased from approximately 0.6 to 1.0 on the F-111 and the YF-12 aircraft, the peak-tone noise of the fan at the fundamental blade passage frequency was reduced approximately 25.0 dB along the forward inlet axis and approximately 20.0 dB along a 50° angle from the forward inlet axis. Additional acoustic inlet tests (refs. 25 and 26) showed similar noise-level reductions. It is therefore reasonable to expect that the fan noise of a VSCE could be reduced 10.0 to 15.0 dB prior to propagating to the observer position, if the variable-geometry inlet is designed with sufficient local-flow Mach number range. This feature is a natural part-power operational characteristic of this type of inlet because the required inlet variable geometry is also necessary during cruise flight. However, as stated in reference 8, full benefit of this procedure will depend on whether the engine can be operated without the need for opening inlet blow-in doors.

Noise Trade-offs

The FAR noise standards (ref. 1) dictate a maximum stage 2 EPNL limit of 108.0 dB at the approach-, sideline-, and flyover-noise-measuring stations for airplanes having maximum gross weights of 2669 kN (600 000 lbf) or more. (See fig. 8 for location of noise-measuring stations.) However, reference 1 allows trade-offs between the approach-, sideline-, and flyover-noise levels if: (1) The sum of the EPNL exceedance is not greater than 3 dB; (2) no EPNL exceedance is greater than 2 dB; and (3) the EPNL exceedances are completely offset by reductions at other required measuring stations. Therefore, these noise-trade-off rules were applied to the noise levels calculated during the previously discussed takeoffs and landings performed using various piloting (operational) procedures.

<u>Takeoffs and landings with standard procedures</u>.- The term "standard procedure," as used in this paper, applies to the piloting procedure used that abides by all present-day Federal Air Regulations, and in particular the noise-certification regulations of reference 1. The minimum flyover EPNL obtained with standard procedures was 107.7 dB (fig. 12) and the sideline EPNL produced was 114.8 dB (fig. 18). Therefore, since the approach EPNL was 101.5 dB (fig. 24), the traded EPNL is 112.8 dB. It should be mentioned that this traded-noise level could be reduced by using less initial thrust for takeoff, thereby reducing the sideline noise to some extent and allowing the flyover noise to become greater. For example, if 100 percent thrust were used for takeoff as opposed to 116.4 percent, the flyover EPNL would increase to 111.7 dB and the sideline EPNL would decrease to 112.3 dB, producing a traded EPNL of 110.5 dB. However, the traded EPNL for either procedure is still well above the allowed 108.0 dB.

<u>Advanced procedures used for takeoff</u>.- The term advanced procedure, as used in this paper, applies to the piloting procedure used that did not abide by the recommended noise test procedures for airplane certification in reference 1. Advanced piloting procedures were developed in an attempt to decrease the sideline noise generated during takeoff. These procedures were discussed previously and results are presented in figure 19. The takeoff EPNL's from these proce-

dures were calculated to be 108.1 dB for flyover, 109.8 dB for sideline, and 101.5 dB for approach, resulting in a traded EPNL of 107.8 dB. Therefore, by using these advanced procedures, the traded EPNL was reduced by 5.0 dB. It should also be noted that this traded EPNL (107.8 dB) meets the noise-limit requirements of 108.0 dB.

<u>Advanced procedures and modified VSCE used for takeoff</u>.- As discussed previously, the simulated VSCE was modified in order to retain the coannular-nozzle acoustic benefit at much lower thrust settings than the basic engine design. Also, the use of this modified engine reduced the flyover EPNL from 108.1 dB to 106.0 dB when the same piloting procedures were used for takeoff as those described as advanced procedure I. However, the modified engine did not improve the sideline EPNL in the area of maximum sideline noise; therefore the traded EPNL would remain at 107.8 dB.

A new takeoff procedure was developed for use with the modified engine in an attempt to further reduce the sideline EPNL (allowing the flyover EPNL to increase above 106.0 dB) and thus reduce the traded EPNL below 107.8 dB. The piloting procedure used, which was discussed previously and is designated advanced procedure II (fig. 21), produced a flyover EPNL of 106.8 dB and a maximum sideline EPNL of 108.2 dB, resulting in a traded EPNL of 106.2 dB.

Advanced procedure III was developed for two primary reasons: (1) To show that if the present noise-certification rules were changed so that the sideline noise is not restricted on airport properties, the flyover noise as well as the overall traded noise could be reduced; and (2) to show that number (1) could be accomplished by violating only one noise-certification test procedure, as opposed to three noise-certification-procedure violations required for advanced procedures I and II. It can be seen from figure 23 that for advanced procedure III, the sideline EPNL at $X = 4572$ m (15 000 ft) was 107.0 dB and the flyover EPNL was 107.2 dB, resulting in a traded EPNL of 105.6 dB.

The histogram presented in figure 28 summarizes the traded EPNL's calculated for the various conditions and test procedures flown during the present study. By using advanced takeoff procedures, the traded EPNL for the subject SCR transport concept can be reduced by approximately 5.0 dB. It is therefore concluded from these results that by using advanced takeoff procedures, the simulated SCR transport with the modified VSCE's readily meets the stage 2 noise-certification standards of reference 1.

Noise Contours

Of the various ways of presenting aircraft-noise results, a meaningful method is the noise contour (footprint). The noise contour represents the boundary of the area enclosing effective perceived noise levels equal to or greater than the specified contour level. Noise contours were determined for some of the takeoffs and landings simulated during the present study in order to indicate the noise-reduction advantages of using operational procedures other than standard. Although several EPNL contours are indicated for each takeoff and landing procedure, the 108.0-dB and the 90.0-dB EPNL's were selected for discussion of takeoffs and landings, respectively. The total areas within

the contours were determined for each case. The areas presented for the takeoff contours were measured for the boundary described from the point of lift-off (a distance of approximately 2500 m (8202 ft) from brake release) to the boundary closure, whereas the areas presented for the landing-approach contours were measured for the boundary described from the runway threshold to the boundary closure. Again, it should be noted that the noise values discussed represent jet-noise only, as predicted by the NASA ANOPP program.

Takeoffs.- The calculated takeoff-noise contours with the respective net-thrust and altitude time histories are presented in figure 29, and the areas of the 108.0-dB EPNL contours for each takeoff are presented in table I. The advanced procedures basically satisfied the maximum-allowed noise requirements of reference 1. The areas of the 108.0-dB contours are also smaller for the advanced procedures than for the standard, particularly in terms of percentage. For example, the area of contour for advanced procedure II is 50 percent less than that for the standard procedure.

The traded EPNL's (fig. 28) for these two takeoffs indicate that the advanced-procedure traded noise was approximately 6.6 dB less. Although this traded-noise difference suggests a distinct advantage of using the advanced procedure for noise reduction, it is believed that the contour-area differences are much more meaningful.

Landing approaches.- The landing-approach-noise contours for EPNL's of 100.0 dB, 95.0 dB, and 90.0 dB with respective net-thrust and altitude time histories are presented in figure 30, and the areas of these contours are presented in table II. These data indicate that the 6° approach was much less noisy than any of the other procedures simulated, but as discussed previously, this landing-approach procedure is not acceptable from a safety standpoint due to the high rate of sink at altitudes below 152 m (500 ft). Table II also indicates that the noise-contour areas for the constant-speed (V = 158 knots of IAS), two-segment approach ($6^{\circ}/3^{\circ}$ glide angle) were appreciably less than the constant-speed (V = 158 knots of IAS), single-segment (3° glide angle) approach. (See also figs. 30(a) and 30(e).) (The 90.0-dB EPNL contour area for the $6^{\circ}/3^{\circ}$ approach was only 37 percent of that calculated for the single-segment (3°) approach.) As discussed previously, the approach EPNL at the reference 1 measuring station (2000 m (6562 ft) from the threshold on the extended centerline of the runway) was higher for the two-segment approach, and therefore did not indicate the noise-reduction advantage of the two-segment approach.

The noise contours for the decelerating-approach techniques simulated are presented in figures 30(c) and 30(d), and the corresponding contour areas are indicated in table II. The decelerating-approach-noise contour areas are approximately one-third of the constant-speed-approach-noise contour areas, and the 90.0-dB EPNL contour area for the deceleration from 250 to 158 knots of IAS approach is only 70 percent of that for the constant-speed, two-segment approach. (See table II.) It is therefore concluded that the best landing-approach procedure for the simulated SCR transport would be a decelerating approach on a constant 3° glide angle.

Comparison of single-event contour areas.- The 95.0-dB EPNL single-event contour areas for some present-day subsonic jet transports are presented in figure 31 and compared with the 95.0-dB EPNL single-event contour area for the simulated SCR transport. These single-event contour areas are the total land area exposed to EPNL's greater than 95.0 dB during one takeoff and one landing of the specific aircraft. The single-event contour area indicated for the SCR transport was determined by using the advanced-procedure takeoff designated advanced procedure II and a standard 3°, constant-speed landing-approach procedure. (In this instance, the complete area enclosed by the 95.0-dB EPNL contour was used.) The single-event contour areas indicated for the subsonic jet transports were taken from reference 27.

As can be seen from figure 31, the 95.0-dB EPNL single-event contour area of the simulated SCR transport compares favorably with the "narrow-bodied" large subsonic jet transports but compares very unfavorably with the "wide-bodied" subsonic jet transports, even though advanced operating procedures were used for takeoff on the SCR transport. The fact that the 95.0-dB EPNL single-event contour area for the simulated SCR transport was larger than for the wide-bodied transport was not disconcerting, but the degree of difference was unexpected. For example, as shown in figure 32, the takeoff- and approach-noise levels at the reference 1 measuring stations for the SCR transport using the advanced procedure II for takeoff compared favorably to the noise levels indicated for the 747-200B airplane. And, although the sideline noise of the SCR transport compared unfavorably with the 747-200B, the large differences in the single-event contour areas (fig. 32) might not be expected. It is therefore concluded that caution must be exercised when comparing contour areas from different studies for different aircraft. For example, reference 28 indicates that a comparison of two aircraft-noise contour prediction programs (neither being the ANOPP program used in the present study) produced single-event noise-contour areas that differed by as much as 500 percent for some aircraft. Reference 28 gives the principal cause of these contour-area differences as being the differences between the noise data bases in the two computer programs, and listed other causes as being the differences in methods of accounting for excess ground attenuation and differences in specification of engine thrust and flight speed along a flight path.

Most published noise-contour area information is presented with the takeoff noise and the approach noise combined as a single event, and therefore much of the area of a specific noise contour would lie within the airport boundary and would not represent a true change, or difference, in community noise annoyance. For example, the 95.0-dB EPNL single-event contour area indicated for the SCR transport (fig. 31) is 82.78 km^2 (31.96 mi^2). However, if the area included within the 95.0-dB EPNL contour between a distance 2000 m (6562 ft) short of the runway threshold to the distance required for lift-off ($X \approx 2500$ m (8202 ft), which are the approach and sideline measuring stations of reference 1, were not considered, the 95.0-dB EPNL single-event contour area would be reduced by 13.99 km^2 (5.40 mi^2). Furthermore, the 95.0-dB EPNL single-event contour area would be reduced by 23.83 km^2 (9.20 mi^2) if the area from a distance 2000 m short of the runway threshold to a distance 2000 m beyond the end of the runway is not considered. This area would lie within most major airport boundaries and would probably not be considered part of the airport community.

It must be noted that the FAR EPNL requirement (ref. 1) for an aircraft of the weight and class of the subject SCR transport is 108.0 dB at the measuring stations indicated in figure 8, and that the 95.0-dB EPNL single-event contour area comparisons were made only because that was the estimated data available for the subsonic jet transports. That is, if it had been the intent of the present study to develop operating procedures which would produce the minimum area of the 95.0-dB EPNL single-event contour, thereby ignoring the reference 1 measuring-station noise requirements, operating procedures other than those proposed in this paper would be required. It is therefore concluded that the advanced operating procedures presented in this paper are the best procedures for the subject SCR transport concept in order to meet the noise requirements of reference 1 but may not be the best procedures for producing the minimum area of any specific EPNL single-event contour.

In addition to using advanced operating procedures to minimize the EPNL single-event contour areas, it must be pointed out that other methods could also be used, not only to reduce the contour areas but also to reduce further the EPNL's at the prescribed measuring stations. As discussed previously, the VSCE used during this simulation program has coannular nozzles for improved jet-noise characteristics. As stated in reference 8, other possible methods for engine-noise reduction would be the use of "mechanical jet-noise suppressors" and the "fluid-shield technique." (In the fluid-, or heat-, shield technique a layer of heated low-velocity air is introduced around the lower half of the jet exhaust stream which reflects and refracts the noise upwards, thus shielding the observer on the ground.) This technique could be applied in addition to the coannular-nozzle technique and/or the mechanical-suppressor technique to provide even further noise reductions. It is also believed that the noise levels and contours discussed in this paper are conservative in that the ANOPP program does not account for any jet-noise shielding between engines - that is, the jet exhaust from one engine shields the sideline noise from another engine or engines.

Flight Safety

The major difference in the present study and other such studies is that this investigation was performed with a piloted, moving-base simulator in order to determine if a pilot with average skills could perform the task of flying various suggested noise-abatement procedures during takeoff and landing without compromising flight safety. The advanced takeoff procedures developed for the subject SCR transport involved violating some of the current FAA noise-certification test conditions (ref. 1) in order to meet the required noise levels. (No violations were required to meet the required noise levels during landing approach.) The three violations were as follows:

(1) Reference 1 requires that takeoff power or thrust be used from the start of takeoff roll to at least an altitude of 214 m (700 ft) for airplanes with more than three turbojet engines. During the present simulation program, thrust reductions were required at altitudes below 214 m in order to meet the takeoff sideline-noise requirement.

(2) Reference 1 states that upon reaching an altitude of 214 m (700 ft), the power or thrust may not be reduced below that needed to maintain level flight with one engine inoperative, or to maintain a 4-percent climb gradient, whichever power or thrust is greater. During the present simulation program, it was determined that larger temporary thrust reductions reduced the flyover noise at the flyover-noise measuring station and that the climb speed could still be maintained.

(3) Reference 1 states that a constant takeoff configuration must be maintained throughout the takeoff-noise test, except the landing gear may be retracted. It was determined during this simulation program that additional noise reduction could be achieved by raising the flaps from 20° to 10° for indicated speeds greater than 233 knots.

Of these three rule violations, number (1) is of primary importance. That is, only minor noise-reduction benefits were realized by violating the rules listed as numbers (2) and (3).

Critical engine failure.- It must be shown that violating the aforementioned FAA rules does not jeopardize flight safety. To demonstrate this, the advanced-procedure takeoffs were repeatedly performed and an outboard engine was failed at various locations during the takeoff. The test pilot felt that the most critical stage of the takeoff was immediately after lift-off. Therefore, one location included during the engine-failure takeoffs was the point immediately following the thrust cutback made upon attaining V_2 (altitude of 10.7 m (35.0 ft)); this time history is presented in figure 33. After the number 4 engine (outboard engine on right wing) was failed, the pilot advanced the thrust on the remaining three engines, attempted to maintain the wings level and the heading constant, and continued to accelerate to $V_c = 250$ knots of IAS. As indicated in figure 33, the wings were kept within $\pm 1^{\circ}$ of being level and the heading was maintained within approximately 2°.

The pilot commented that the aforementioned advanced takeoff procedures posed no safety problems. He stated that above an indicated airspeed of approximately 230 knots, instead of declaring an engine-failure an emergency situation, the pilot could safely choose to continue to follow the noise-abatement procedure because of the excess thrust available on the simulated airplane.

Engine response.- The transient-response times of the simulated variable-stream-control engines (VSCE) used in the present study were approximately $t = 4.8$ sec for acceleration from flight idle to maximum and $t = 3.4$ sec for deceleration from maximum to flight idle. During the course of the present simulation study, response times (unpublished) were predicted for this VSCE that were considerably longer (slower) than those being used on the simulator. These slower engine-response times were therefore used as inputs to the SCR simulation and evaluated by the test pilot as to the effects they may have on flight safety when using advanced operating procedures for community noise reduction. (The corresponding slower engine-response times for full acceleration and full deceleration were 14.0 sec and 8.5 sec.)

During the takeoff and climb tests with the slower engine-response times, there was little noticeable degradation in performance with four engines operating and more than adequate performance when the number 4 engine was failed. Full power on the remaining engines was added approximately 2 sec after the number 4 engine failed, and good acceleration was maintained and the rate of climb was never less than 457 m/min (1500 ft/min). Heading was maintained within approximately 1°, and no problems were evident resulting from the longer engine-response times for the advanced-procedure takeoff.

During the approach tests, a go-around was initiated for each approach so that the airplane did not go lower than a minimum altitude of 61 m (200 ft). With the fast-responding engines, advancing the throttles produced rapid thrust response. As soon as full thrust was commanded, the acceleration was such that a positive climb gradient could be achieved so rapidly that very little altitude was needed to arrest the approach rate of descent and establish a positive rate of climb. Even losing the number 4 engine only degraded the performance slightly. With the slower responding engines (four operating), slightly more time and altitude were needed to arrest the approach rate of descent, accelerate, and achieve a good positive climb. The performance of the slower responding four-engine go-around was very similar to the faster responding three-engine go-around; approximately 15 m (50 ft) of lead altitude were needed to preclude decending below the 61-m (200-ft) minimum altitude. Losing the number 4 engine with the slower response times necessitated more time and altitude to arrest the rate of descent, accelerate, and climb. The pitch-attitude change had to be delayed somewhat to allow for the slower thrust response with three engines (to maintain airspeed), but it was considered to be representative of the present-day jet-transport thrust response and was quite satisfactory. Approximately 23 m (75 ft) of altitude was needed to perform the go-around. Only approximately 2° of heading change was noted and no problems in any areas were encountered.

These simulator tests indicated that even the slower engine response times posed no safety problems for the advanced operating procedures developed during this study.

CONCLUDING REMARKS

The piloted-simulation study was conducted with the AST-105-1 supersonic cruise research (SCR) transport concept to determine: (1) Advanced takeoff and landing procedures for which the Federal Aviation Regulations (FAR) noise-level requirements could be met; (2) whether a pilot with average skills could perform the task of flying the suggested procedures without compromising flight safety; (3) the degree of automation required for the advanced procedures; and (4) the pilot information displays required for the advanced procedures. This paper summarizes the results of this study which support the following major conclusions.

The use of the current FAR test procedures for aircraft noise certification produced the following results: The landing approach effective perceived noise level (EPNL) was 101.5 dB, the flyover EPNL was 107.7 dB, and the sideline EPNL was 114.8 dB.

Advanced takeoff procedures were developed that involved violating three of the current FAR noise-test conditions. These violations involved thrust cutbacks at altitudes below 214 m (700 ft), thrust cutbacks to levels below those presently allowed, and configuration changes other than raising the landing gear. Under the current FAR test conditions with these three exceptions, the calculated effective perceived noise levels for flyover and sideline were 108.1 dB and 109.8 dB.

The basic variable-stream-control engine (VSCE) used in this study was modified in order to retain the coannular-nozzle acoustic benefit at thrust levels approaching 40 percent. With this engine modification, the advanced takeoff procedure was also modified in an attempt to reduce the takeoff EPNL's below the presently allowed 108.0 dB. With this "updated" takeoff procedure and modified engine, the flyover EPNL was calculated to be 106.8 dB and the sideline EPNL was 108.2 dB.

Through the use of current FAR noise-trade-off rules, it was determined that the traded EPNL was 110.5 dB when using current FAR noise-certification test conditions, compared with a traded EPNL of 106.2 dB when advanced takeoff procedures and the modified VSCE were used. This is a traded-noise reduction of approximately 4.3 dB.

During the landing-approach work it was determined that the standard FAR landing-approach (constant configuration, constant airspeed, and constant 3° glide angle) EPNL was 101.5 dB. It was also determined that: (1) Increased glide angles significantly reduced the noise at the FAR measuring station and reduced the approach noise-contour areas, but produced unacceptably high rates of sink (greater than 305 m/min (1000 ft/min)) at altitudes below 152 m (500 ft); (2) two-segment approaches, with a final segment of 3°, produced higher noise levels at the FAR measuring station but smaller noise-contour areas; and (3) decelerating approaches on a 3° glide angle produced lower noise levels at the FAR measuring station and the smallest approach noise-contour areas.

The advanced operating procedures developed in this simulation study are the best procedures for the subject supersonic cruise research transport in order to meet the current noise standards, but may not be the best procedures for producing the minimum area for any specific effective perceived noise level single-event contour.

The advanced takeoff and approach procedures developed and evaluated during this study also did not compromise flight safety.

The subject SCR transport concept, with the augmented variable-stream-control engines modified to maintain the coannular-nozzle acoustic benefit at thrust levels approaching 40 percent, can meet the current noise standards if the current noise-certification test conditions are modified in such a manner to allow maximum performance utilization of the aircraft without jeopardizing flight safety.

It was further concluded that the automation of some of the aircraft functions reduced the pilot work load when performing the advanced procedure takeoffs and landings, and that very simple piloting displays seemed to be adequate for the task.

Langley Research Center
National Aeronautics and Space Administration
Hampton, VA 23665
September 23, 1980

REFERENCES

1. Noise Standards: Aircraft Type and Airworthiness Certification. FAR Pt. 36, FAA, June 1974.

2. Final Environmental Impact Statement Noise Regulation and Type Certification Alternatives for Civil Supersonic Aircraft. FAA, U.S. Dept. Transp., June 1978.

3. Zalovcik, John A.: Effect of Thrust and Altitude in Steep Approaches on Ground Track Noise. NASA TN D-4241, 1967.

4. Schwind, G. K.; Morrison, J. A.; Nylen, W. E.; and Anderson, E. B.: Operational Flight Evaluation of the Two-Segment Approach for Use in Airline Service. NASA CR-2515, 1975.

5. Denery, D. G.; White, K. C.; and Drinkwater, F. J., III: Resume of the Status and Benefits of the Two-Segment Approach and Its Applicability to the Jet Transport Fleet. AIAA Paper No. 74-978, Aug. 1974.

6. Foster, John D.; and Lasagna, Paul L.: Flight-Test Measurement of the Noise Reduction of a Jet Transport Delayed Flap Approach Procedure. NASA TM X-73172, 1976.

7. Grantham, William D.; and Smith, Paul M.: Development of SCR Aircraft Takeoff and Landing Procedures for Community Noise Abatement and Their Impact on Flight Safety. Supersonic Cruise Research '79 - Part 1, NASA CP-2108, 1980, pp. 299-333.

8. Driver, Cornelius; and Maglieri, Domenic J.: Some Unique Characteristics of Supersonic Cruise Vehicles and Their Impact on Airport Community Noise. AIAA-80-0857, May 1980.

9. Raney, John P.: Noise Prediction Technology for CTOL Aircraft. NASA TM-78700, 1978.

10. Baber, Hal T., Jr.; and Swanson, E. E.: Advanced Supersonic Technology Concept AST-100 Characteristics Developed in a Baseline-Update Study. NASA TM X-72815, 1976.

11. Baber, Hal T., Jr.: Characteristics of the Advanced Supersonic Technology AST-105-1 Configured for Transpacific Range With Pratt and Whitney Aircraft Variable Stream Control Engines. NASA TM-78818, 1979.

12. Coe, Paul L., Jr.; Smith, Paul M.; and Parlett, Lysle P.: Low-Speed Wind Tunnel Investigation of an Advanced Supersonic Cruise Arrow-Wing Configuration. NASA TM-74043, 1977.

13. Smith, Paul M.: Low-Speed Aerodynamic Characteristics From Wind-Tunnel Tests of a Large-Scale Advanced Arrow-Wing Supersonic-Cruise Transport Concept. NASA CR-145280, 1978.

14. Wrenn, G. A.; McCullers, L. A.; and Newsom, J. R.: Structural and Aeroelastic Studies of a Supersonic Arrow Wing Configuration. NASA CR-145325, 1978.

15. Coe, Paul L., Jr.; and Thomas, James L.: Theoretical and Experimental Investigation of Ground Induced Effects for a Low-Aspect-Ratio Highly Swept Arrow-Wing Configuration. NASA TM-80041, 1979.

16. Freeman, Delma C., Jr.: Low Subsonic Flight and Force Investigation of a Supersonic Transport Model With a Highly Swept Arrow Wing. NASA TN D-3887, 1967.

17. USAF Stability and Control Datcom. Contracts AF33(616)-6460 and F33615-76-C-3061, McDonnell Douglas Corp., Oct. 1960. (Revised Apr. 1978.)

18. Martin, D. J., Jr.: A Digital Program for Motion Washout on Langley's Six-Degree-of-Freedom Motion Simulator. NASA CR-145219, 1977.

19. Airworthiness Standards. Transport Category Airplanes. FAR Pt. 25, FAA, June 1974.

20. Tomlinson, B. N.; and Wilcock, T.: A Piloted Simulation of the Take-off of a Supersonic Transport Aircraft, With and Without a Take-off Director. R. & M. No. 3594, British A.R.C., 1969.

21. Padula, S. L.: Prediction of Noise Constrained Optimum Takeoff Procedures. AIAA-80-1055, June 1980.

22. Russell, James W.: A Method for Predicting the Noise Levels of Coannular Jets With Inverted Velocity Profiles. NASA CR-3176, 1979.

23. Pao, S. Paul: A Correlation of Mixing Noise From Coannular Jets With Inverted Flow Profiles. NASA TP-1301, 1979.

24. Wright, B. R.; Clauss, J. S.; Averett, B. T.; Oatway, T. P.; Hays, A. P.; and Sakata, I. F.: Supersonic Cruise Vehicle Technology Assessment Study of an Over/Under Engine Concept - Volume I. NASA CR-159003, 1978.

25. Putman, Terrill W.; and Smith, Ronald H.: XB-70 Compressor-Noise Reduction and Propulsion-System Performance for Choked Inlet Flow. NASA TN D-5692, 1970.

26. Cawthorn, Jimmy M.; Morris, Garland J.; and Hayes, Clyde: Measurement of Performance, Inlet Flow Characteristics, and Radiated Noise for a Turbojet Engine Having Choked Inlet Flow. NASA TN D-3929, 1967.

27. Williams, Louis J.: An Analysis Method for Assessing the Impact of Aircraft Noise Reduction Options. NASA TM X-62276, 1973.

28. Chapkis, Robert L.; Blankenship, Gary L.; and Marsh, Alan H.: Comparison of Aircraft Noise-Contour Prediction Programs. AIAA-80-1057, June 1980.

TABLE I.- EFFECT OF PILOTING PROCEDURE ON TAKEOFF NOISE

[Jet noise only]

Takeoff procedure	VSCE	EPNL at reference 1 measuring station, dB				EPNL contour, dB	Area of contour (a)	
		Flyover	Sideline	Standard	Traded		km^2	mi^2
No cutback	Basic	118.4	116.3	101.5	116.4	108.0 110.0	41.78 25.90	16.13 10.00
Standard (ref. 1)	Basic	107.7	114.8	101.5	112.8	108.0 110.0	8.00 6.42	3.09 2.48
Advanced procedure I	Basic	108.1	109.8	101.5	107.8	108.0 110.0	6.58 4.14	2.54 1.60
Advanced procedure I	Modified	106.0	109.8	101.5	107.8	108.0 110.0	5.34 4.07	2.06 1.57
Advanced procedure II	Modified	106.8	108.2	101.5	106.2	108.0 110.0	4.04 3.16	1.56 1.22
Advanced procedure III	Modified	107.2	107.0	101.5	105.6	108.0 110.0	4.90 4.01	1.89 1.55
Advanced procedure IV	Modified	109.5	108.2	101.5	107.5	108.0 110.0	4.45 3.32	1.72 1.28

[a]Measured from lift-off to contour closure.

TABLE II.- EFFECT OF PILOTING PROCEDURE ON APPROACH NOISE

[Jet noise only]

Approach procedure	Glide angle, deg	Indicated airspeed, knots	EPNL, dB (a)	EPNL contour, dB	Area of contour (b)	
					km^2	mi^2
Standard (ref. 1)	3	158	101.5	90.0	9.95	3.84
				95.0	3.76	1.45
				100.0	.44	.17
Steep	6	158	86.9	90.0	.16	.06
				95.0	.003	.0012
				100.0	-----	------
Two segment	6/3	158	102.0	90.0	3.73	1.44
				95.0	1.84	.71
				100.0	.34	.13
Decelerating	3	200/158	100.8	90.0	3.44	1.33
				95.0	2.02	.78
				100.0	1.04	.40
Decelerating	3	250/158	98.8	90.0	2.67	1.01
				95.0	1.48	.57
				100.0	.16	.06

[a]Measured at FAR-36 measuring station.
[b]Measured from runway threshold to contour closure.

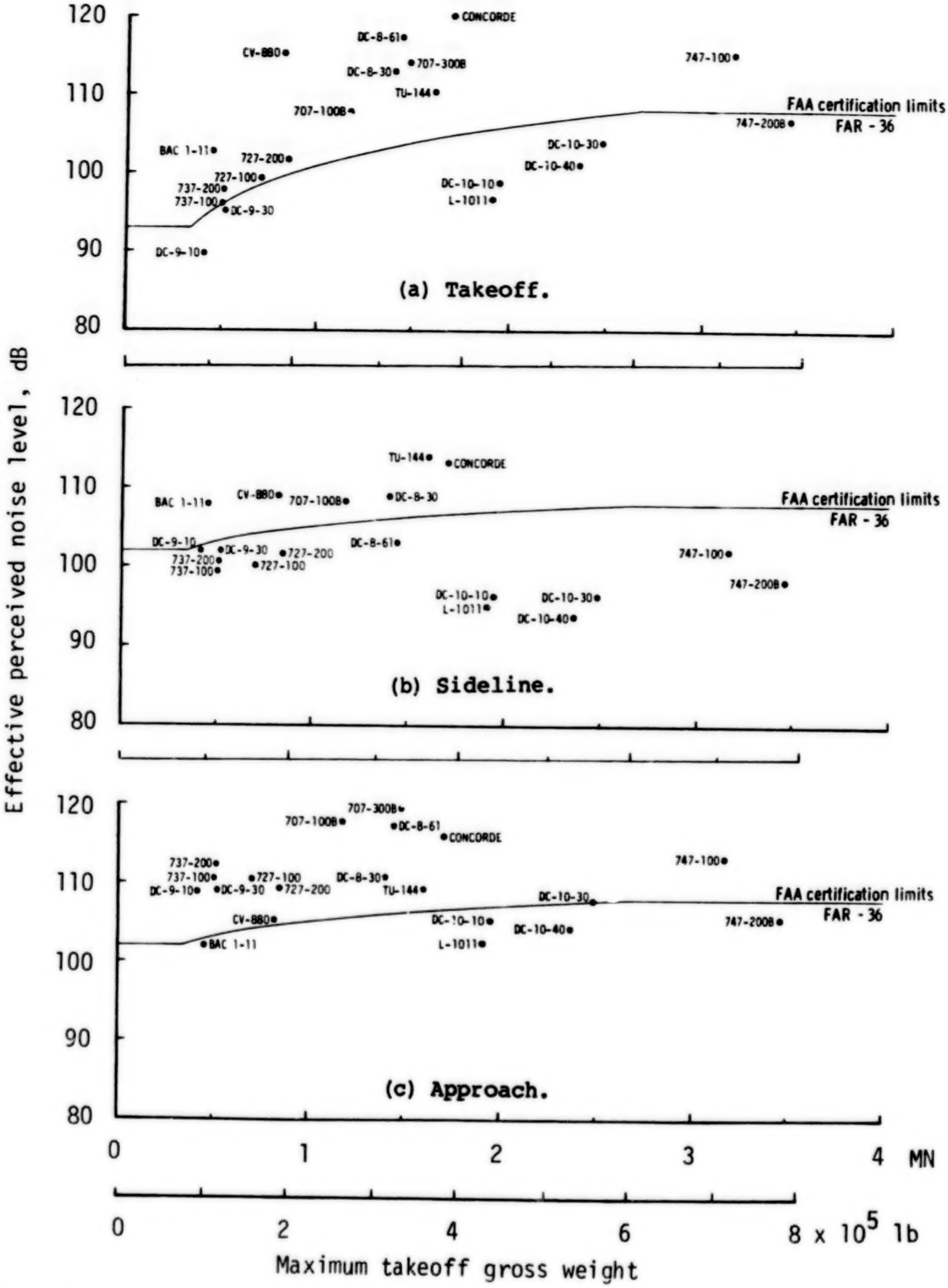

Figure 1.- Noise limits of FAR (ref. 1) as function of aircraft weight, with some present-day aircraft noise levels indicated. (Noise levels indicated for various aircraft were taken from ref. 2.)

Four VSCE-516 engines

8334 km (4500 n. mi.) range

Cruise at M = 2.62

273 passengers

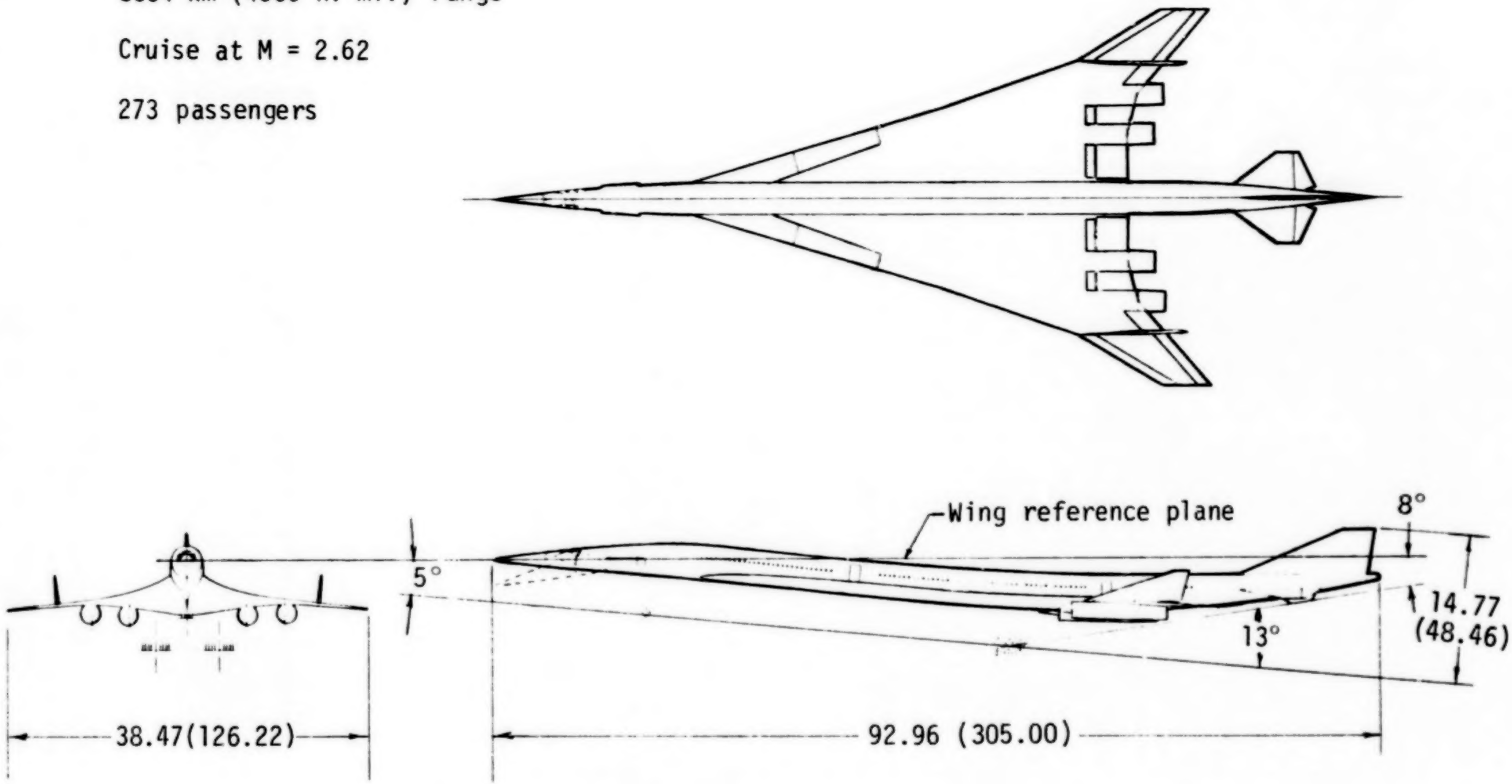

Figure 2.- Three-view sketch of simulated SCR transport concept (AST-105-1). All linear dimensions in meters (feet).

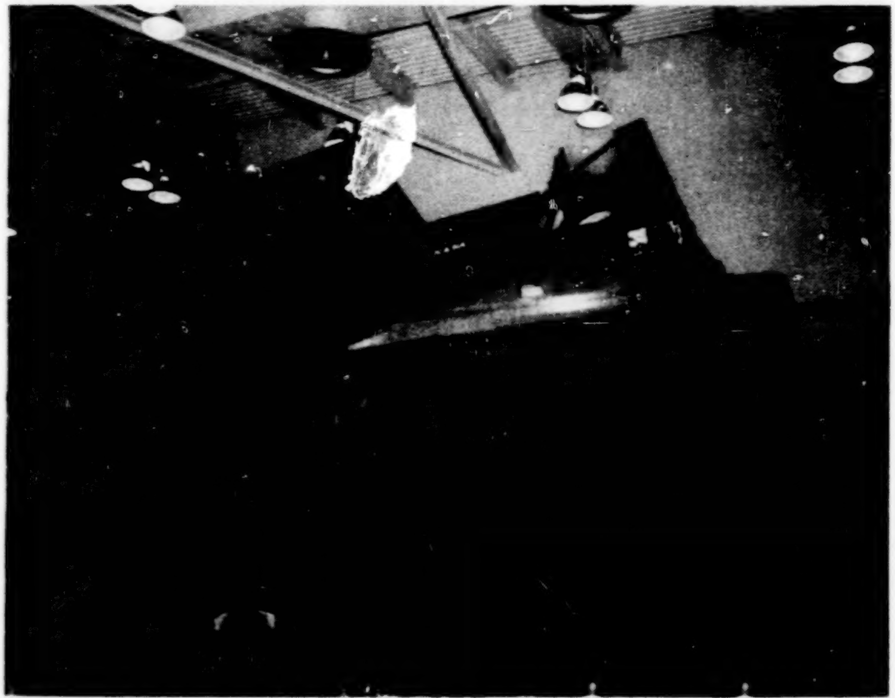

L-75-7570

(a) Langley Visual/Motion Simulator.

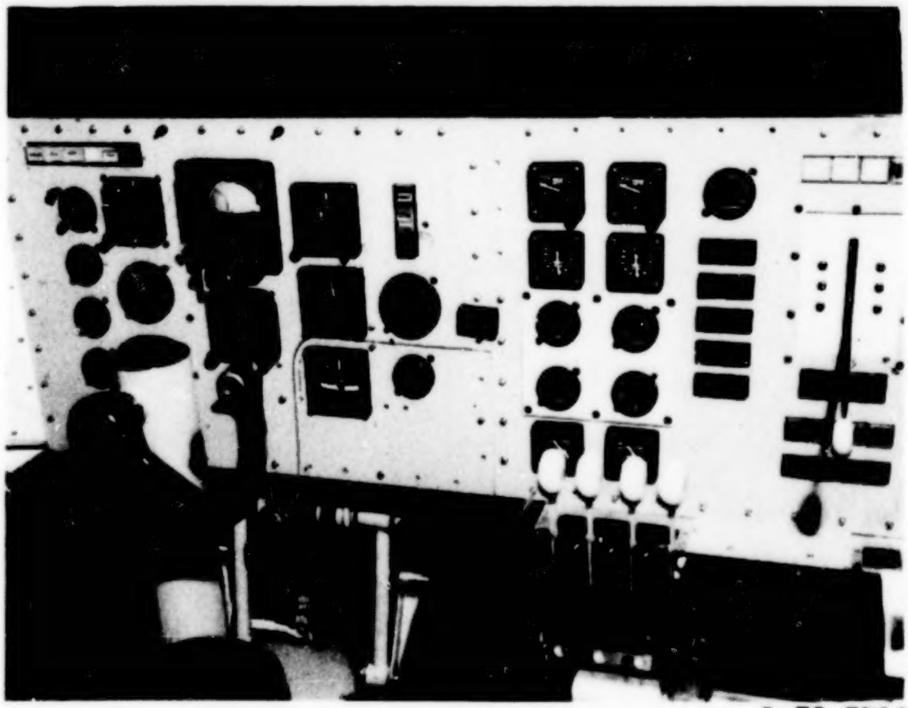

L-78-7794

(b) Instrument panel.

Figure 3.- Langley Visual/Mction Simulator and instrument panel display.

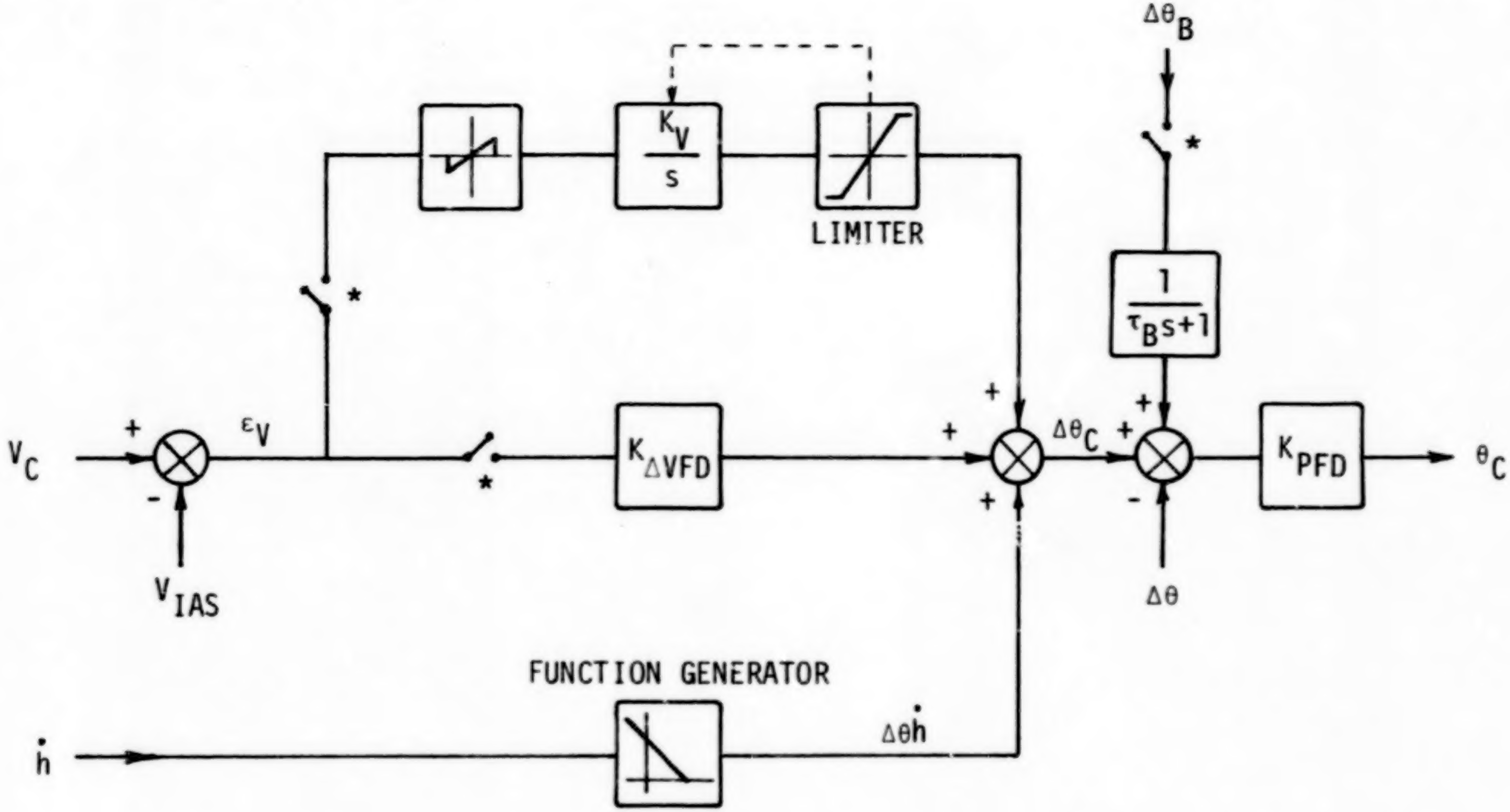

* Switches activated at predetermined capture velocity.

Figure 4.- Block diagram of takeoff director.

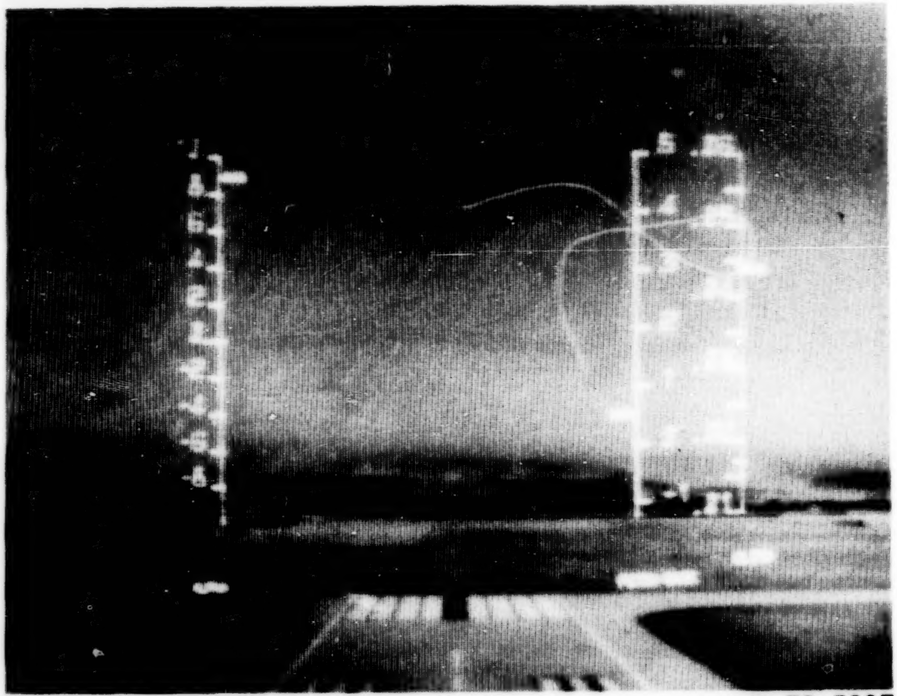

L-79-5997

(a) Head-up display superimposed on airport scene at takeoff.

L-79-5999

(b) Approach scene.

Figure 5.- View of airport scene as seen by pilot.

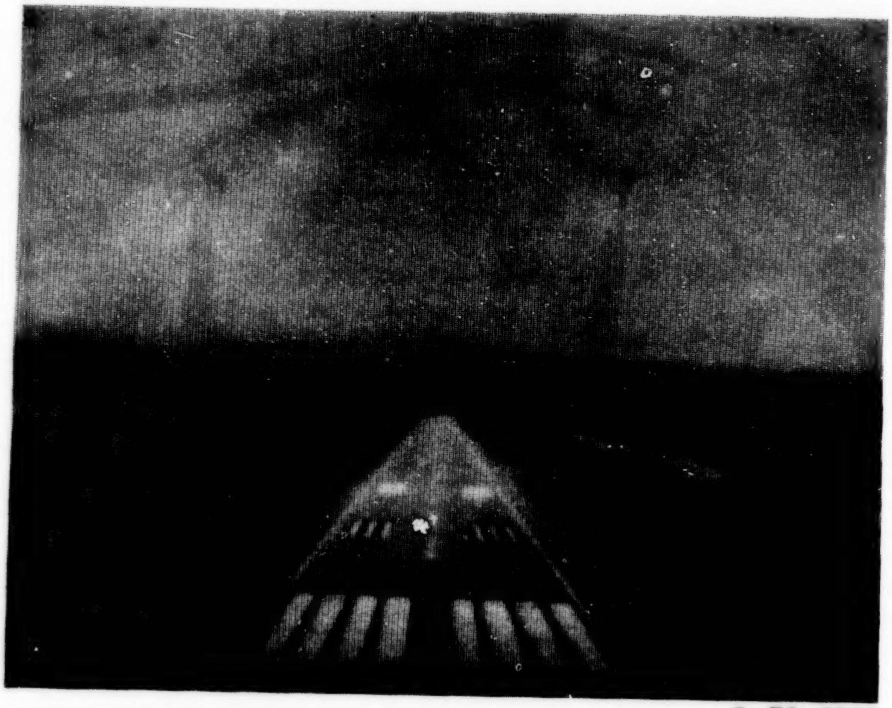

L-79-6000

(c) Landing scene.

Figure 5.- Concluded.

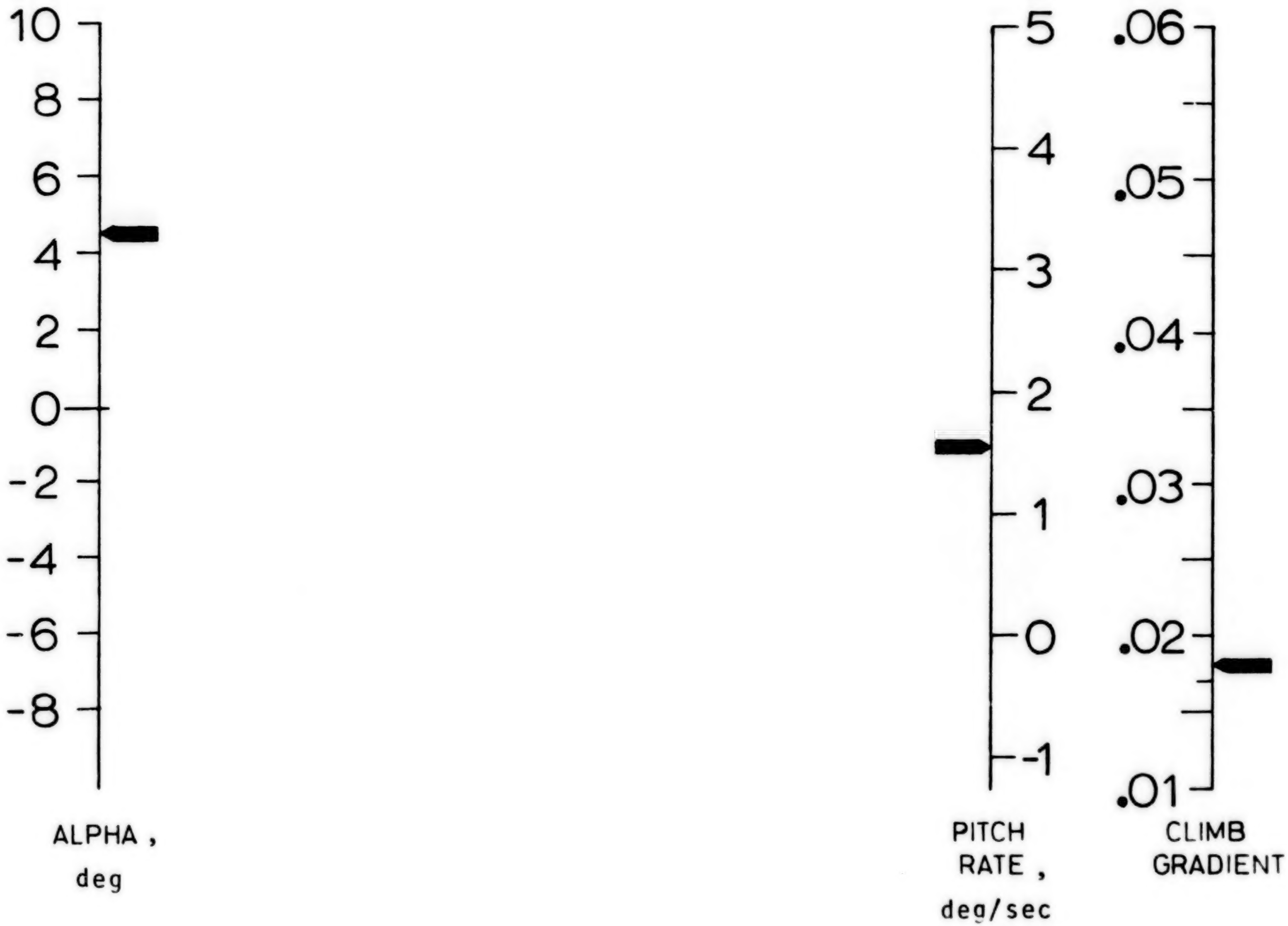

Figure 6.- Sketch of head-up display used during takeoff and climb.

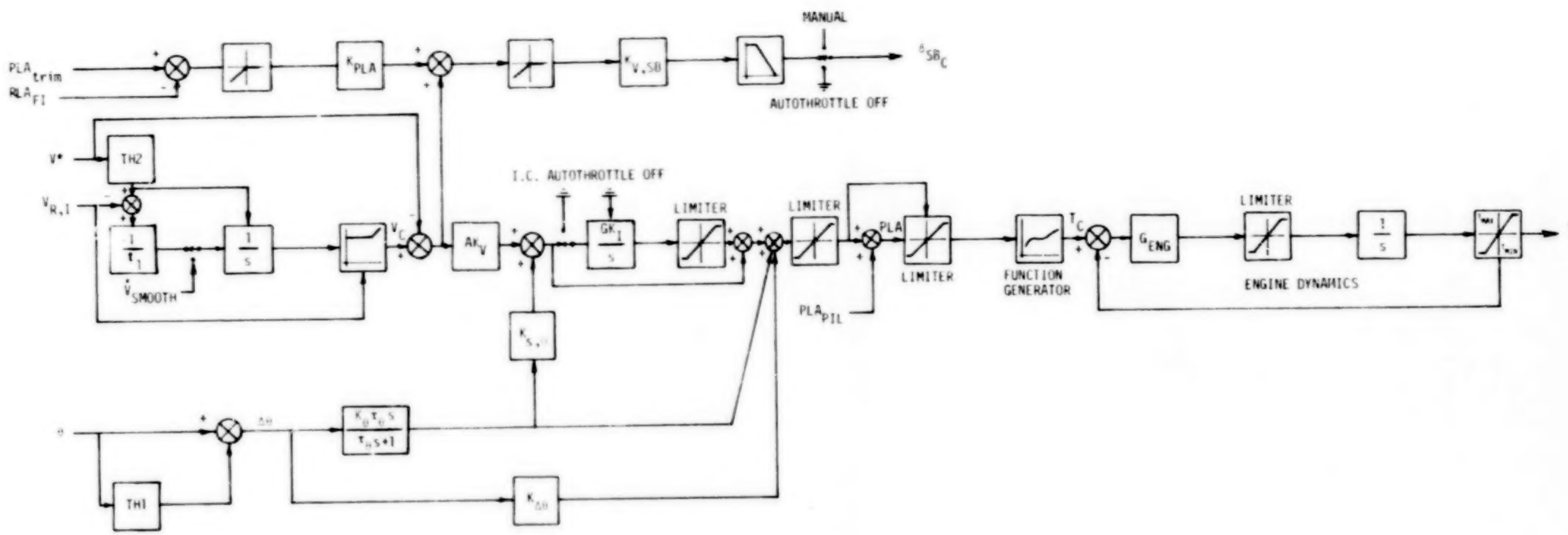

Figure 7.- Block diagram of autothrottle.

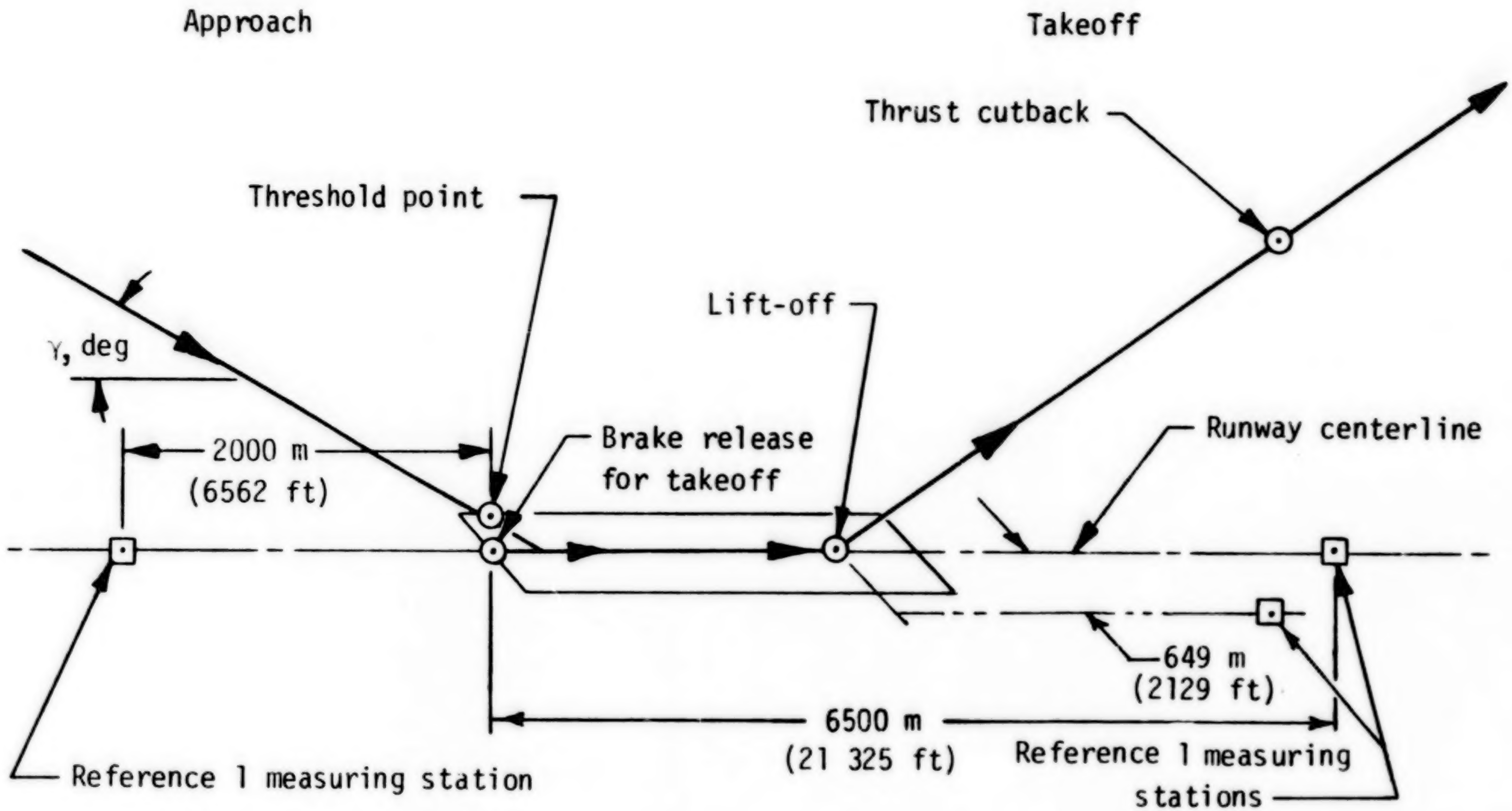

Figure 8.- Noise measurement locations for takeoff and landing. (Sideline noise is measured where noise level after lift-off is greatest.)

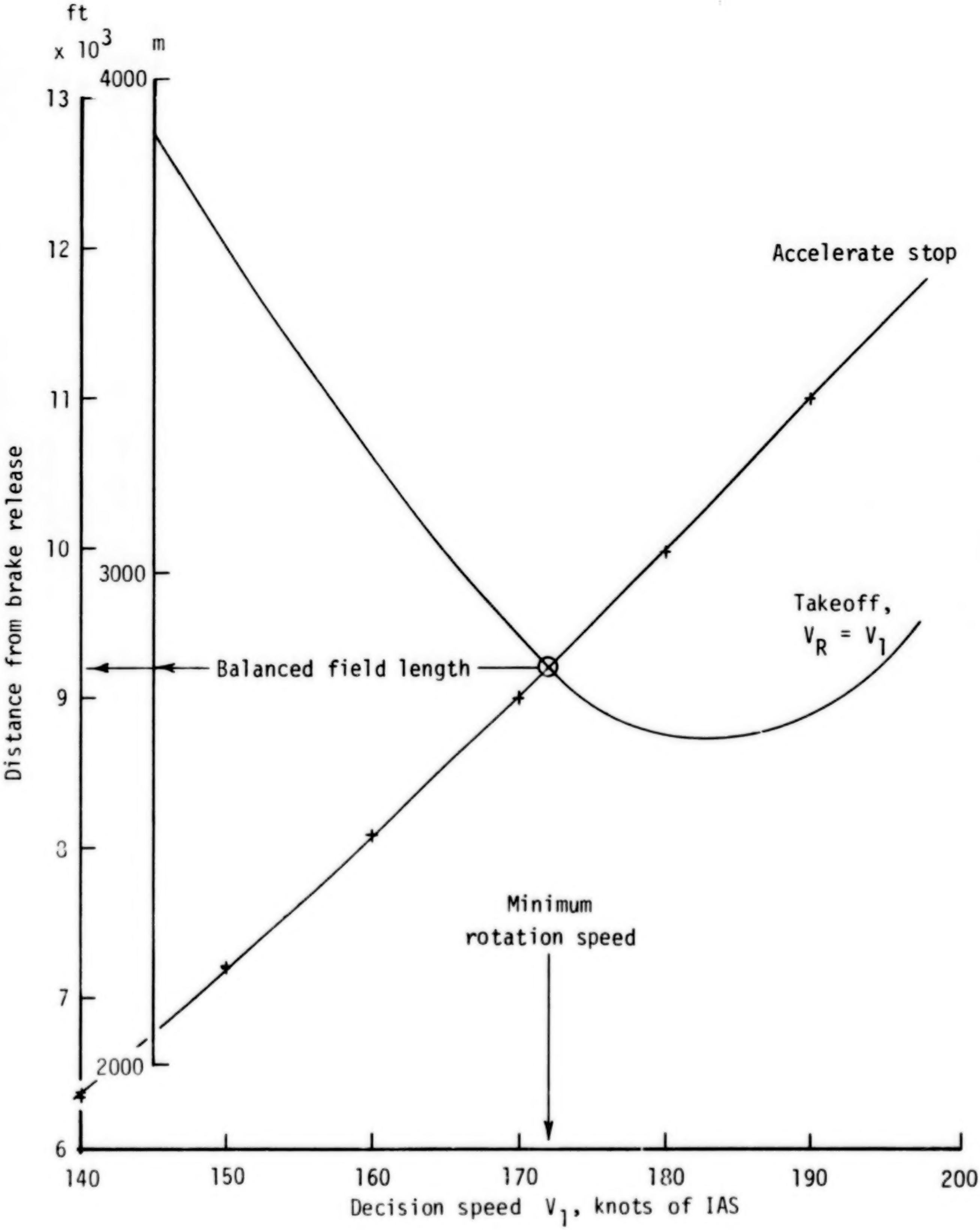

Figure 9.- Indication of three-engine balanced field length at takeoff weight.

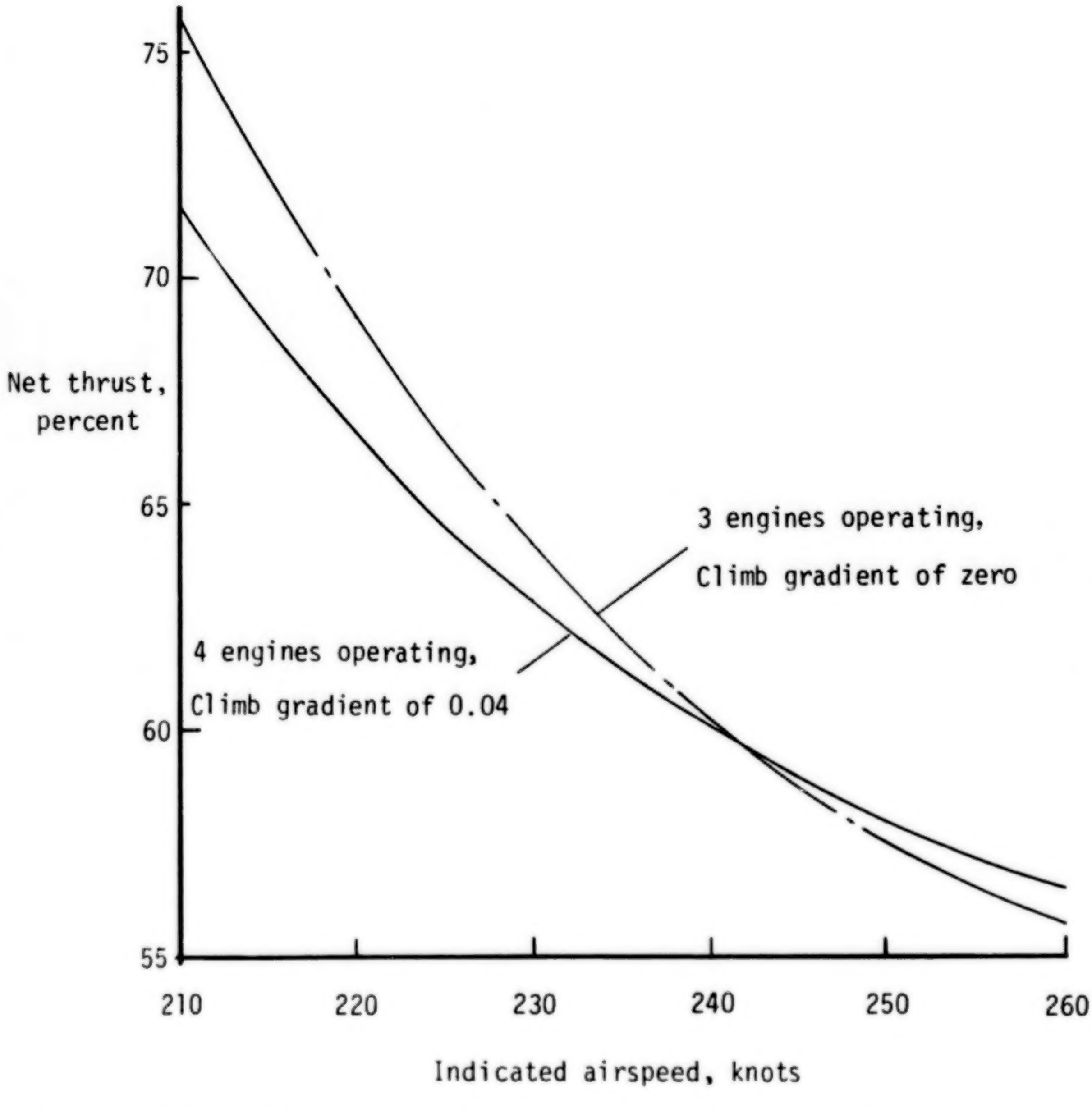

Figure 10.- Trimmed net thrust used in establishment of allowable thrust cutback.

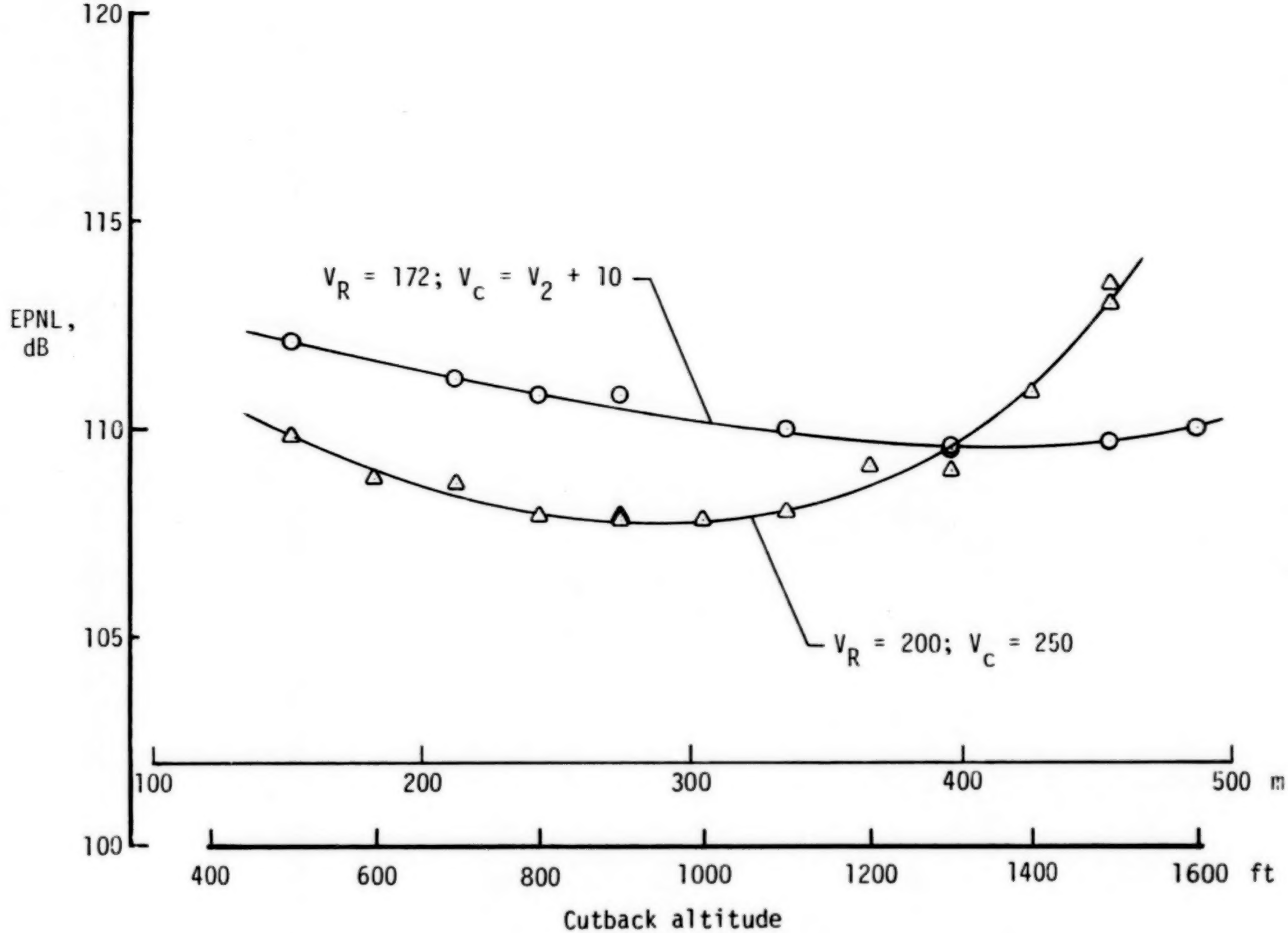

Figure 11.- Effect of rotation speed, climb speed, and cutback altitude on flyover noise. (Noise levels indicated for jet noise only; $\delta_f = 20^{\circ}$.)

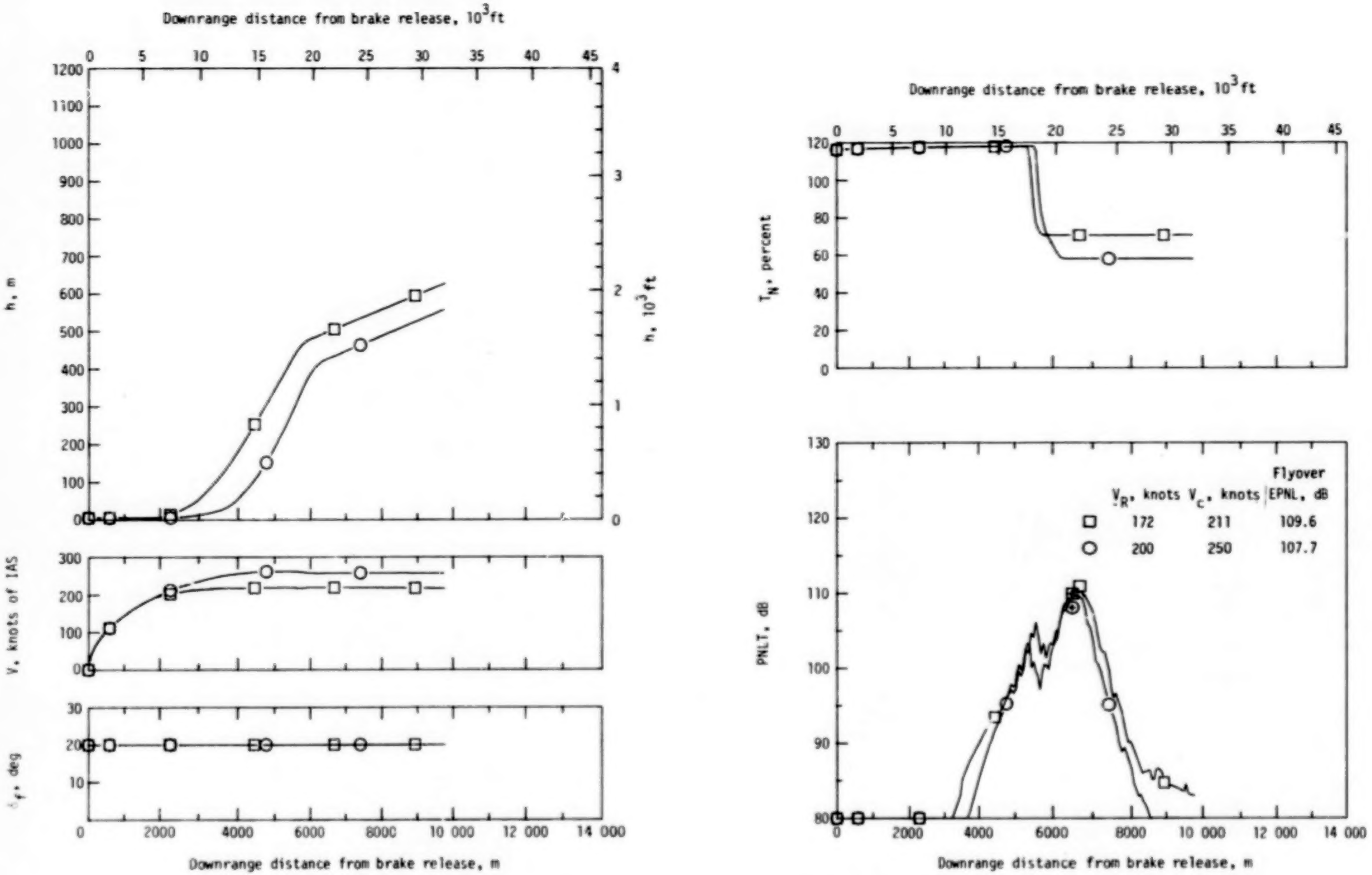

Figure 12.- Takeoff profiles and flyover noise generated for minimum and maximum simulated rotation and climb speeds. (Noise levels indicated for jet noise only; symbols with +'s indicate values at measuring station.)

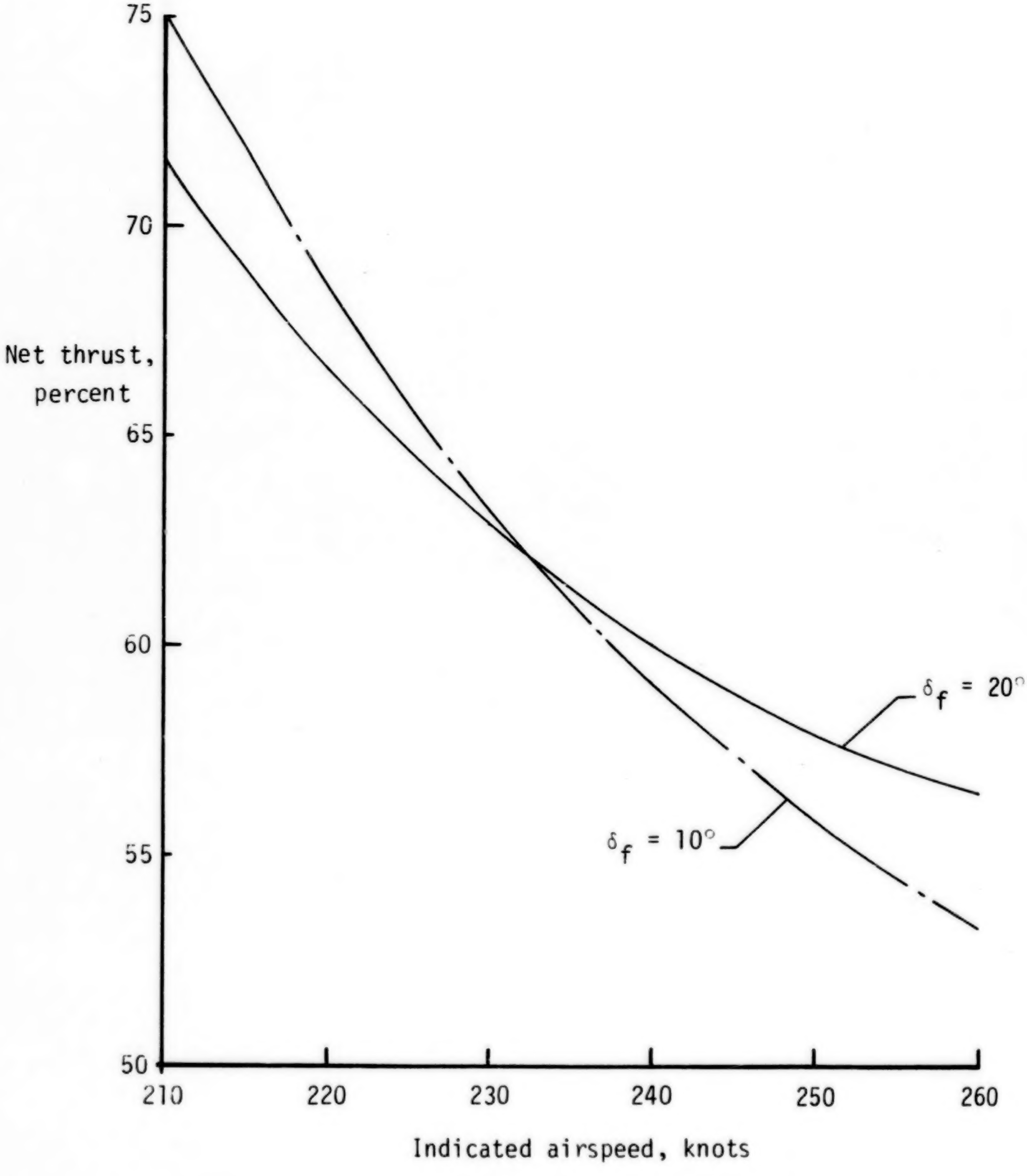

Figure 13.- Effect of trailing-edge flap deflection and airspeed on trimmed net thrust at takeoff weight and climb gradient of 0.04.

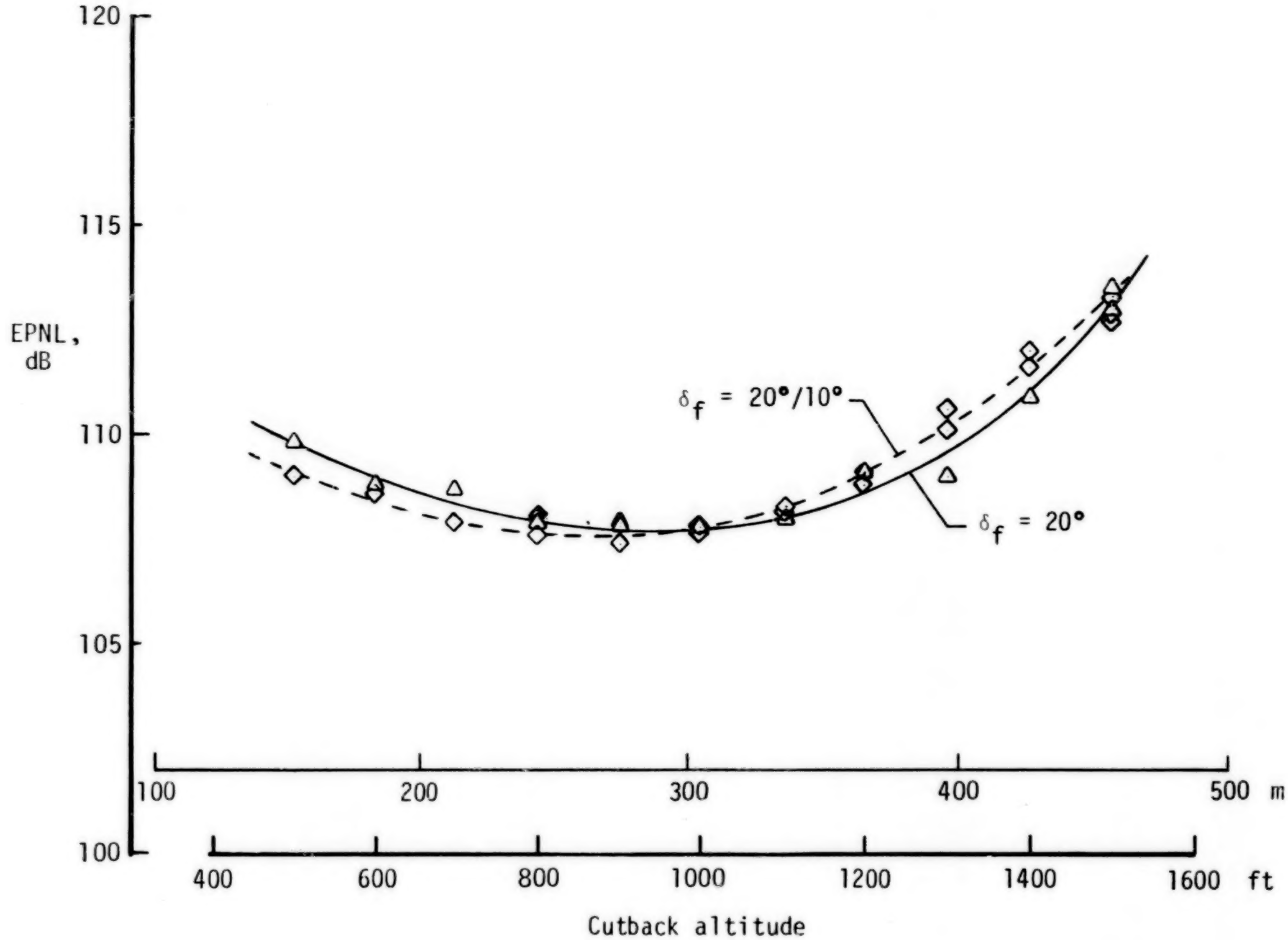

Figure 14.- Effect of trailing-edge flap setting and cutback altitude on flyover noise. (Noise levels indicated for jet noise only.)

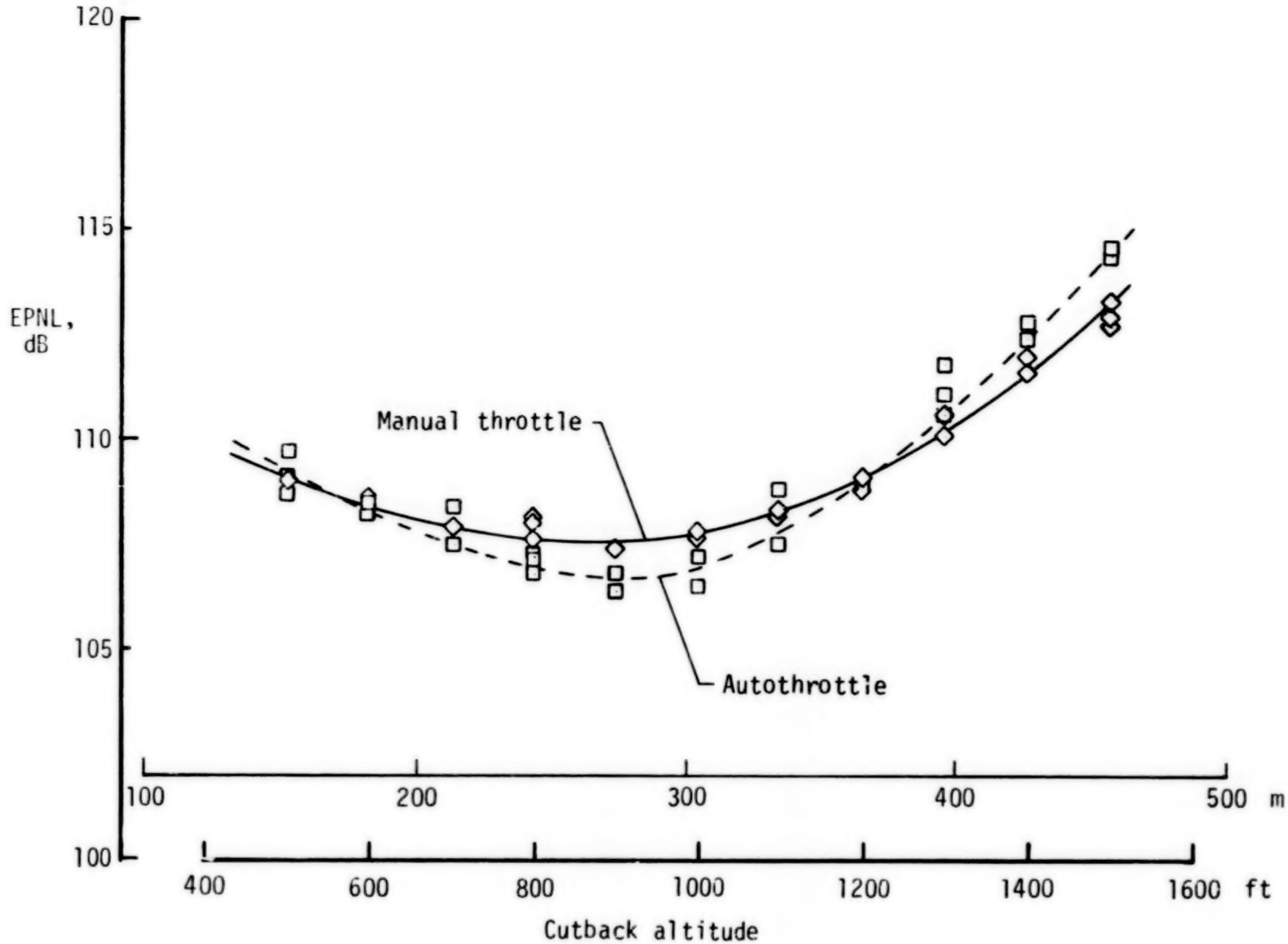

Figure 15.- Effect of thrust cutback procedure and cutback altitude on flyover noise. (Noise levels indicated for jet noise only.)

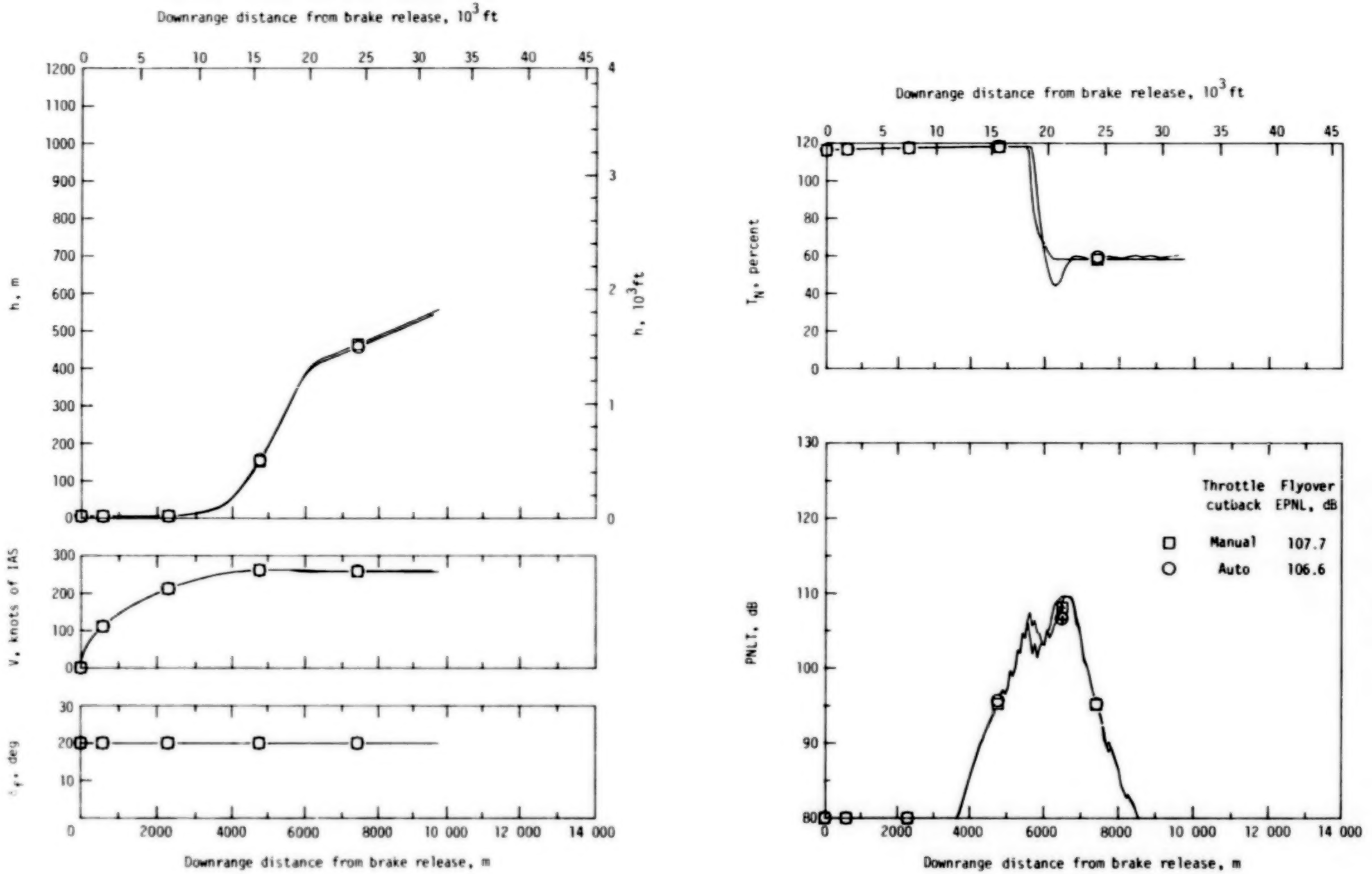

Figure 16.- Takeoff profiles and flyover noise for different cutback procedures. (Noise levels indicated for jet noise only; symbols with +'s indicate values at measuring station.)

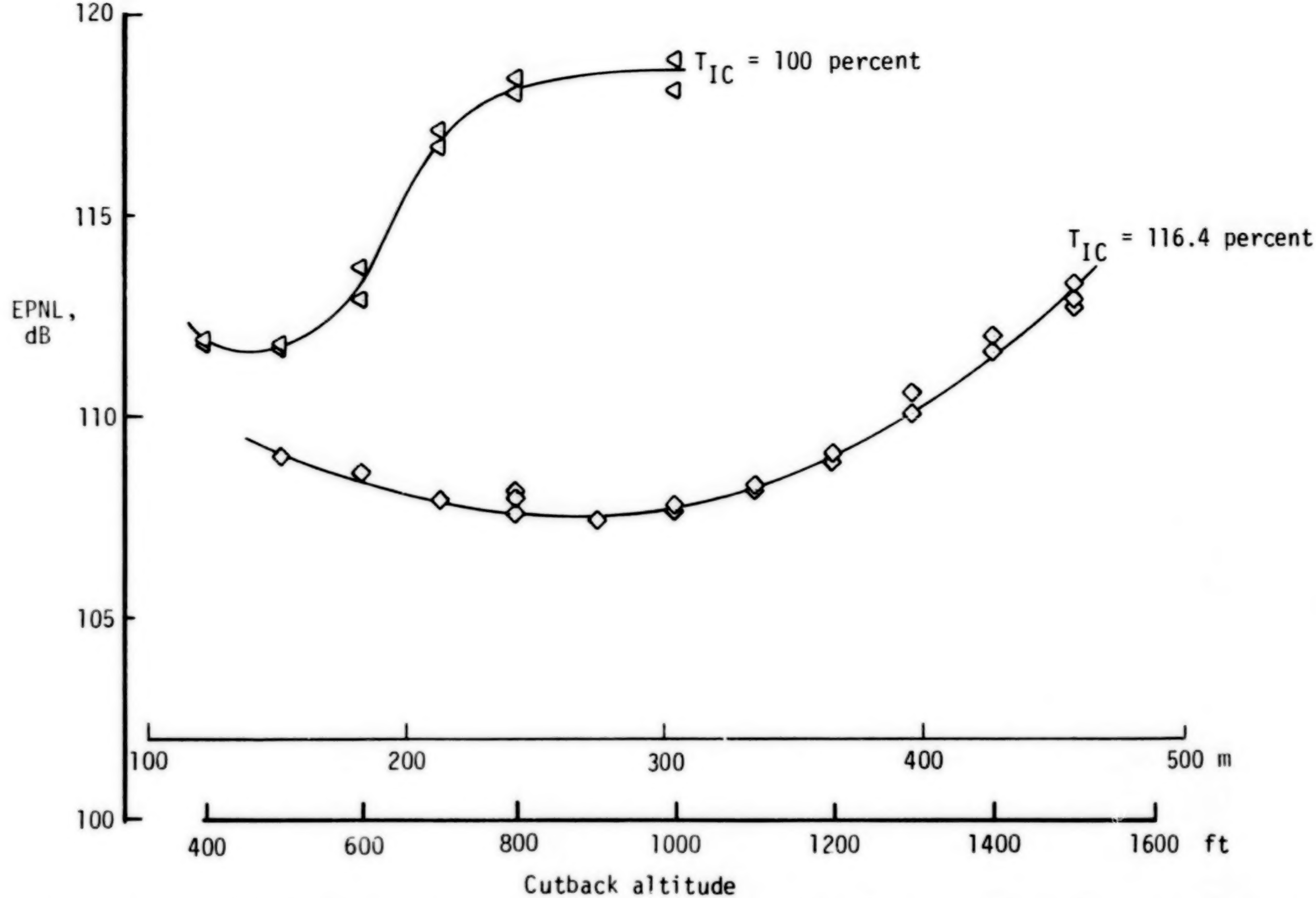

Figure 17.- Effect of initial thrust setting and cutback altitude on flyover noise. (δ_f changed from 20° to 10° at $V_c \leq 235$ knots; noise levels indicated for jet noise only.)

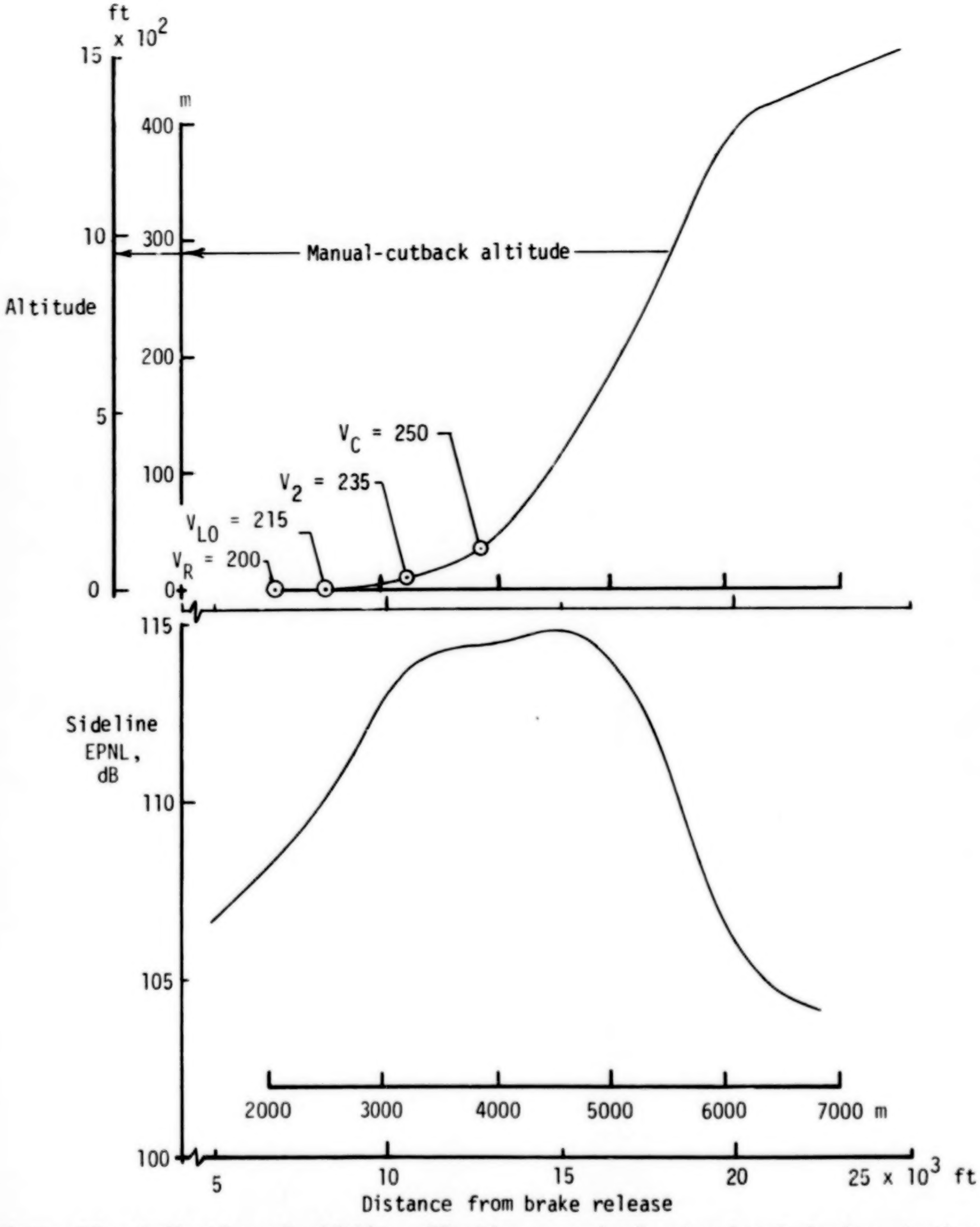

Figure 18.- Indication of sideline effective perceived noise level during standard procedure takeoff. (Flyover EPNL = 107.7 dB; noise levels indicated for jet noise only.)

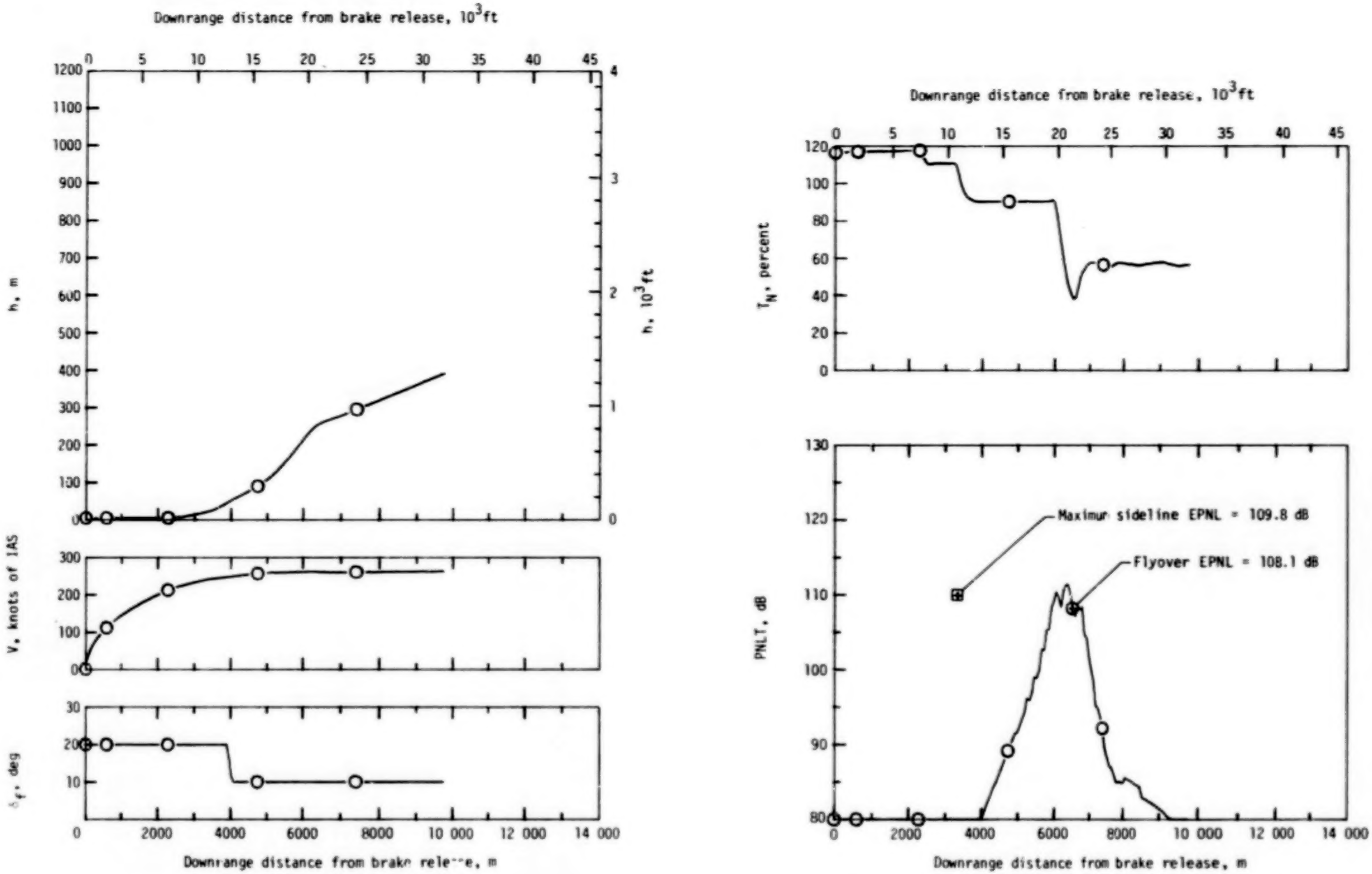

Figure 19.- Advanced-procedure-I takeoff profile and corresponding calculated sideline and flyover noise. (Noise levels indicated for jet noise only; symbols with +'s indicate values at measuring stations.)

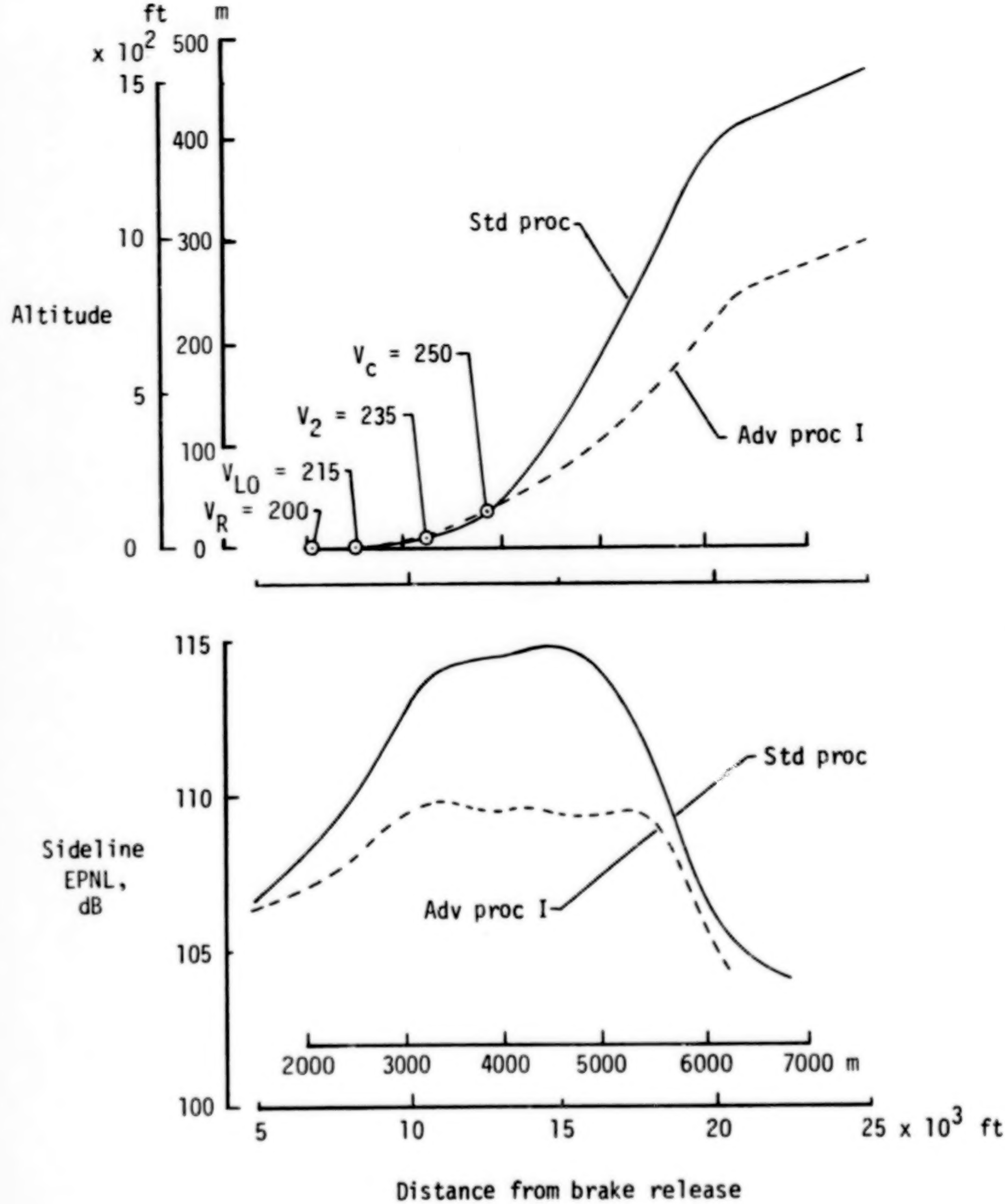

Figure 20.- Comparison of sideline EPNL's generated for standard-procedure and advanced-procedure-I takeoffs. (Noise levels indicated for jet noise only.)

BLANK PAGE

BLANK PAGE

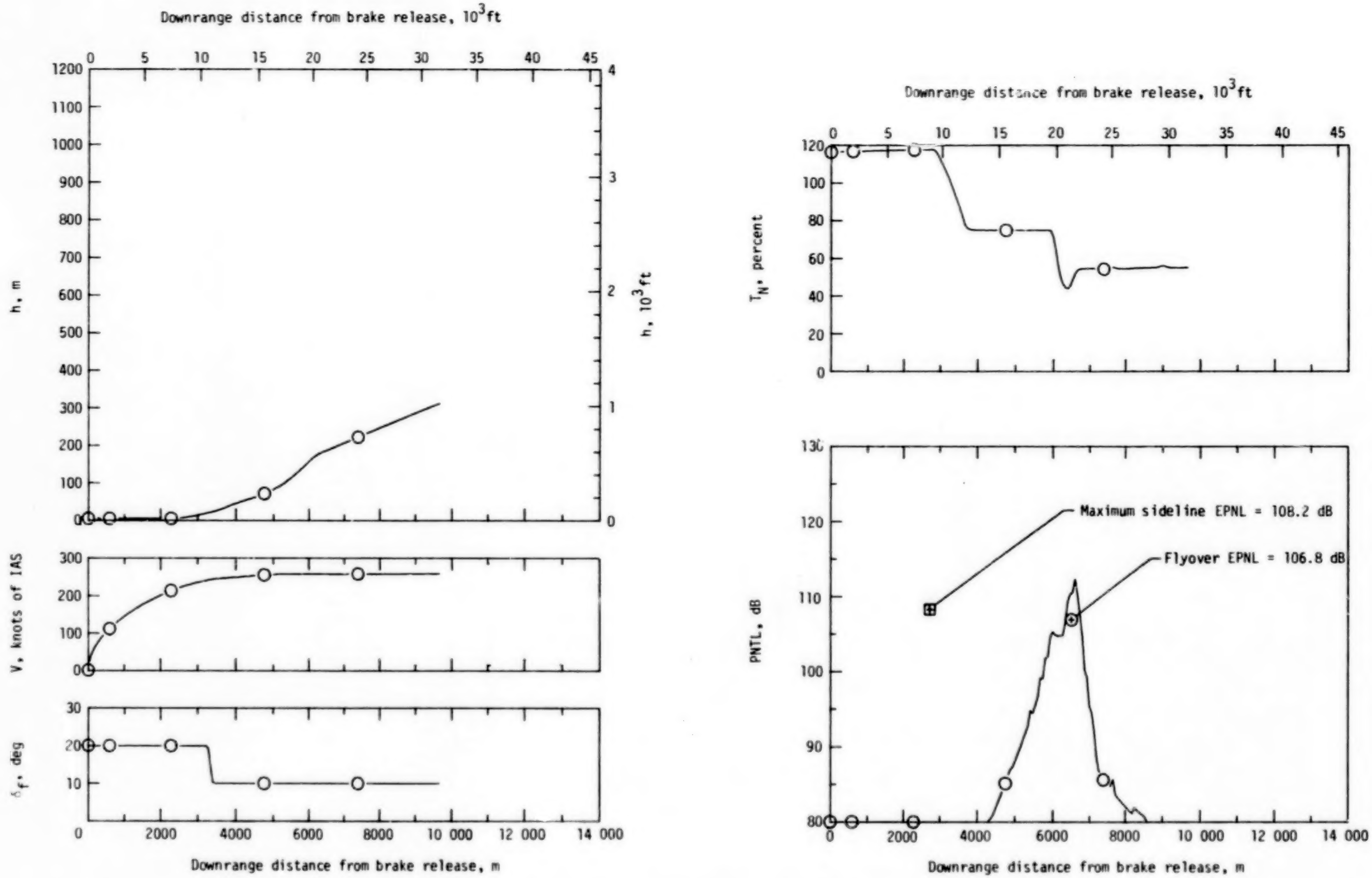

Figure 21.- Advanced-procedure-II takeoff profile and corresponding calculated sideline and flyover noise. (Noise levels indicated for jet noise only; symbols with +'s indicate values at measuring stations.)

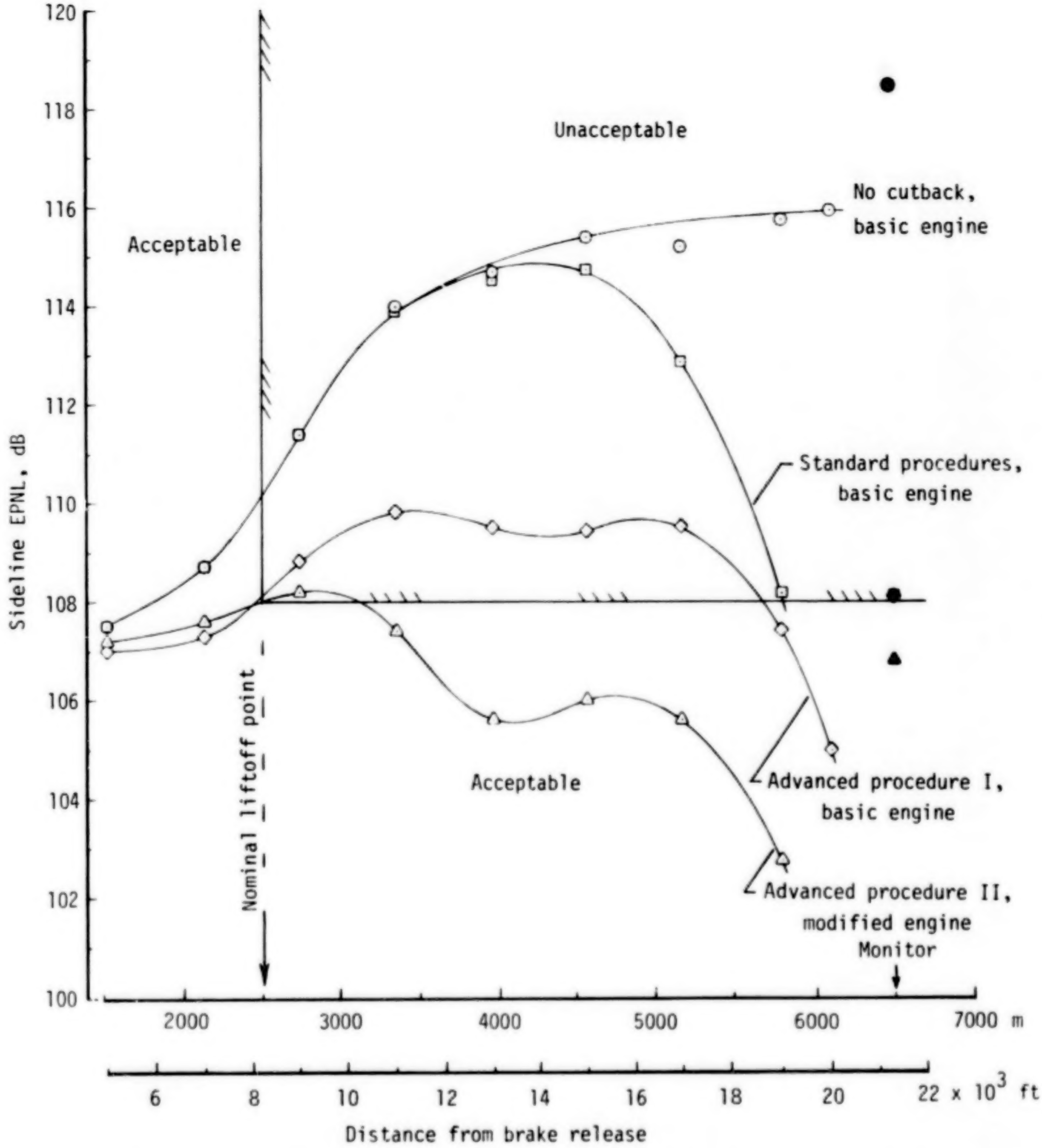

Figure 22.- Sideline effective perceived noise levels generated during takeoff for various operating procedures. (Noise levels indicated for jet noise only; solid symbols indicate flyover values at measuring station.)

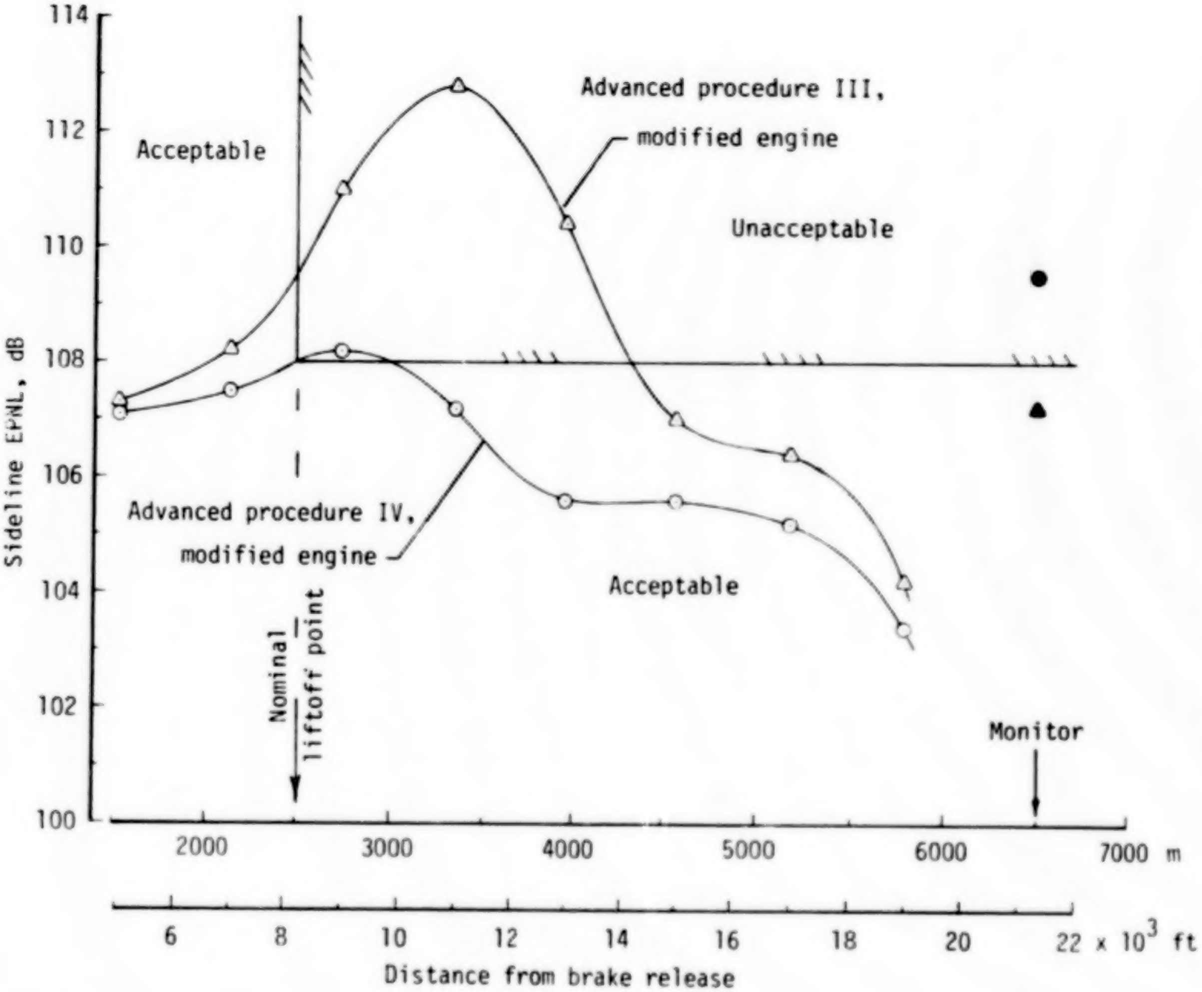

Figure 23.- Comparison of sideline and flyover effective perceived noise levels generated during takeoff with advanced procedures III and IV. (Noise levels indicated for jet noise only; solid symbols indicate flyover values at measuring station.)

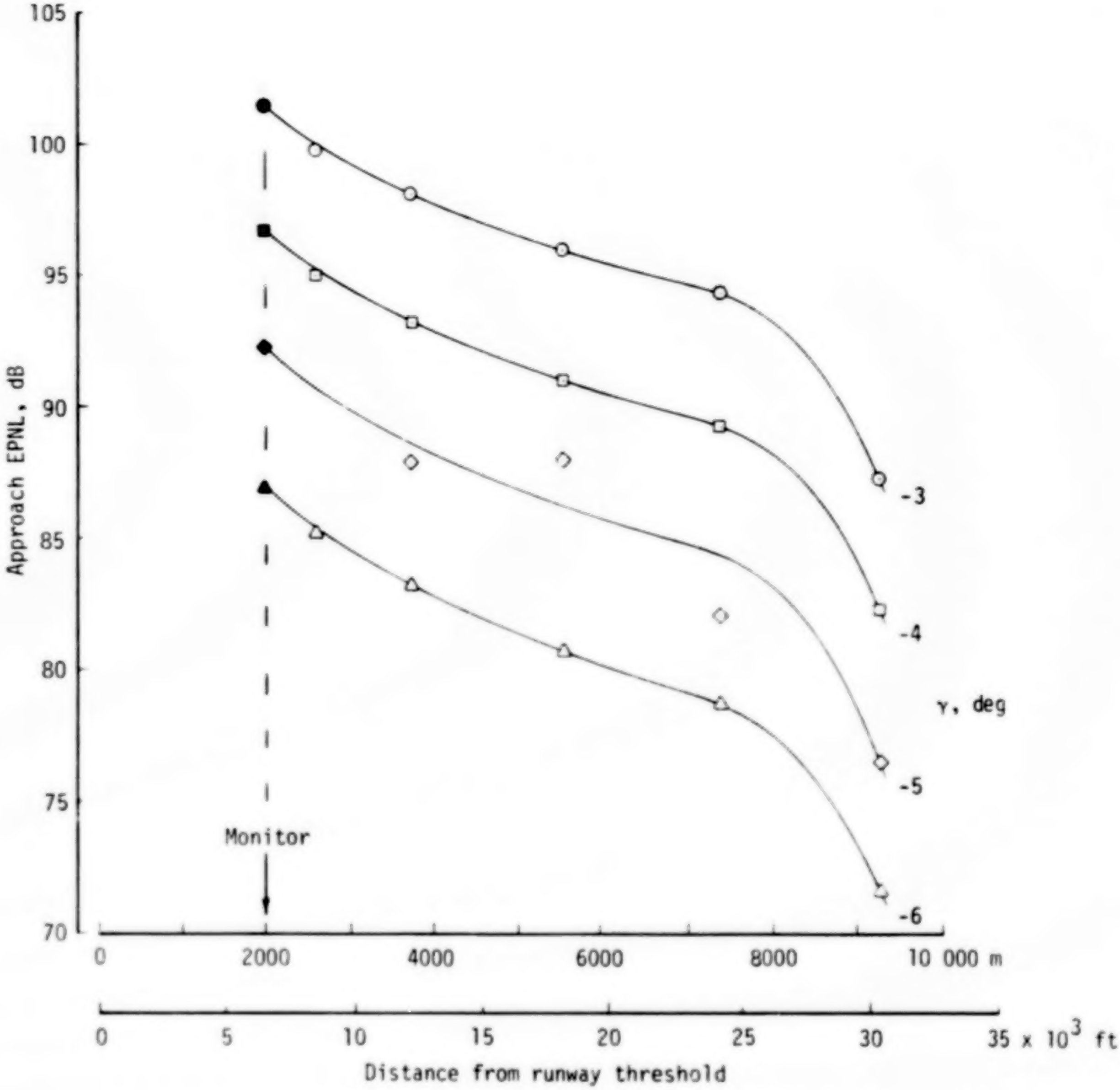

Figure 24.- Indication of effect of approach glide angle on the effective perceived noise levels generated at various distances from the runway threshold. (Noise levels indicated for jet noise only; solid symbols indicate flyover values at measuring station.)

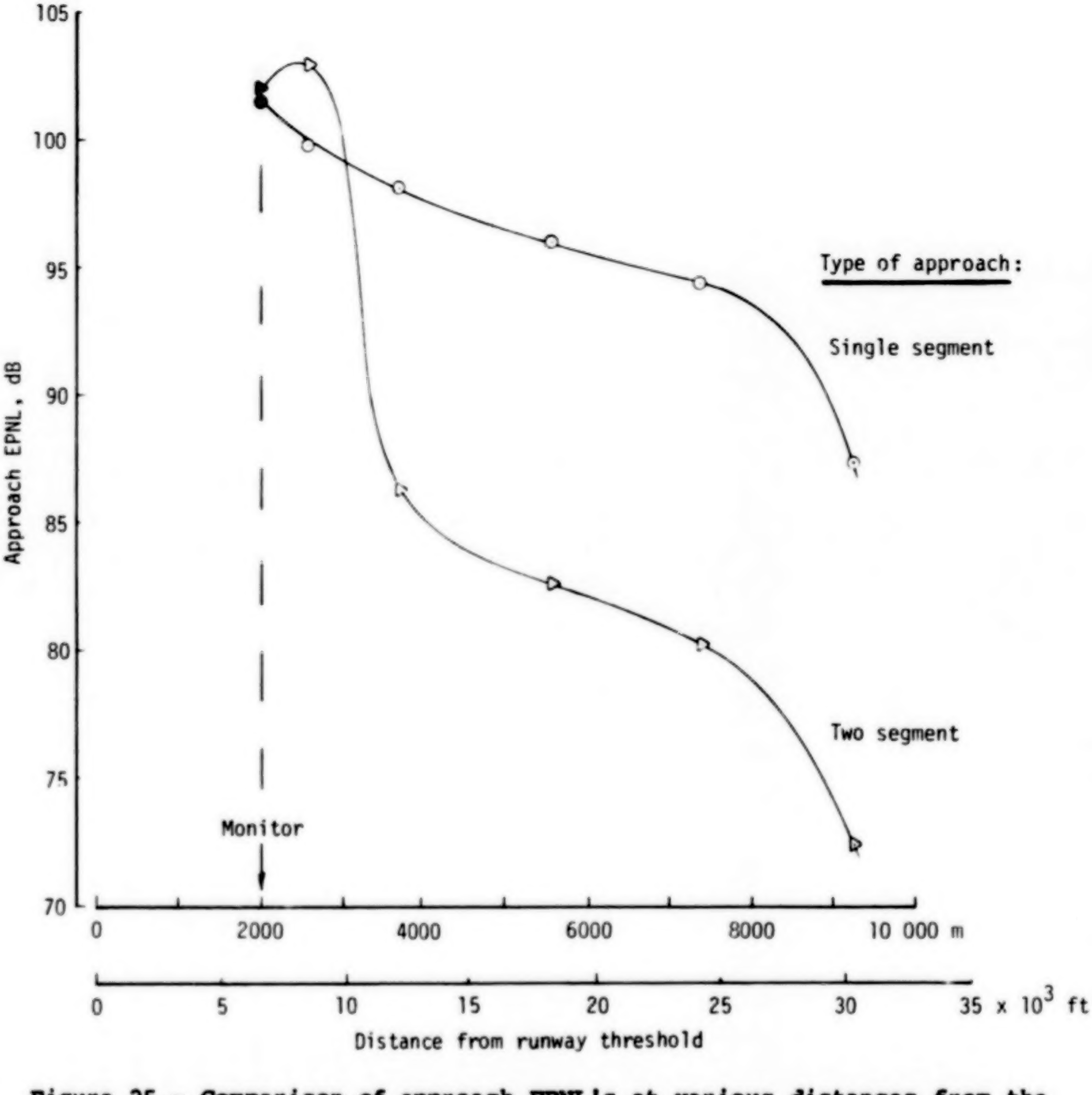

Figure 25.- Comparison of approach EPNL's at various distances from the runway threshold for two-segment ($6^{\circ}/3^{\circ}$) and single-segment (3°) approaches. (V = 158 knots of IAS; noise levels indicated for jet noise only; solid symbols indicate values at measuring station.)

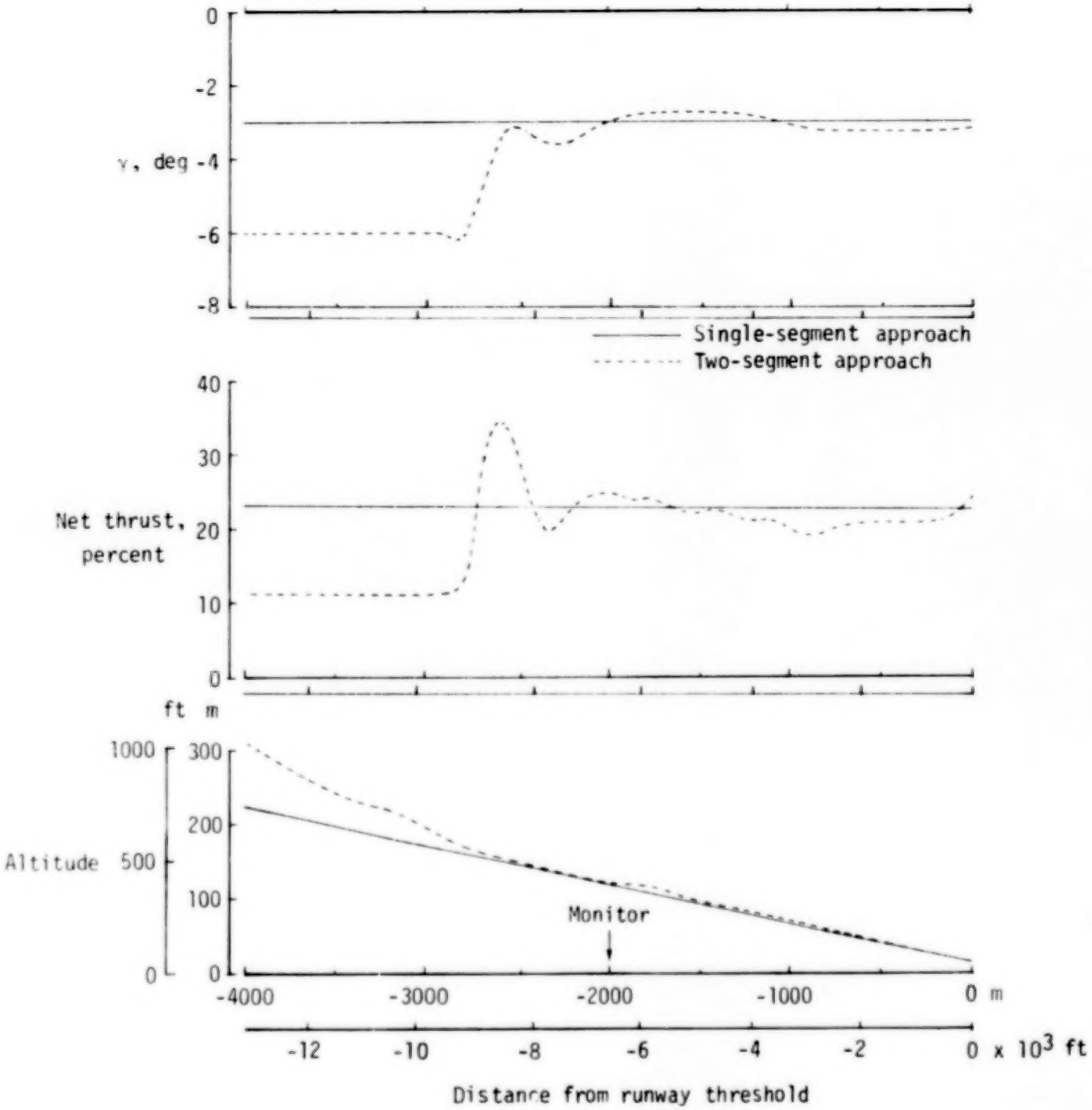

Figure 26.- Comparison of approach profiles for 6°/3° and constant 3° approaches. (V = 158 knots of IAS).

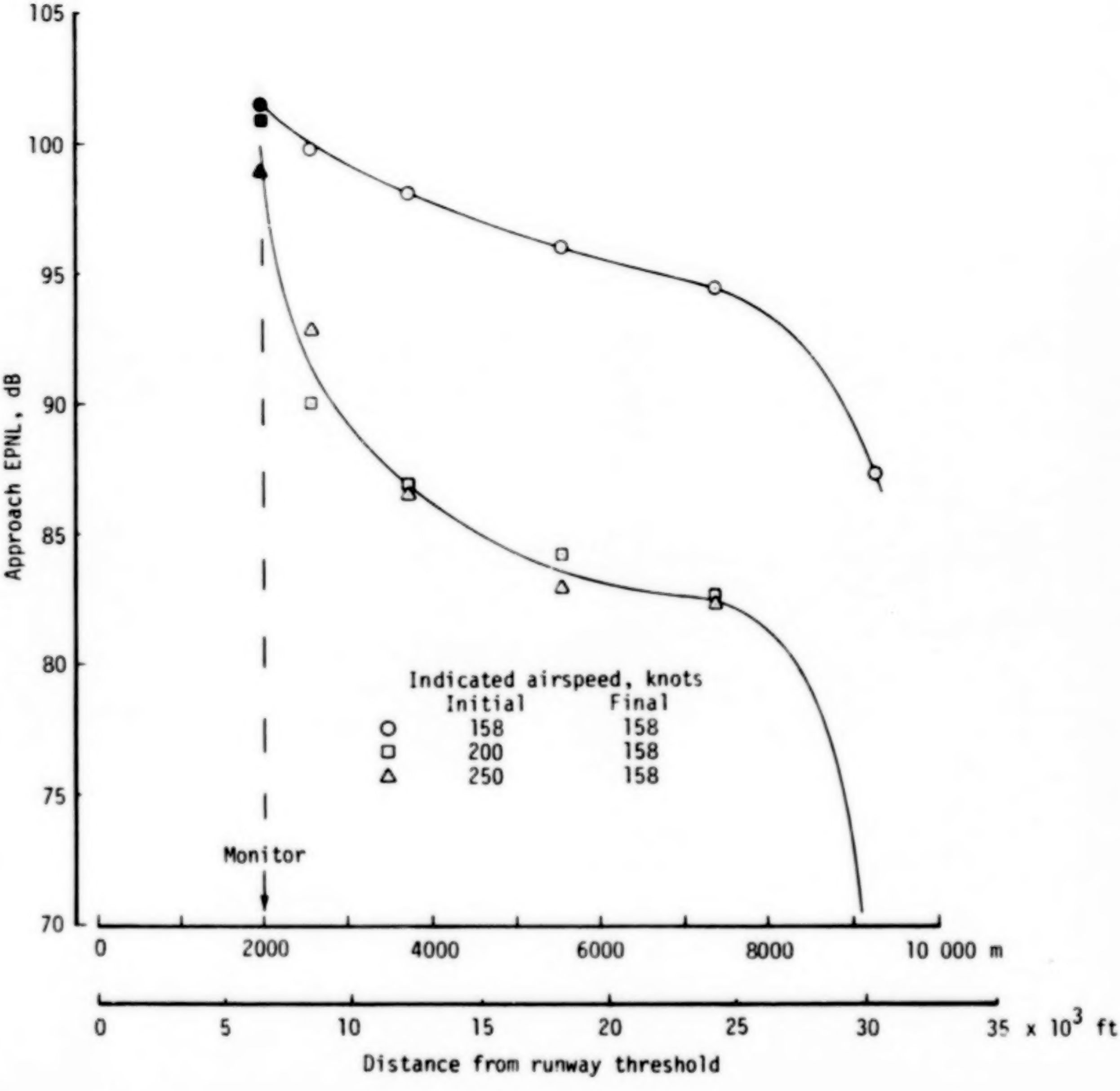

Figure 27.- Comparison of approach EPNL's at various distances from the runway threshold for two decelerating approaches and a constant-speed approach. ($\gamma = -3^o$; noise levels indicated for jet noise only; solid symbols indicate values at measuring station.)

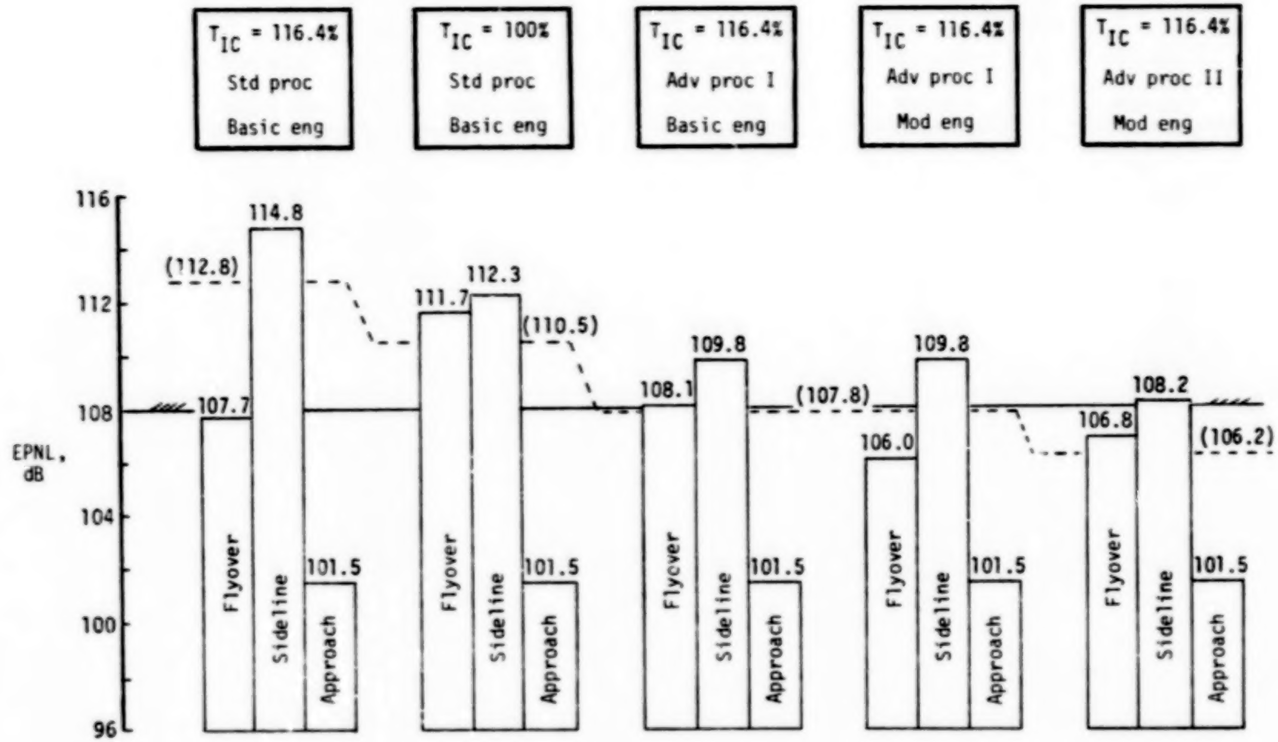

Figure 28.- Histogram of the traded noise levels calculated for some of the conditions and test procedures flown. (Numbers in parentheses indicate traded noise levels. All noise levels indicated for jet noise only.)

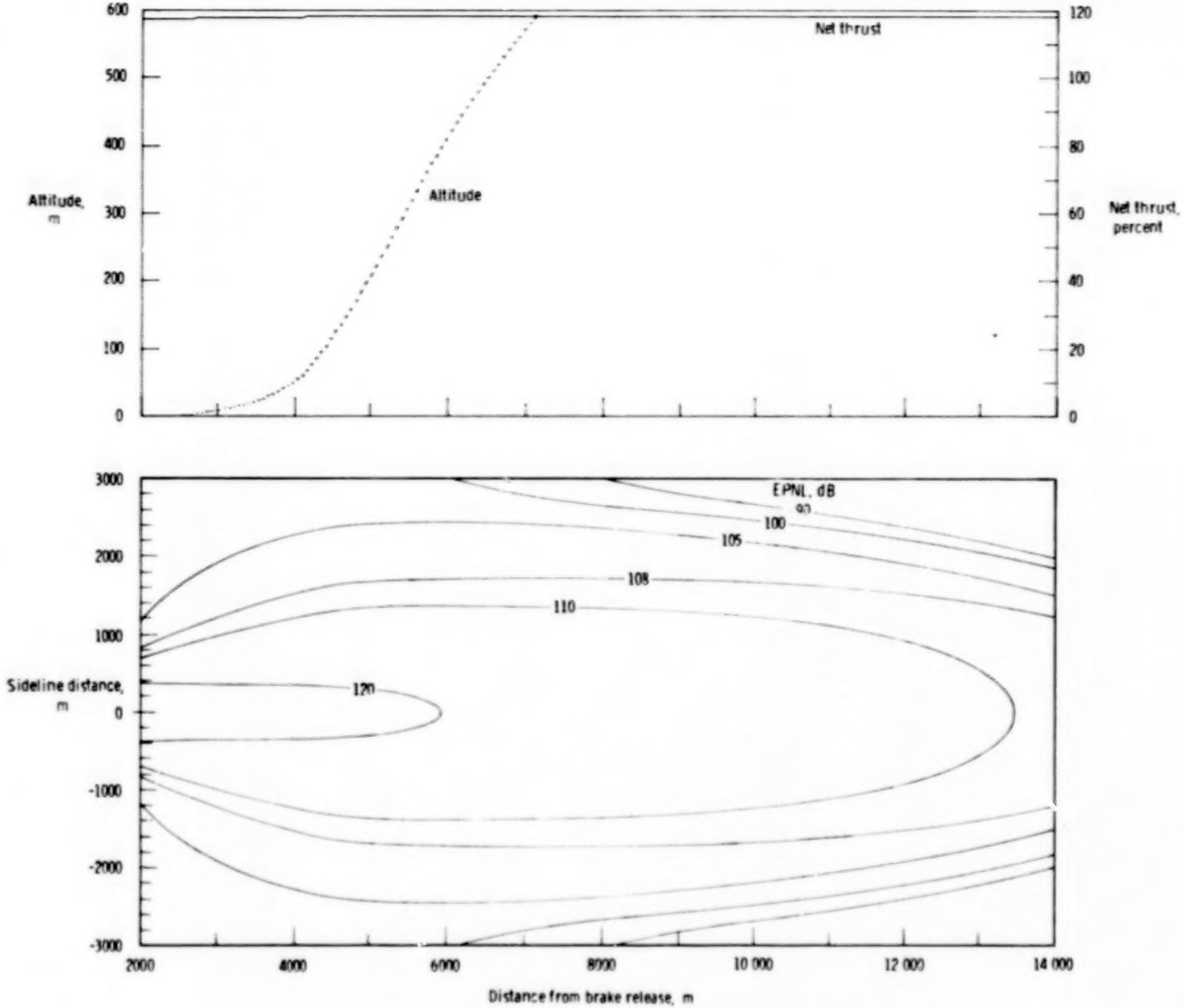

(a) No cutback (basic engine).

Figure 29.- Takeoff-noise contours and net-thrust and altitude time histories for the simulated SCR transport for various operating procedures. (Jet noise only.)

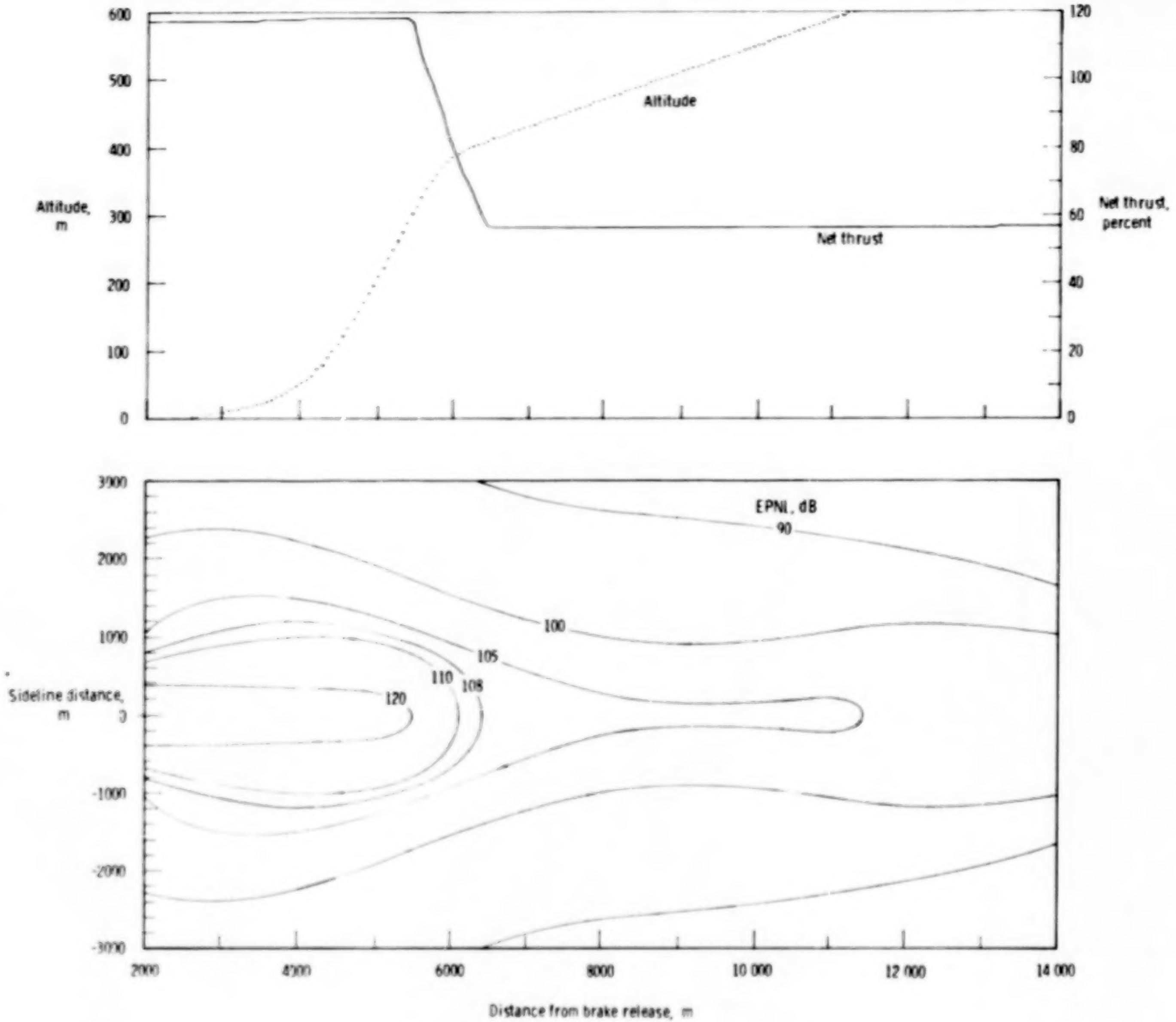

(b) Standard procedures (ref. 1, basic engine).

Figure 29.- Continued.

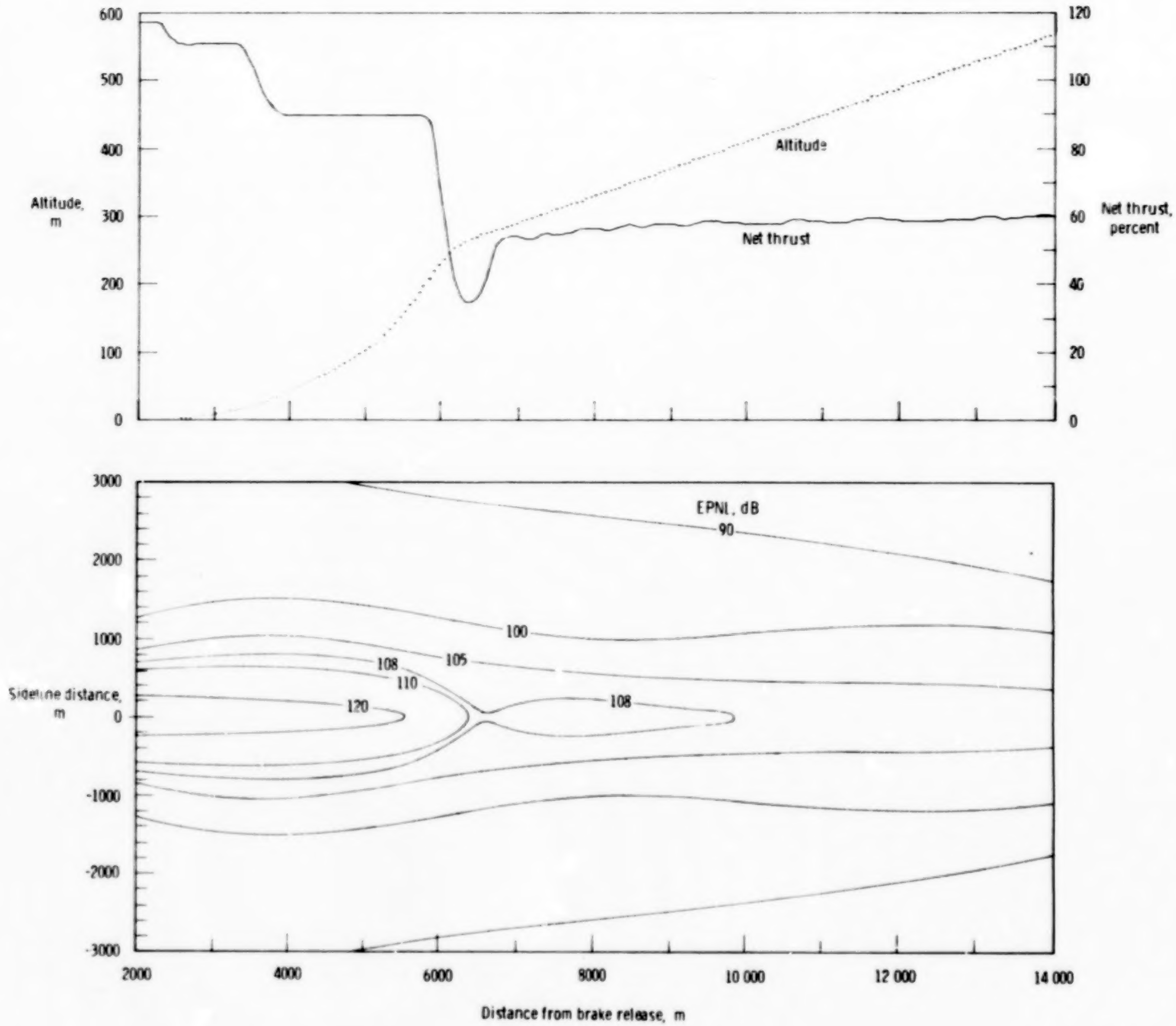

(c) Advanced procedure I (basic engine).

Figure 29.- Continued.

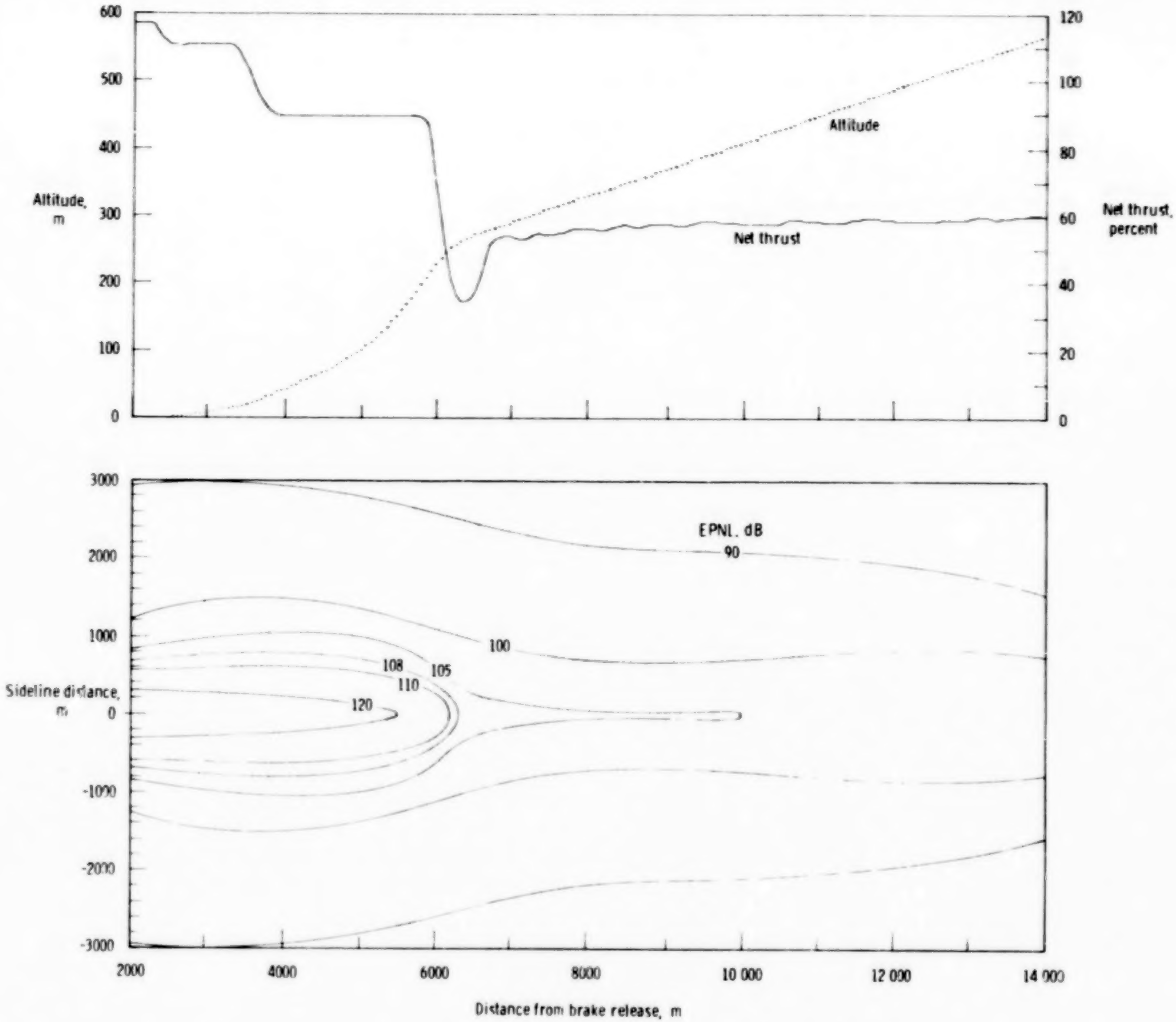

(d) Advanced procedure I (modified engine).

Figure 29.- Continued.

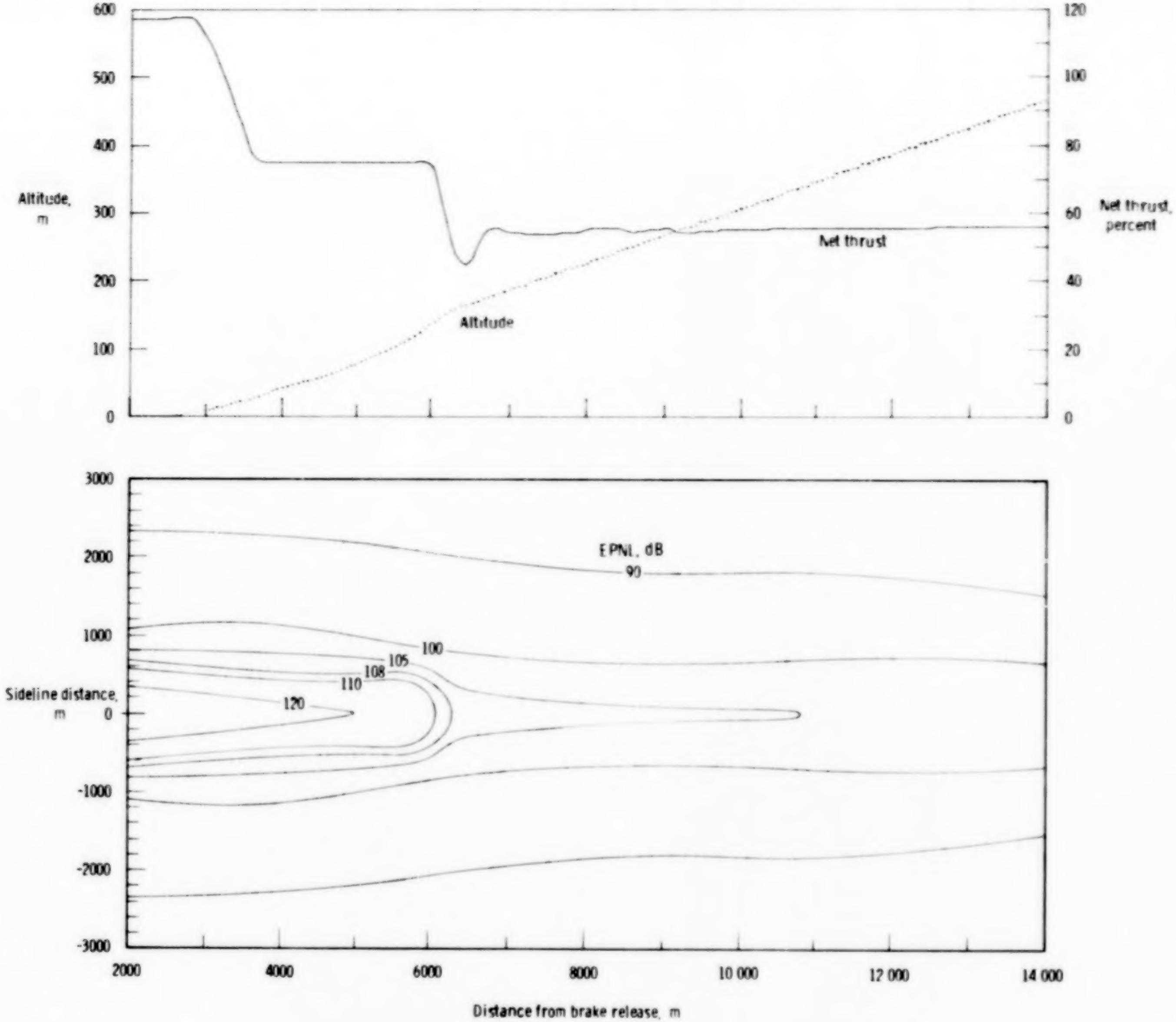

(e) Advanced procedure II (modified engine).

Figure 29.- Continued.

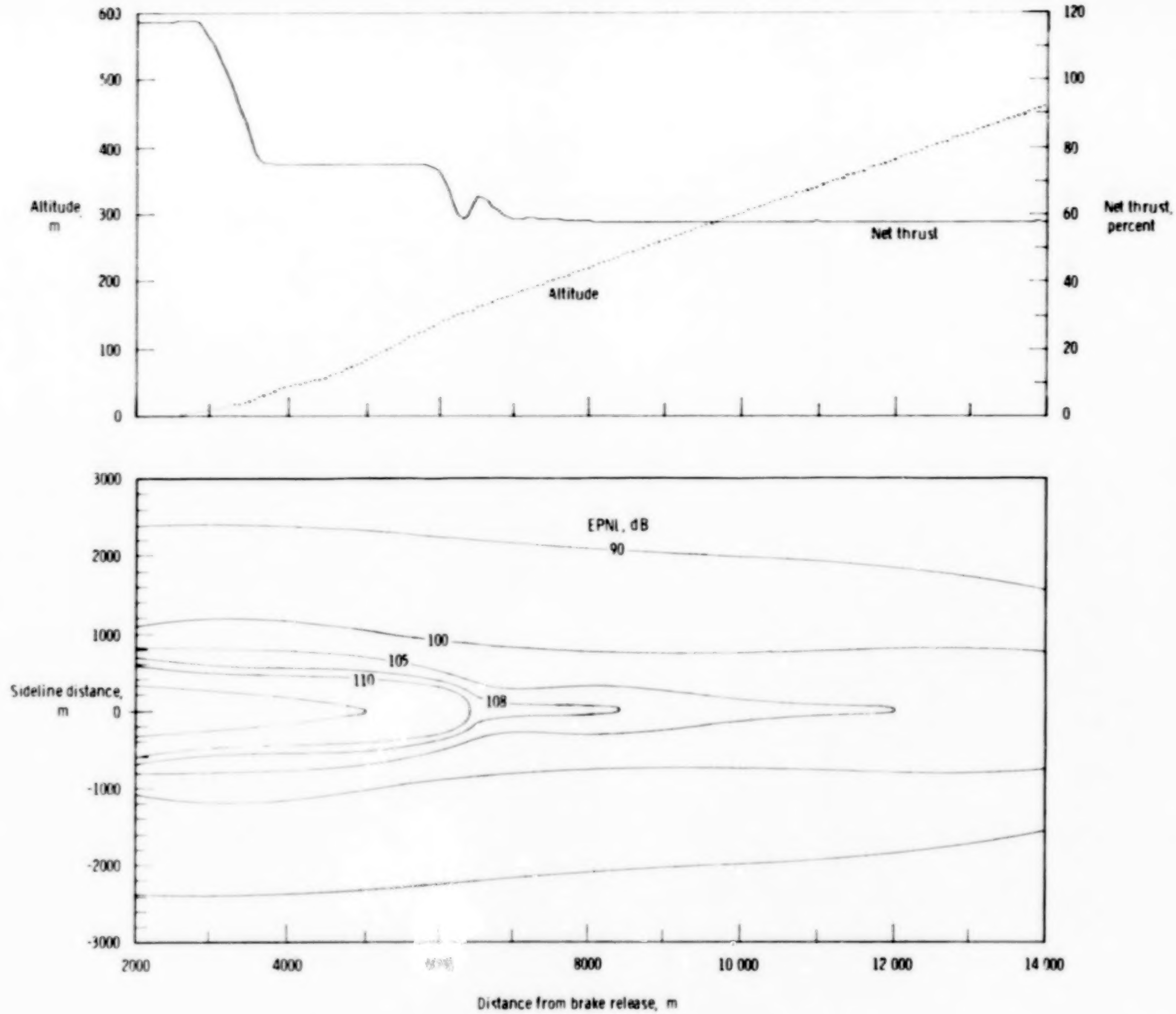

(f) Advanced procedure IV (modified engine).

Figure 29.- Continued.

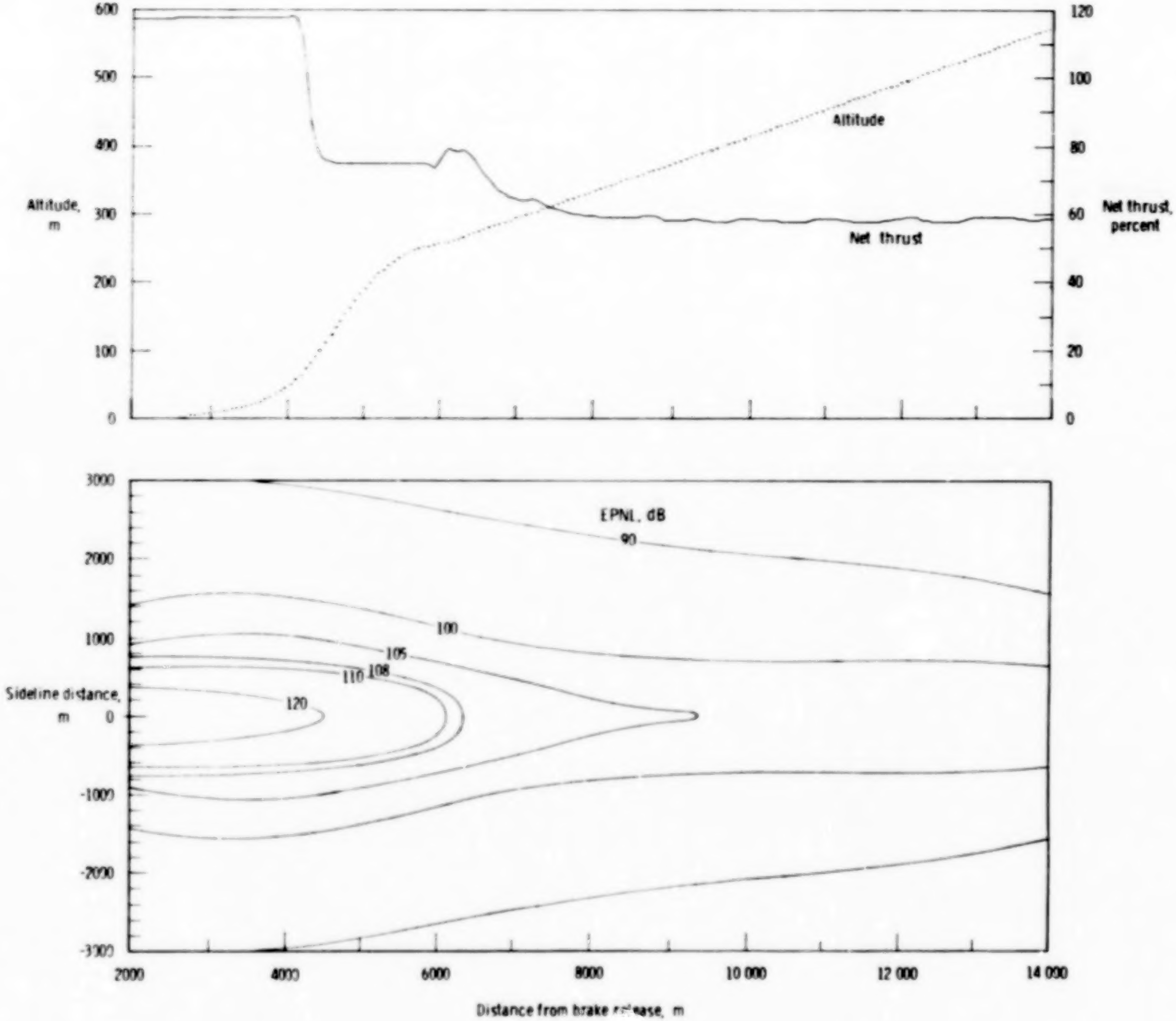

(g) Advanced procedure III (modified engine).

Figure 29.- Concluded.

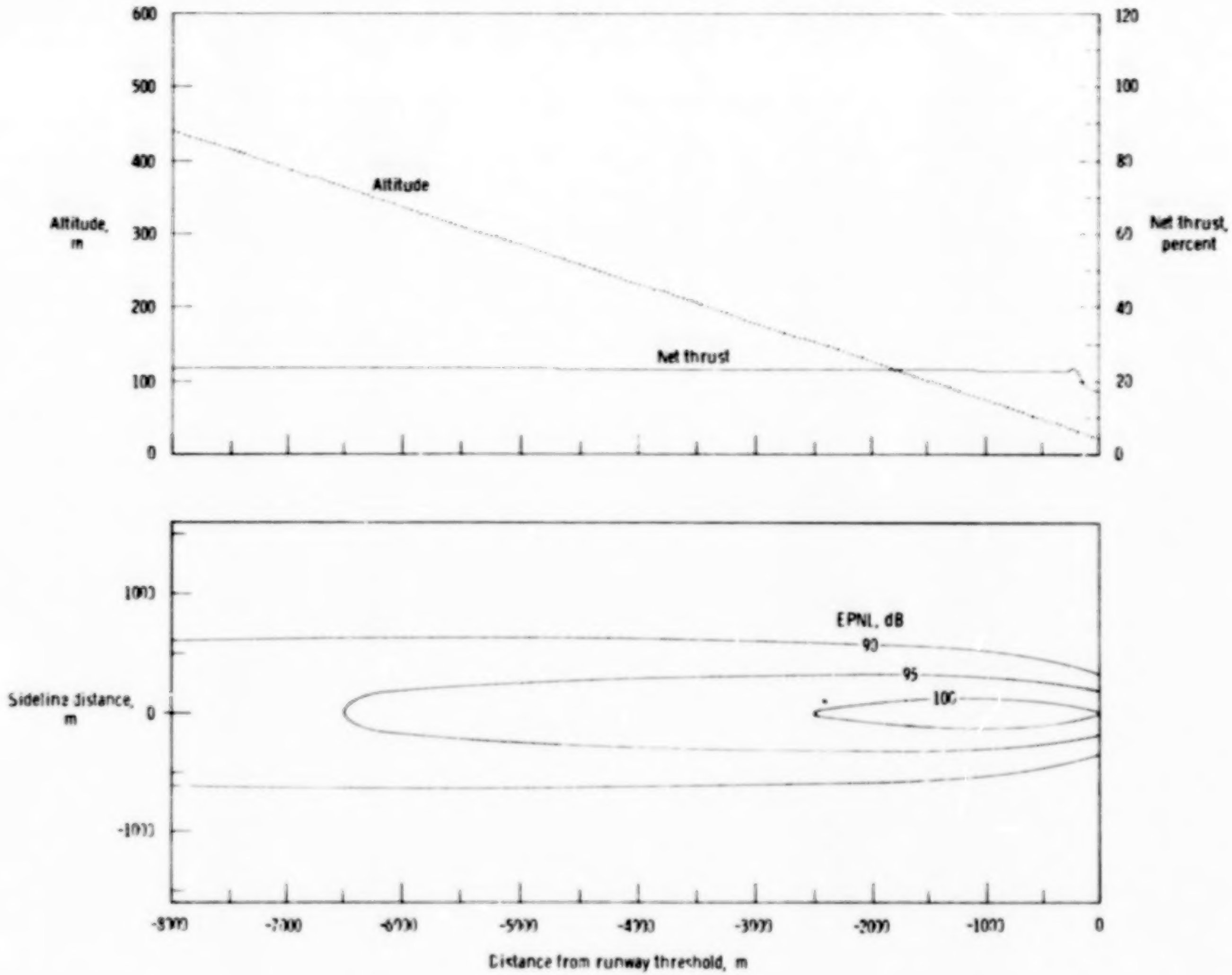

(a) Glide angle of 3°, constant IAS of 158 knots.

Figure 30.- Landing-approach noise contours and net-thrust and altitude time histories for the simulated SCR transport, for various operating procedures. (Jet noise only.)

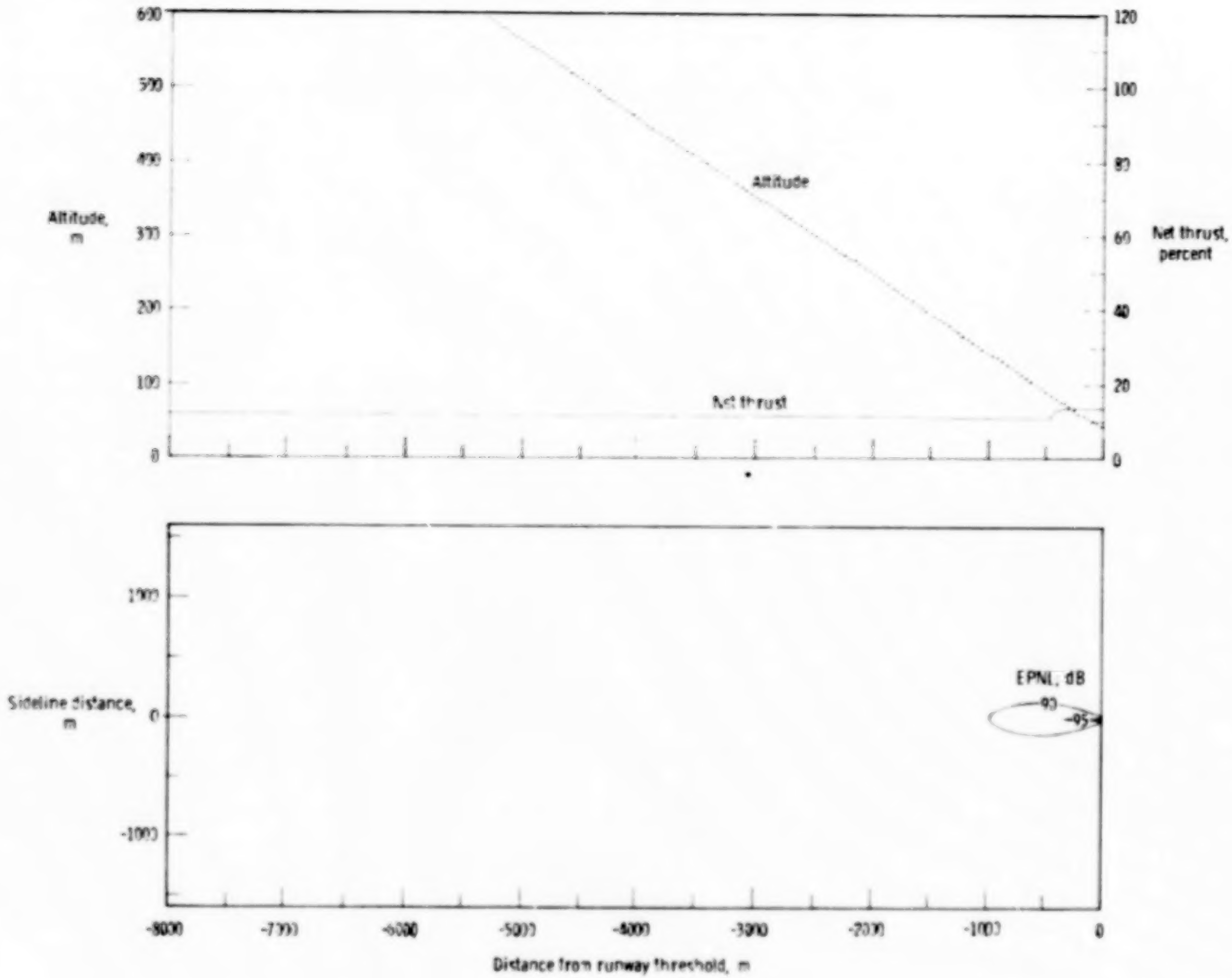

(b) Glide angle of 6°, constant IAS of 158 knots.

Figure 30.- Continued.

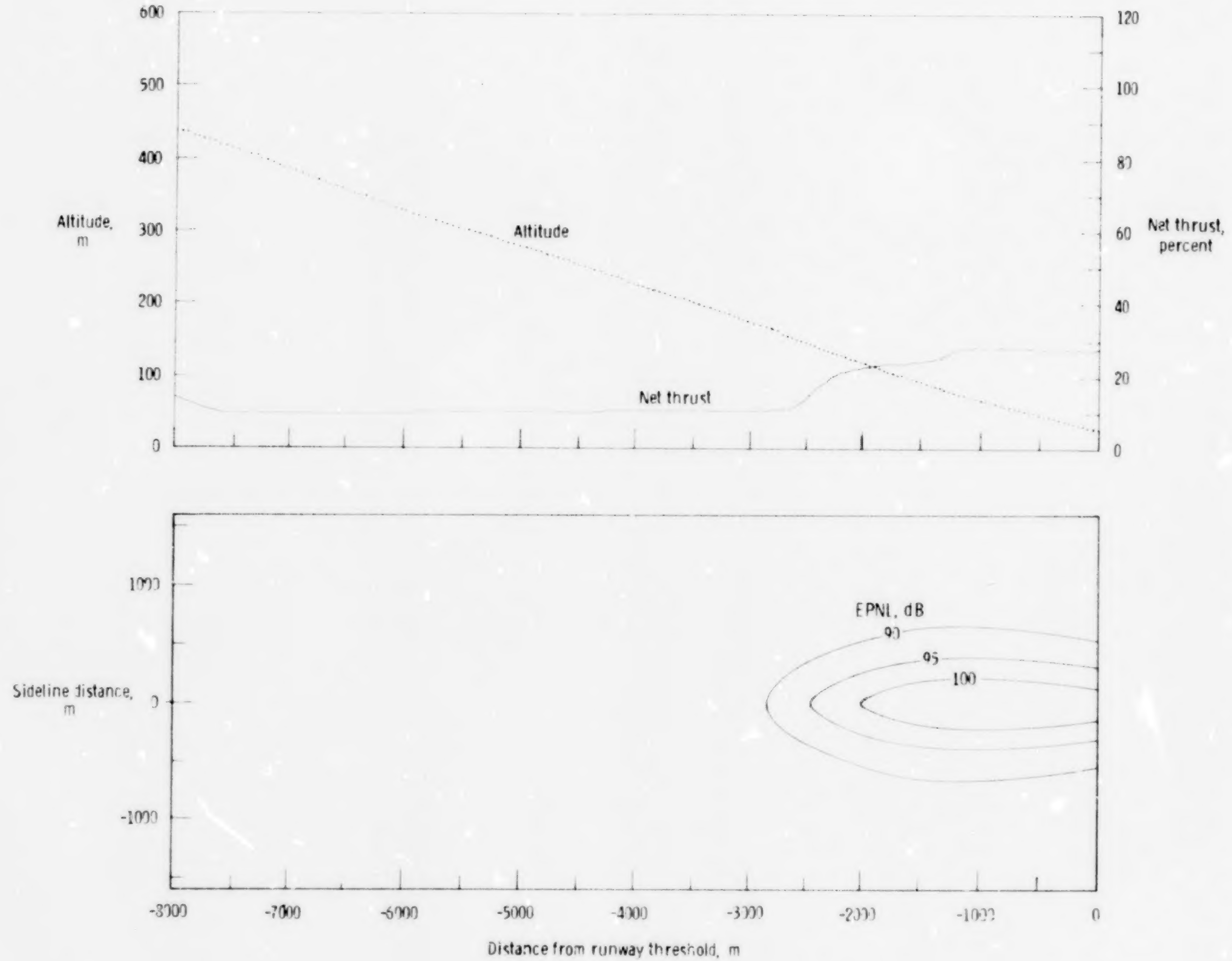

(c) Glide angle of 3°, decelerating IAS from 200 to 158 knots.

Figure 30.- Continued.

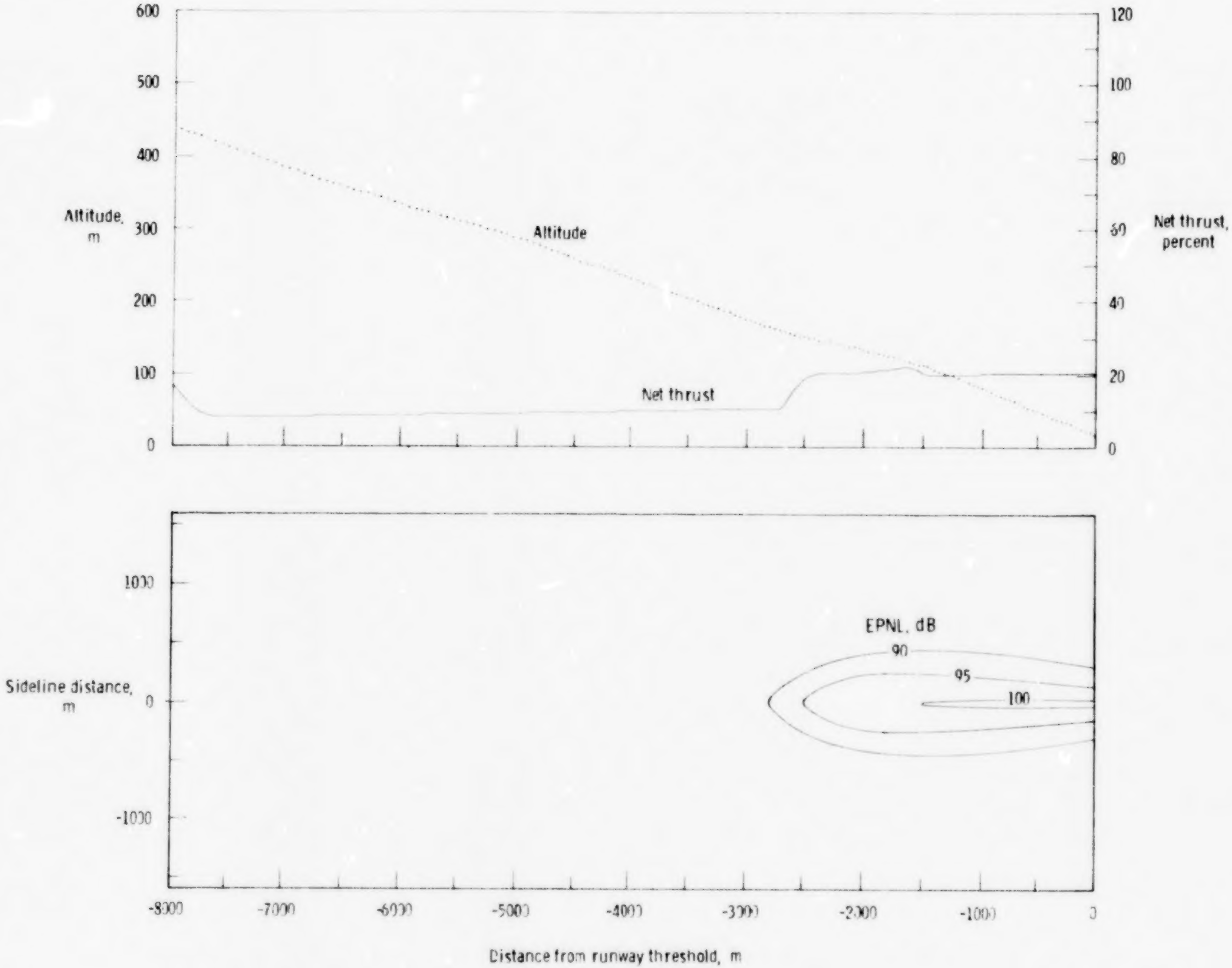

(d) Glide angle of 3°, decelerating IAS from 250 to 158 knots.

Figure 30.- Continued.

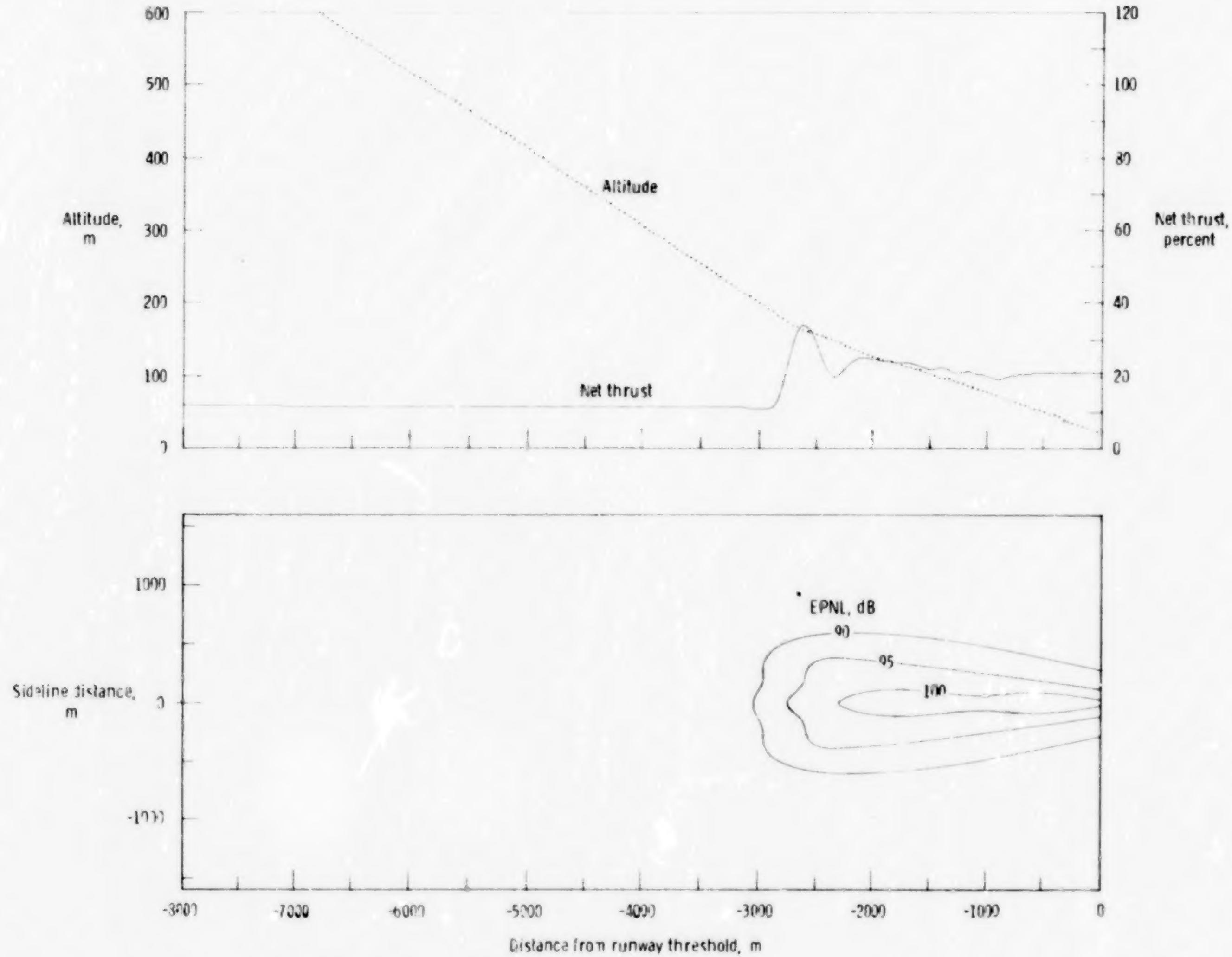

(e) Two-segment ($6^{o}/3^{o}$) glide angle, constant IAS of 158 knots.

Figure 30.- Concluded.

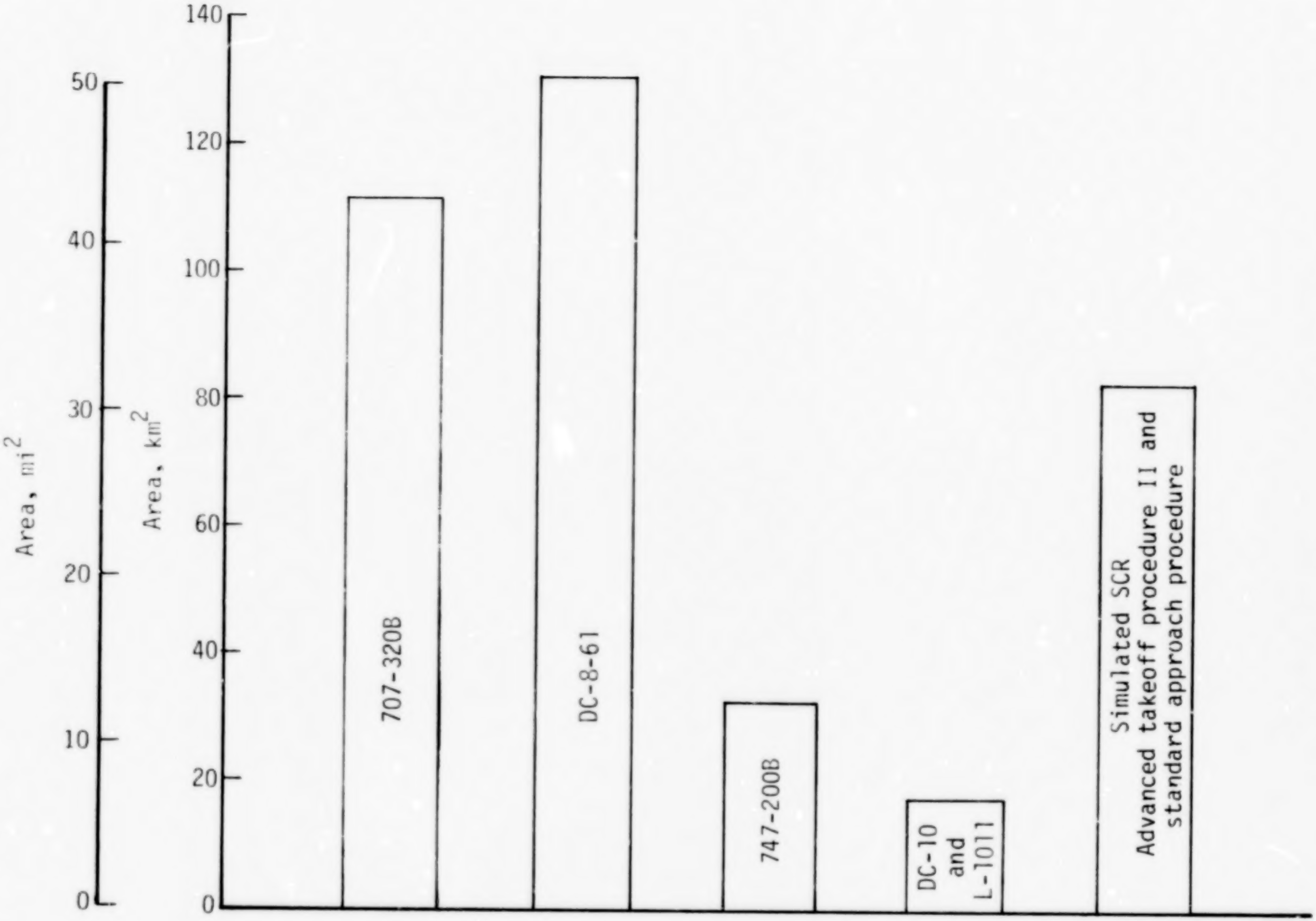

Figure 31.- Comparison of 95.0-dB EPNL single-event contour areas.

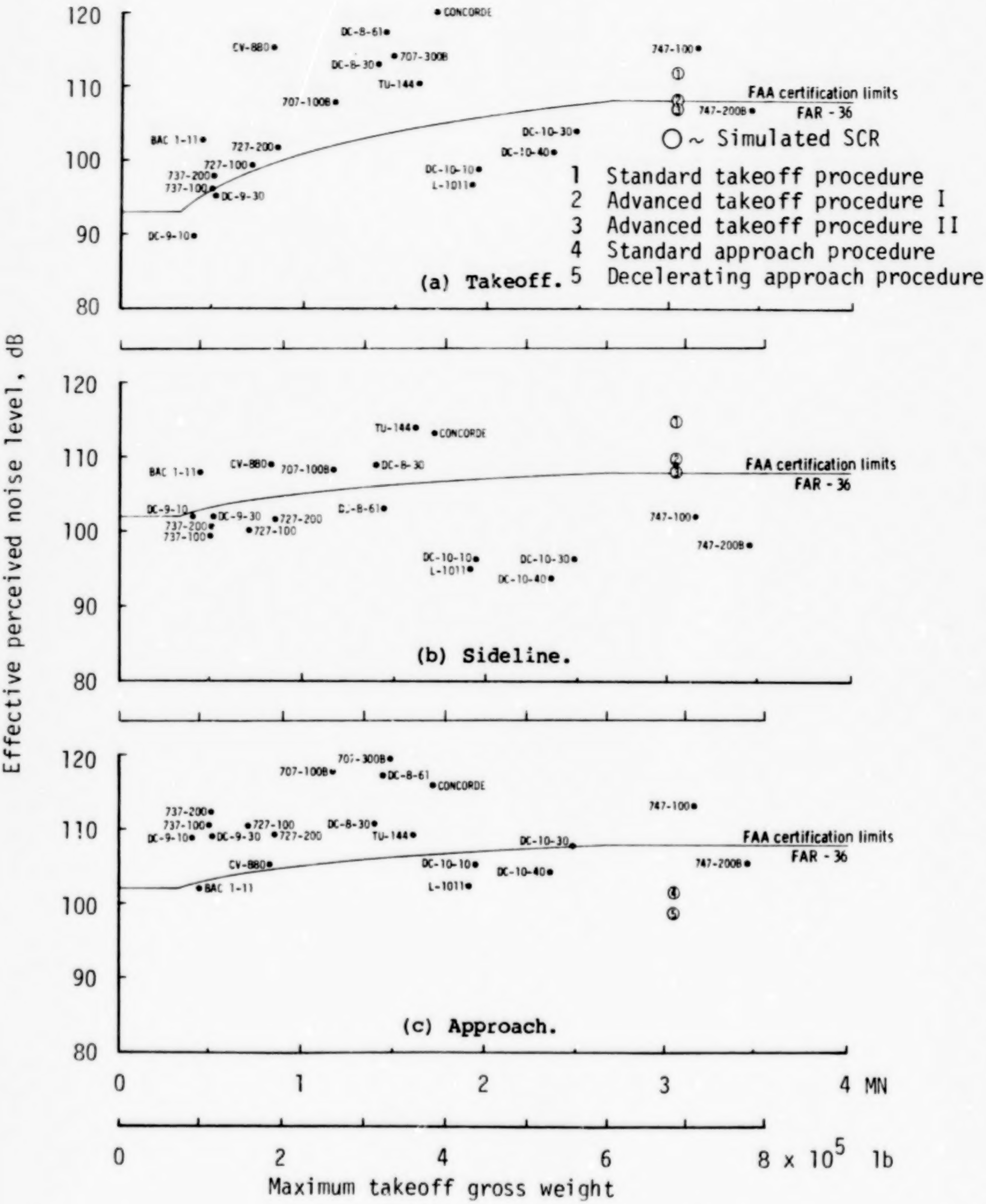

Figure 32.- Comparison of SCR results with some present-day aircraft EPNL's.

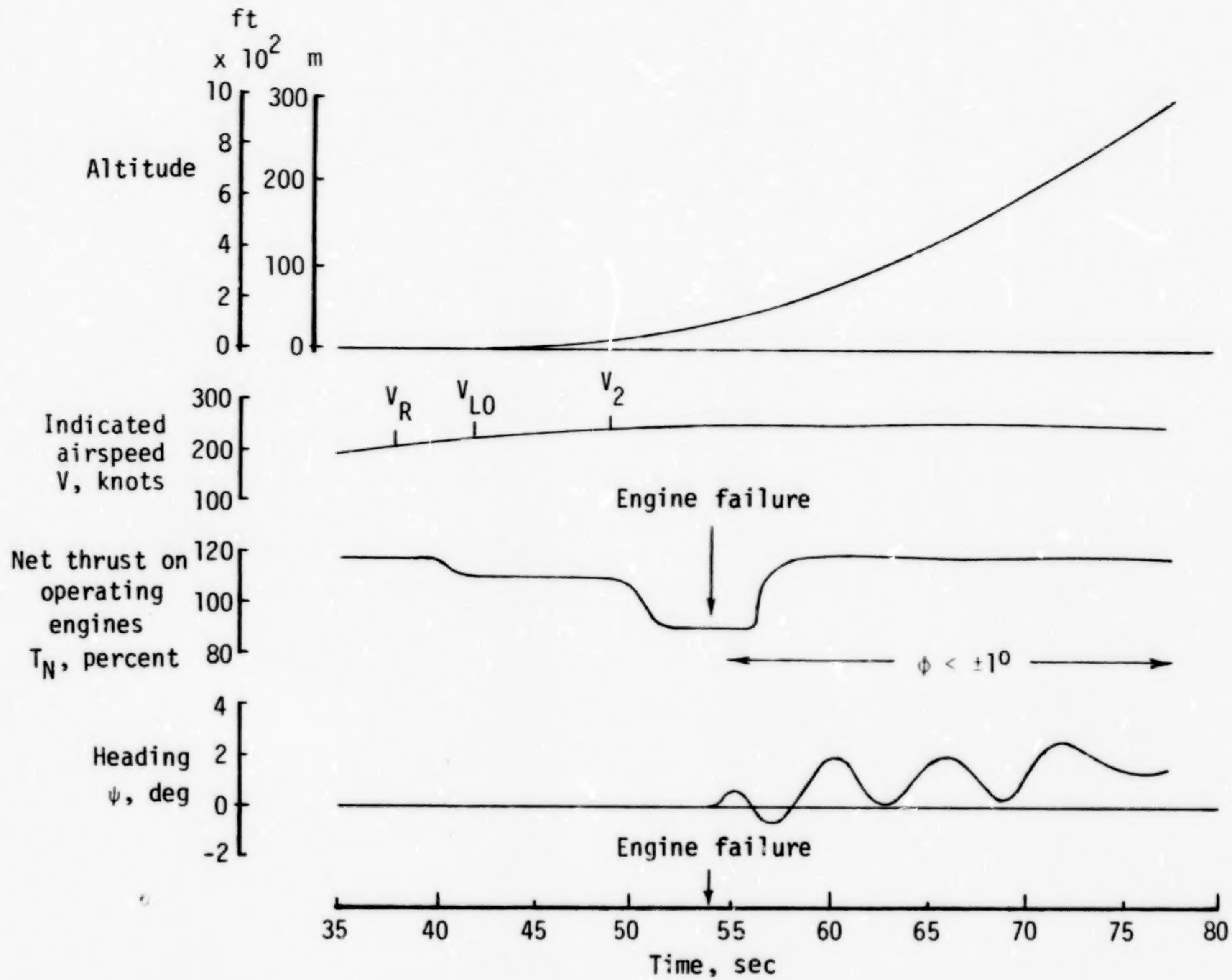

Figure 33.- Indication of bank angle and heading excursion following failure of number 4 engine while performing an advanced-procedure takeoff. (Advanced-procedure takeoff shown in fig. 18.)

1. Report No. NASA TP-1742	2. Government Accession No.	3. Recipient's Catalog No.
4. Title and Subtitle A SIMULATOR STUDY FOR THE DEVELOPMENT AND EVALUATION OF OPERATING PROCEDURES ON A SUPERSONIC CRUISE RESEARCH TRANSPORT TO MINIMIZE AIRPORT-COMMUNITY NOISE		5. Report Date November 1980
		6. Performing Organization Code 533-01-43-01
7. Author(s) William D. Grantham, Paul M. Smith, and Perry L. Deal		8. Performing Organization Report No. L-13881
		10. Work Unit No.
9. Performing Organization Name and Address NASA Langley Research Center Hampton, VA 23665		11. Contract or Grant No.
		13. Type of Report and Period Covered Technical Paper
12. Sponsoring Agency Name and Address National Aeronautics and Space Administration Washington, DC 20546		14. Sponsoring Agency Code
15. Supplementary Notes William D. Grantham and Perry L. Deal: Langley Research Center. Paul M. Smith: Kentron International, Inc., Hampton, VA.		

16. Abstract

Piloted-simulator studies have been conducted to determine takeoff and landing operating procedures for a supersonic cruise research transport concept that result in predicted noise levels which meet current Federal Aviation Administration (FAA) certification standards.

The results of the study indicate that with the use of standard FAA noise-certification test procedures, the subject simulated aircraft did not meet the FAA traded-noise-level standards during takeoff and landing. However, with the use of advanced procedures, this aircraft meets the traded-noise-level standards for flight crews with average skills. The advanced takeoff procedures developed involved violating some of the current Federal Aviation Regulations (FAR), but it was not necessary to violate any FAR noise-test conditions during landing approach.

Noise contours were also determined for some of the simulated takeoffs and landings in order to indicate the noise-reduction advantages of using operational procedures other than standard.

The takeoff and landing approach procedures developed and evaluated during this study did not compromise flight safety.

17. Key Words (Suggested by Author(s)) Aircraft noise; Supersonic transport; Piloted simulation; Takeoff and landing		18. Distribution Statement Unclassified - Unlimited. Subject Category 03	
19. Security Classif. (of this report) Unclassified	20. Security Classif. (of this page) Unclassified	21. No. of Pages 76	22. Price A05

For sale by the National Technical Information Service, Springfield, Virginia 22161

NASA-Langley, 1980

77

END

February 18, 1981